GL02144

Open File 82-466

Open File 82-466

UNITED STATES
DEPARTMENT OF THE INTERIOR
GEOLOGICAL SURVEY

Electrical Studies at the Proposed Wahmonie and Calico Hills Nuclear Waste Sites, Nevada Test Site, Nye Co., Nevada

by

D. B. Hoover, M. P. Chornack, K. H. Nervick and M. M. Broker

Open-File Report 82-466

1982

Prepared by the U.S. Geological Survey

for

Nevada Operations Office
U.S. Department of Energy
(Interagency Agreement DE-AI08-78 ET 44802)

Table of Contents

Illustrations

Illustrations (Continued)

Electrical Studies of the Proposed Wahmonie and Calico Hills Nuclear Waste Sites, Nevada Test Site, Nye Co., Nevada

by

D. B. Hoover, M. P. Chornack, K. H. Nervick, and M. M. Broker

Abstract

Two sites in the southwest quadrant of the Nevada Test Site (NTS) were investigated as potential repositories for high-level nuclear waste. These are designated the Wahmonie and Calico Hills sites. The emplacement medium at both sites was to be an inferred intrusive body at shallow depth; the inference of the presence of the body was based on aeromagnetic and regional gravity data. This report summarizes results of Schlumberger VES, induced polarization dipole-dipole traverses and magnetotelluric soundings made in the vicinity of the sites in order to characterize the geoelectric section.

At the Wahmonie site VES work identified a low resistivity unit at depth surrounding the inferred intrusive body. The low resistivity unit is believed to be either the argillite (Mississippian Eleana Formation) or a thick unit of altered volcanic rock (Tertiary). Good electrical contrast is provided between the low resistivity unit and a large volume of intermediate resistivity rock correlative with the aeromagnetic and gravity data. The intermediate resistivity unit (100-200 ohm-m) is believed to be the intrusive body. The resistivity values are very low for a fresh, tight intrusive and suggest significant fracturing, alteration and possible mineralization have occurred within the upper kilometer of rock. Induced polarization data supports the VES work, identifies a major fault on the northwest side of the inferred intrusive and significant potential for disseminated mineralization within the body. The mineralization potential is particularly significant because as late as 1928, a strike of high grade silver-gold ore was made at the site.

The shallow electrical data at Calico Hills revealed no large volume high resistivity body that could be associated with a tight intrusive mass in the upper kilometer of section. A drill hole UE 25A-3 sunk to 762 m (2500 ft) at the site revealed only units of the Eleana argillite thermally metamorphosed below 396 m (1300 ft) and in part highly magnetic. Subsequent work has shown that much if not all of the magnetic and gravity anomalies can be attributed to the Eleana Formation. The alteration and doming, however, still argue for an intrusive but at greater depth than originally thought. The electrical, VES, and IP data show a complex picture due to variations in structure and alteration within the Eleana and surrounding volcanic units. These data do not suggest the presence of an intrusive in the upper kilometer of section. The magnetotelluric data however gives clear evidence for a thick, resistive body in the earth's crust below the site. While the interpreted depth is very poorly constrained due to noise and structural problems, the top of the resistive body is on the order of 2.5 km deep. The IP data also identifies area of increased polarizability at Calico Hills, which may also have future economic mineralization.

Introduction

The U.S. Geological Survey (USGS) working under a memorandum of understanding with the Department of Energy (memorandum EW-78-A-08-1543), is engaged in a broad program to assess and identify potential repositories for high-level nuclear waste on the Nevada Test Site (NTS fig. 1). The USGS program consists of integrated geologic, hydrologic, and geophysical studies of regional and site-specific scope. This report discusses the results of electrical studies from Schlumberger vertical electrical soundings (VES), dipole-dipole induced polarization (IP), and magnetotelluric soundings (MT) at the Calico Hills and Wahmonie sites. The aim of this work is to characterize the geoelectrical section at and immediately adjacent to the sites.

The two sites are in the southwest quadrant of NTS adjacent to Jackass Flats (fig. 1). The two sites were originally selected based on previous geologic, aeromagnetic, and regional gravity data suggesting that a shallow intrusive was present at each site. The aeromagnetic data was particularly convincing because of similarity in signature with known granitic intrusions elsewhere in the region. The sought-for repository medium at these two sites was the inferred intrusive. At Calico Hills, Paleozoic argillite of the Eleana Formation also was present at the surface. Secondary consideration was given to the argillite as a potential repository medium should a sufficiently large and homogeneous body be identified.

Site-specific characterization work started in the fall of 1978 with emphasis on the Calico Hills site because it was thought to have the larger intrusive body. At the same time as the geological and geophysial studies were undertaken, a 2500 ft exploratory drill hole UE25a-3 was drilled at Calico Hills (Maldonado and others, 1979).

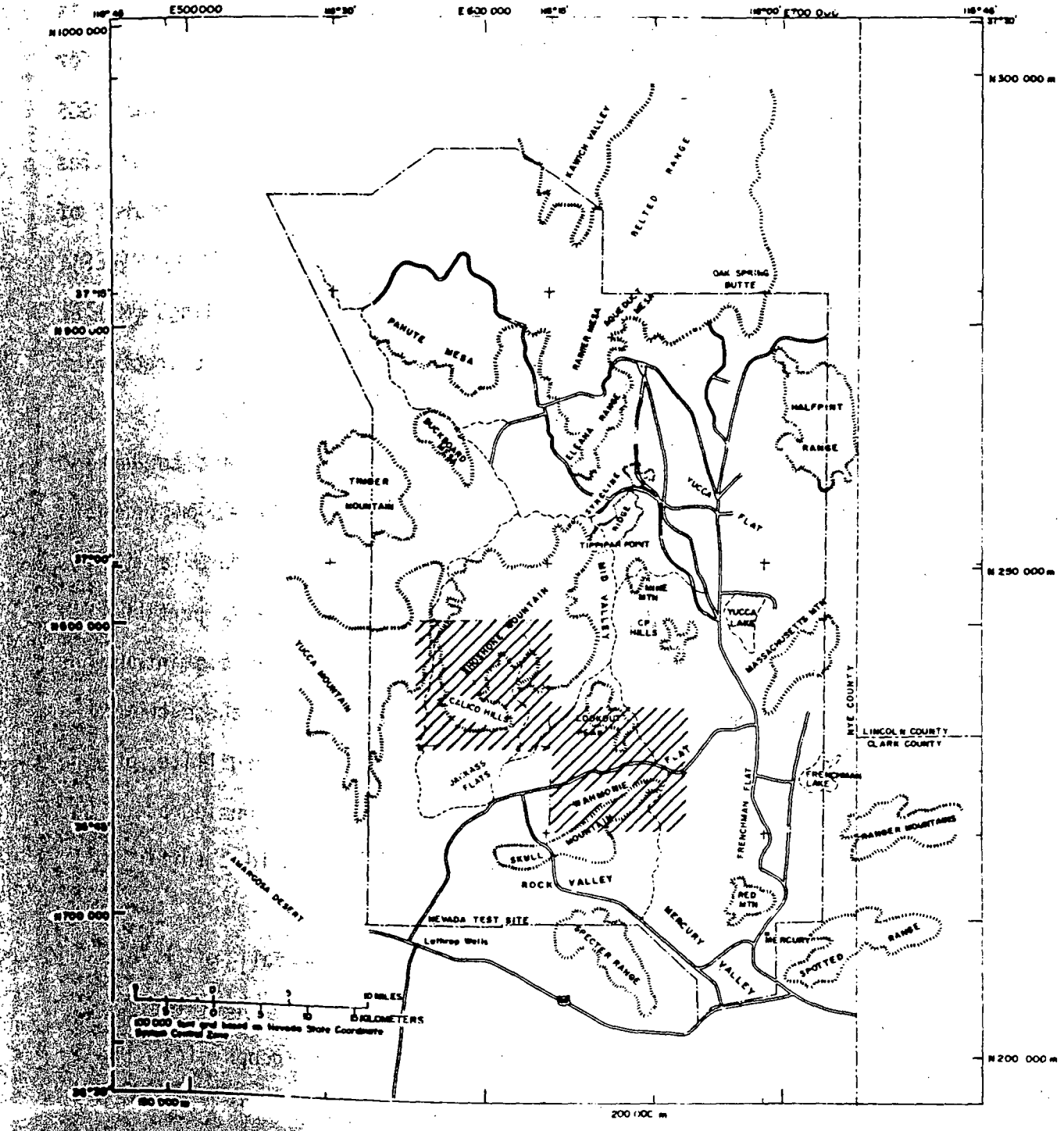

Figure 1: Index map of the Nevada Test Site showing the location of Calico Hills and Wahmonie Flat

Generalized repository criteria used in this program were the identification of a large homogeneous rock mass having low permeability in the depth range of 300 to 1500 m (1000 to 5000 ft). The areal extent is to be two square miles or more. The repository volume is to be relatively simple geologically so that it can be readily characterized. The geological conditions at the site should be such that potentially adverse conditions, high seismicity, uplift, faulting, fracturing, and so forth will not be present or can be demonstrated to not adversely affect the repository performance. Additional criteria may be found in the Nuclear Regulatory Commission Technical Criteria 10CFR Part 60 (1980).

Acknowledgments

We wish to express our sincere appreciation to the many people at the NTS who helped resolve the various problems that arose in the daily operations of our contractors-particularly the staffs of the DOE security and communications divisions and of the USGS core library at Mercury. Our appreciation also goes to the various geologists of Fenix and Scisson, Inc.[1] of Mercury, Nevada, who assisted Mr. M. P. Chornack in providing background information, guidance and monitoring of the contract operations. We also express our thanks to Mr. Charles Stearns who ran many of the VES inversions.

Electrical Methods Used

This report discusses results from Schlumberger VES, induced polarization IP, and magnetotelluric MT surveys. Other electrical methods were tried at Calico Hills on an experimental basis but will be reported on separately. Field data acquisition was contracted to private concerns for all three electrical methods (VES, IP, and MT). The VES field data was provided by Phoenix Geophysics Inc. of Denver, Colo. The IP field data provided by Heinrichs Geoexploration of Tucson, Arizona, were lines TR1, TR2, and CH1 on

Calico Hills, the remaining IP data were provided by Phoenix Geophysics, Inc., of Denver, Colo. The MT field data, data processing and one-dimensional inversion were provided by Williston McNeil, Inc., Denver, Colo.

Field procedures followed standard methods that have been discussed by Zohdy (1974) and Flathe and Liebold (1976) for VES and by Sumner (1976) for IP. The MT procedures in general followed those described by Vozoff (1972) or see Gamble and others (1979).

One-dimensional inversion of the VES data was done using computer programs of Zohdy (1974, 1975). The VES expansions were confined to areas of relatively flat topography because the inversion cannot take into account effects due to topography.

The IP data is presented as conventional pseudosections with qualitative interpretation Sumner (1976). Two-dimensional modeling was applied to selected data using an interactive computer code of Killpack and Hohmann (1979). This finite element program, originally developed by Rijo (1977), is able to take into account the effects of two-dimensional structure and topography. Four of the IP lines were modeled using this code by the University of Utah Research Institute, (UURI) Earth Science Laboratory. IP data is emphasized in this work because it provides good definition of lateral variations in electrical properties and it can be acquired in topographically rough and difficult terrain. The presence of the Horn Silver mine at Wahmonie and various small prospects at Calico Hills also suggested mineralization potential that might be identified by IP methods.

The MT data were processed and inverted by the contractor using proprietary computer programs. Much of the MT data is quite noisy. The noise could be due in part to low natural signal levels during the field operations.

Wahmonie Site

Geology

A simplified geological map of the Wahmonie site is shown in figure 2 adapted from Ekren and Sargent (1965). Figure 3 shows topography, the location of all the electrical data at the site, and identifies the principal geographic features. In figure 2 Tertiary volcanics have been lumped into a single unit because individually mapped units are not directly pertinent to the problem.

Surrounding Wahmonie flat and the Horn Silver mine is a zone of hydrothermal alteration (fig. 2 and fig. 3), which corresponds approximately with the inferred intrusive. Within the zone of alteration a north-northeast-trending horst block is present 1.5 km wide and 4 km long, which can be identified by a lack of alteration (fig. 2). On the southeast margin of this horst are two small granodiorite bodies giving distinct magnetic highs in low-level aeromagnetic data (G. D. Bath, oral communication, 1980). Within the horst and outside the area of alteration the exposed bedrock is principally rhyodacite. A small patch of Mississippian Eleana Formation, not shown in figure 2, overlies part of the Tertiary granodiorite within the horst.

Extensive block faulting is present in the exposed areas with the principal trends being northwest and northeast. The narrow southwest nose in the alteration pattern is probably an expression of hydrothermal solutions moving along an extension of a major fault zone on the southeast side of the horst.

The water table in the area is at approximately 732 m (2400 ft) above sea level or about 580 m (1900 ft) below the surface at Wahmonie flat (Winograd and Thordarson, 1975). The nearest well information is at J 11 (also called well 74-6) 10 km southwest of the Horn Silver mine. Water in J 11 is

high insulfate content in contrast to water from wells J 12 and J 13 (Winograd and Thordorson, 1975) located further west along Forty Mile Canyon.

Mining took place along faults in and adjacent to the southeast corner of the horst, at the Horn Silver Mine prior to 1905. In 1928 the district was reopened with a strike of high grade silver-gold ore (Cornwall 1977). Ball (1907) reports quartz stringers with gypsum present with the ore in the mine. The gypsum presumably comes from oxidation of primary sulfides and provides a possible source of sulfate for the water in J 11.

Geophysics

Both high level (8000 ft barometric) and draped (400 m terrain clearance) aeromagnetic surveys and a regional gravity map were available prior to this study. The aeromagnetic and gravity data supported inferences from the geology of the presence of a buried intrusive and some idea of its extent (G. D. Bath, oral communication, 1980; H. W. Oliver, oral communication, 1980). The high-level aeromagnetic map, figure 4, shows anomalies identified with both the Wahmonie and Calico Hills sites. The major anomalous magnetic body at Wahmonie is contained within the alteration halo and centered near the Horn Silver mine.

Ground magnetic, detailed gravity, seismic refraction, and seismic reflection studies have been done in addition to the electrical studies reported here. Results from the non-electrical studies are not yet available so reference to the supplementary studies are preliminary and tentative.

Schlumberger VES data

Individual sounding curves are shown in appendix 1 with their corresponding one-dimensional inversions. Figure 5 shows a cross-section interpreted from the inverted data. The section begins with sounding 79-3 in Jackass Flat (not shown in fig. 3) 4.7 km west-southwest of sounding 79-8,

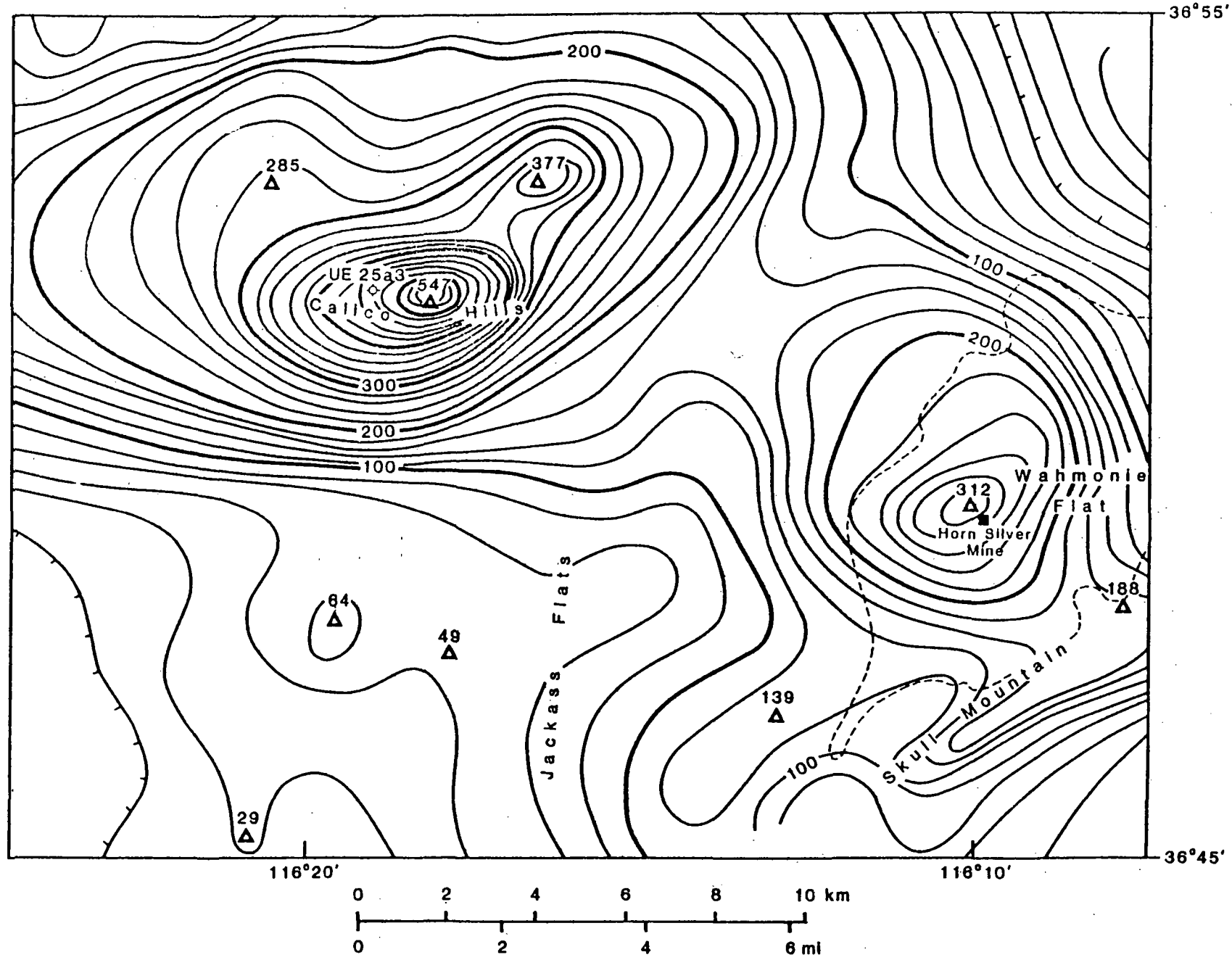

Figure 4. Aeromagnetic map of the Wahmonie and Calico Hills sites. Flight elevation in 8000 ft barometric and contour interval is 20 nT.

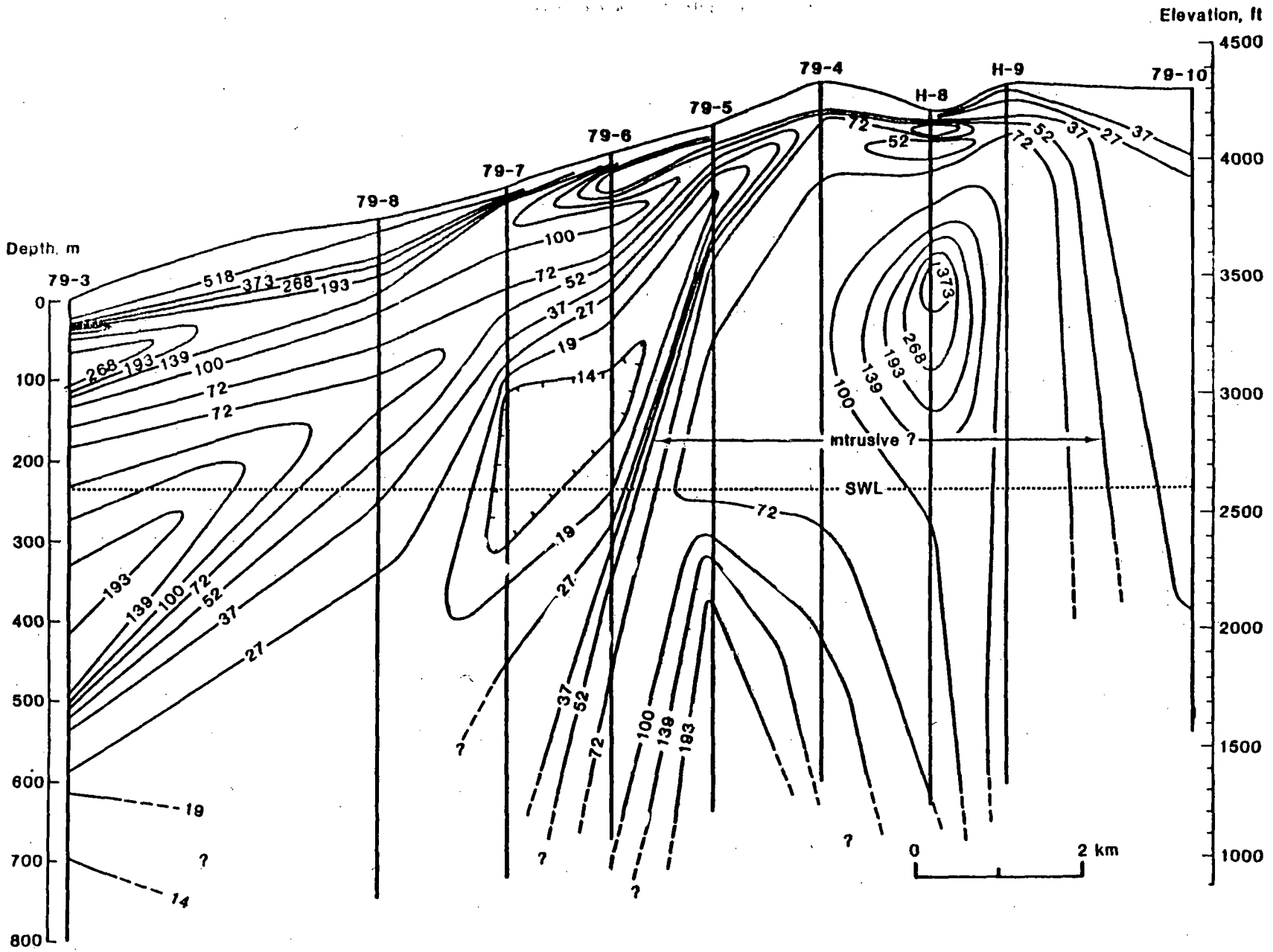

Figure 5. VES geoelectric cross-section at the Wahmonie Site. Contour interval is logarithmic and resistivities are in ohm-meters.

proceeds eastward to 79-8, 79-7, 79-6, 79-5 and 79-4. At 79-4 the section bends northward to H-8, H-9 and 79-10 (fig. 3). Soundings 79-4, 79-5, H-8, and H-9 are within the alteration halo. Near surface detail in the sounding data was omitted for clarity in figure 5.

Data from J-11 2.5 km northwest of sounding 79-3, provides the nearest lithologic control for the soundings at Wahmonie. A thick alluvial section (300 m) was found at J-11 below which basalt and tuff were encountered to a total depth of 406 m. Correlating the lithology with sounding 79-3 (appendix 1) suggests that the alluvium has a wide variation in resistivity (about 70-1000 ohm-m). The basalt and tuff correlate with a horizon of about 200 ohm-m at approximately 300-400 m depth. Below 500 m depth, the resistivity drops to 60 ohm-m or less and remains low indicating a minimum thickness of 400 m for this unit. This deep low resistivity unit is identified in the geoelectric section as the wedge shaped block defined by the 52 ohm-m contour. The depth to the top decreases and the thickness decreases as the alteration halo is approached.

The thick, low resistivity body cannot be directly correlated with a known lithology in the absence of deep drilling information. Either Eleana argillite or altered volcanics are believed to be the most probable lithologies correlative with the low resistivity body. Eleana Formation crops out within the horst at the Wahmonie Site but with very limited extent. However, it crops out extensively at Calico Hills (fig. 1) 12 km northwest of the Horn Silver mine and has the necessary thickness and resistivity. The electrical characteristics of the Eleana argillite at Calico Hills will be discussed later in this paper. Altered volcanic units crop out or are inferred to be beneath shallow alluvium. Resistivity inversions within the alteration halo all show a thin low-resistivity horizon at about 10 m depth

which probably correlates with the mapped altered volcanics. If altered volcanics correlate with the thick, low-resistivity body in the western half of the geoelectric section then alteration about the inferred intrusive is more extensive than surface mapping indicates.

The geoelectric section (fig. 5) shows a significant change going from sounding 79-6 to 79-5. VES 79-5 is 1200 m northeast of VES 6, 600 m inside the zone of alteration and presumably above the intrusive body. At a depth of about 150 m a more resistive body is inferred from the data; it extends in depth to the limit of the sounding gradually increasing in resistivity with depth. The sounding curve at this point however is not rising steeply enough for the resistive body to be several thousand ohm-m representative of a tight intrusive. This suggests that the intrusive is sufficiently altered, mineralized, or fractured in the upper part so as to reduce its resistivity.

VES 79-4 shows only a single shallow, low-resistivity zone that could be either argillite (Eleana) or altered volcanics. At 30 m depth, the resistivity increases to 70-100 ohm-m and remains fairly uniform to a depth of 700 m.

A resistive body reaching 300-400 ohm-m at a depth of 200-350 m is seen in the section below sounding H-8. This may represent a less altered part of the intrusive. The decrease in resistivity below 350 m may be due to lateral effects. The last data point on this sounding was dropped as it was believed to be perturbed by underground utilities.

VES H-9 shows a similar picture to VES 79-4 with the electrical basement found at 40-50 m but the resistivities are very low not rising above 100 ohm-m. An intrinsic resistivity of 100 ohm-m is a very low value for an unaltered, unfractured and unmineralized intrusive body. These data from H8 and H9 are in excellent agreement with results from an IP line, W1, run close to these two soundings and discussed below.

The last sounding in this cross-section, VES 79-10, on the northwest side of the intrusive shows a single thick, low-resistivity zone similar to VES 79-7 again presumed to be the Eleana Formation or altered volcanics.

The other soundings (VES 79-1, 79-2, H10 and 79-9, appendix 1,) are all on the edges of the intrusive and give a similar picture to those of figure 5 except for details in the upper part, which most likely represents the alluvial cover.

Induced Polarization Data IP

Two dipole-dipole IP lines were run across the central region of the inferred intrusive in a northwest-southeast direction (lines w1 and w2 in figure 3) and close to old workings of the Horn Silver mine. Line W1 was measured using a 305 m (1000 ft) dipole spacing; it is the only line at Wahmonie modeled by UURI (Smith and others, 1981). The modeling results and the observed pseudosection from line W1 are shown in figure 6 and the observed pseudosections from line W2 are shown in figure 7.

Because there are no large variations in topography along line W1, the modeling was not corrected for two-dimensional topography. Between stations 80W to 110W (8000-1100 ft west of the zero position) the small hills to the side of the line would have a small perturbation on the apparent resistivity values measured from these positions. The frequency effect values shown on the sections provide a measure of polarizable minerals within the rock matrix. These are the metallic-luster sulfides, magnetite and some clays and zeolites for the most part. Sumner (1976) discusses the responses of various rocks which have been noted as giving greater than normal background response. Metallic sulfides are not stable in the oxidizing environment above

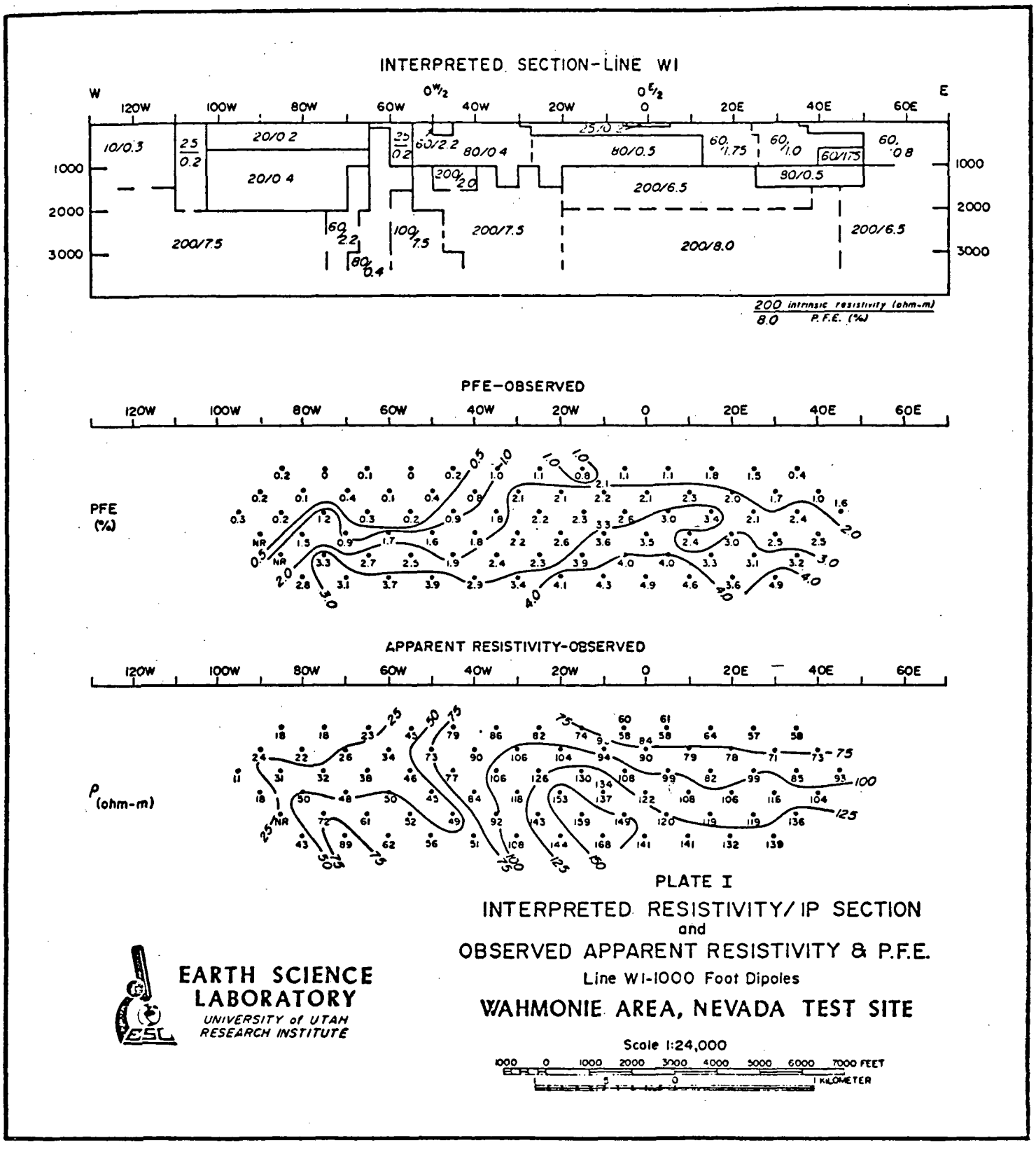

Figure 6. Induced polarization line W1 at the Wahmonie Site showing the derived two-dimensional model and the pseudosections.

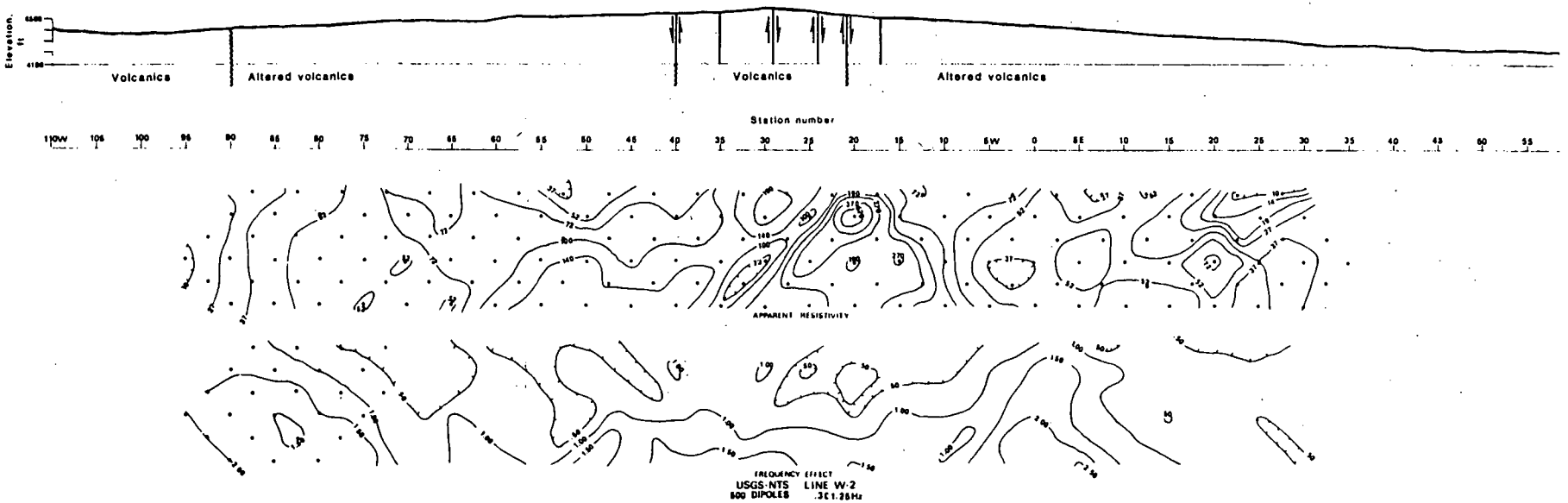

Figure 7. Induced polarization line W2 at the Wahmonie Site showing the surface lithologies and pseudosections. The resistivity pseudosection is contoured logarithmically and values are in ohm-meters.

the water table but are chemically changed to secondary minerals which have very low polarizability. We would not expect to see much polarization from altered sulfides above the water table and in fact we see low polarizability in the upper part of the inverted model in figure 9. The intrinsic polarizability increases significantly below about 300 m depth with another increase inferred at 600 m depth. This is the approximate water table. The modeled intrinsic polarizabilities go as high as 8% frequency effect, PFE, and large values are seen at depth along almost the whole line. A large disseminated mineral deposit is consistent with these data.

Smith and others (1981) estimated the grade using an empirical relationship of

$$W = \frac{45 \times PFE^{1/2}}{\rho},$$

where w = weight percent sulfide

ρ = intrinsic resistivity

PFE = intrinsic percent frequency effect,

which implies a minimum grade of 1 to 2 weight percent sulfide. Using the relationship w = PFE/3 (Sumner, 1976) gives 2.7% sulfide. Metal factor is another measure used to indicate the grade of a deposit (Sumner, 1976). The apparent metal factor on line W1 at depth is in the range of 150 to 180. We made a brief search of case histories to see if a similar prospect had been reported in the literature. A similar prospect at Quartzite Arizona, was found (McPhar Geophysics Corp., 1966) where a very uniform 200-300 ohm-m resistivity section showed apparent metal factors increasing with depth to 100-150 or 3-5% PFE. The line was about 5000 ft long with mineralization indicated at depth all along the line. The similarity with Wahmonie data on line W-1 is striking. The drilling results showed thick Tertiary overburden, a thick schist sequence with oxidized sulfides and granite at depth containing

2 to 4% sulfides. Drilling depths and thicknesses are not given in the case history.

The IP evidence for disseminated mineralization and the presence of the Horn Silver Mine provides strong evidence for a large disseminated sulfide body at depth. The area near the Horn Silver Mine offers an exceedingly attractive minerals exploration target. The data do indicate that the shallowest disseminated mineralization is between 20W and 20E. This zone is closest to and on the trend of the Horn Silver Mine workings.

Some structural information can also be obtained from the data on line W1. Approximately at station 60 W, faulting is inferred from the pseudosections and model data. To the northwest the section appears to have been downdropped about 300 m (1000 ft). This is consistent with a steep gravity gradient at this position (H. W. Oliver, oral communication, 1980) that also suggests a major fault or lithologic boundary. The upper 300-600 m of section in this northwest block was modeled with 10-20 ohm-m material, which we infer to be the Eleana argillite or altered volcanics. Several faults are inferred from geological data to cross line W1 east of station 60W yet the entire line southeast of 60W shows no distinct boundaries that could be inferred as faults. The fact that the faults were not sensed may be due to the large dipole length, (300 m), which makes the data show values averaged over large volumes of rock.

Line W2 runs across prospects and between shafts of the Horn Silver Mine. The line has not been modeled, but qualitative interpretations can be based on the pseudosection of figure 7. The dipole spacing on this line was 152 m (500 ft) so that at an "n" of six, we are at best just starting to sample rocks below the water table (550-670 m depth on line W-2). At an "n" of six the PFE values are about 1.5; this value is consistent with the

observations on line W1 at an equivalent depth. The increase in PFE with depth suggests that the survey may just be beginning to sense sulfides.

The resistivity section suggests the existence of a high-resistivity block near 20W that is probably fault bounded. The Horn Silver Mine workings were in a northeast-trending zone that crosses line W2 in the 15-25 W interval. No increased polarization is noted in this region presumably because the sulfides have been oxidized. The high-resistivity zone between 10W and 20W may also be due to induration of the host rock by mineralizing solutions. The horst is mapped geologically between 20W and 40W on line W2 and as mapped is distinguished by a lack of rock alteration. The eastern boundary is clearly seen in the electrical data near 15W but there is no clear evidence for an electrical boundary on the west. Neither the resistivity nor the frequency effect pseudosection show a significant change in value across the mapped contact between altered and unaltered volcanic units on the western edge of the horst.

Conclusions Wahmonie Study Area

The foregoing data interpretation is considered preliminary as much additional geophysical data is presently being analyzed, which should provide additional constraints. However, the tentative conclusions to be drawn from these data suggest that the Wahmonie site is inappropriate for a nuclear waste repository.

There may be a volume of intrusive rock at the site sufficient to hold a waste repository. The resistivity of the mass, however, shows that it is not a fresh, tight, and unaltered intrusive. The resistivity indicates significant porosity attributable to fracturing, faulting, alteration, mineralization or any combination of these. Many mapped faults do not appear to be reflected in the electrical data, but two prominent faults were

identified; one at station 20W line W2 on the southeast margin of the horst and another at station 60W on line W1.

The data show the edges of the inferred intrusive correspond approximately with the alteration halo. This correspondence is not substantiated on the north and east sides due to a lack of data.

The most significant finding is the disseminated sulfide mineralization in the intrusive. IP data suggest that 2% or more sulfides may be present below the water table. This evidence of mineralization with the presence of once-active silver-gold mining at the site suggest that it is a very attractive exploration target. This serendipitous result, although detrimental to siting of a waste repository, indicates that further exploration and drilling might outline a deposit of importance to our inventory of strategic metals.

Calico Hills

Geology

A simplified geological map of the Calico Hills region is shown in figure 8, adopted from Orkild and O'Connor (1970) and McKay and Williams (1964). All extrusive volcanic units were lumped in preparing the map. The Calico Hills are part of a structural dome, (Maldonado and others, 1979) elongate in a northeast direction, on the north-central edge of Jackass Flat (fig. 1, fig. 8). Extensive radial and ring faulting is associated with the doming. Faults not associated with the doming are high-angle Basin and Range faults generally trending north-south or thrusts which have left some remnants of Devonian limestone on the structurally higher parts of the dome. The Mine Mountain fault is a major northeast-trending strike-slip fault 5.5 km southeast of the dome axis. A fault has been inferred (Orkild and O'Connor, 1970) along the center of Topopah Wash on the long axis of the dome, which parallels the Mine Mountain fault (fig. 8).

The oldest rock units in the area are thin islands of Devonian carbonate rocks that are remnants of an upper thrust plate. The Devonian carbonates overlie younger Mississippian rocks of the Eleana Formation composed primarily of argillite with some quartzite. The Eleana crops out in the south central part of the dome (fig. 8) and is assumed to exist beneath thin alluvial cover along Topopah Wash. Unconformably overlying the Mississippian rocks, extrusive Tertiary volcanics 8-14 m.y. old (Maldonado and others, 1979) crop out principally along the margins of the dome and also to the north. The extrusive volcanic units are composed of rhyolite flows and welded to non-welded tuffs. Several small rhyolite intrusions are present within the outcrop area of the Eleana Formation. Quaternary alluvium is present along Topopah Wash and in Jackass Flat to the south.

A generalized lithologic section from drill hole UE25a-3 (fig. 9) along with VES data and electric logs are shown in figure 10. Unit J of the Eleana Formation composed principally of argillite in unaltered or essentially unaltered condition, occurred in the upper 415 m (1360 ft). The clay minerals (kaolinite, nacrite and dickite) found in fractures indicate that hydrothermal solutions moved along fractures but caused little alteration in the main mass (Maldonado and others, 1979). From 415 m to 721 m (1361 to 2364 ft) of depth, unit J is present but has been thermally altered. The lowest 46 m (150 ft) of this interval is composed of a calcareous argillite. The remainder of the hole (721 to 772 in depth) was drilled through marble believed to be unit I of the Eleana Formation.

Nine fault zones, some of which showed brecciation, were encountered in the core; their apparent dips ranging from 45^{o} to -90^{o}. Bedding plane dips measured in the argillite ranged from 10^{o} to 52^{o}. The calcareous argillite was essentially horizontal, while the marble dipped at about 50^{o}.

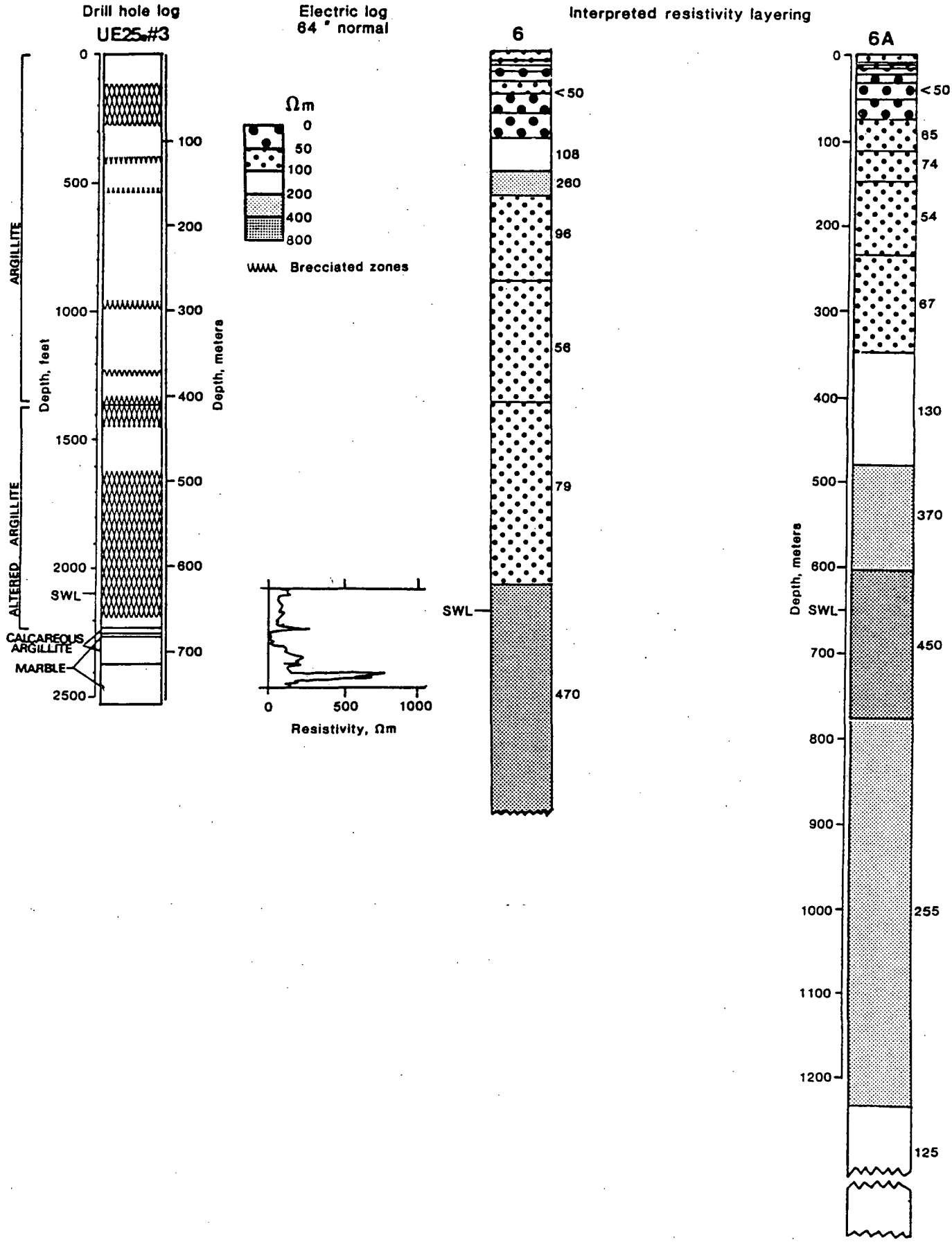

Figure 10. Diagram comparing the lithologic log of UE 25A-3 with crossed VES 6 and 6A at the well site.

Magnetite and pyrite are present along fractures in the argillite. Within the altered part sufficient magnetite occurs so that a significant part if not all of the magnetic anomaly (discussed below) can be attributed to the argillite rather than a buried intrusive (G. D. Bath, oral communication, 1980). Measured porosity on 10 core samples of the unaltered argillite averaged 10.8%, and on nine samples of altered argillite 6.7% (Maldonado and others, 1979).

The measured static water level in UE25a-3 is at an elevation of 748 m (2453 ft) or 639 m (2097 ft) below the surface. Temperature logs were run in April 1979 after the hole had reached thermal equilibrium. The average thermal gradient in the lower part of the drill hole was 45°C/km and the temperature on bottom was 46.8°C. The calculated heat flow is quite high, (3.3 HFU), which suggests an upwelling hydrothermal system below the bottom of the hole (Sass, 1980).

Geophysics

The aeromagnetic data on which much of the inference of a shallow intrusive was based is shown in figure 4. Drilling has shown that the intrusive, if present, is deeper than 2500 ft near the center of the dome and that much of the magnetic anomaly can be attributed to magnetic mineralization within the argillite. Subsequent detailed gravity work has also shown that the gravity anomaly can be attributed to a density contrast between the Paleozoic rocks and the surrounding low density Tertiary volcanics, (Snyder and Oliver, 1981). Nevertheless the doming and alteration provide evidence that an intrusive is present at depth. The electrical studies presented here are an attempt to identify the intrusive and to characterize the subsurface geoelectric section including the extent and location of unit J of the Eleana Formation.

VES data and results

Figure 10 shows the interpreted electrical sections from two coincident, orthogonal soundings (6 and 6A) made at the site of drill hole UE25a-3. The lithologic log is also shown for comparison. The soundings were completed prior to the drilling so they are not perturbed by drill casing. The interpreted sections are similar; the observed differences are attributed to lateral variations in electrical properties. The unaltered argillite in the lithologic section correlates with an electrical section having an average resistivity of about 50 ohm-m. The high-resistivity unit at 150 m depth on sounding 6 is attributed to a narrow remnant of carbonate rock that was crossed while making the sounding. At 350-400 m depth the resistivity increases reaching a maximum of about 460 ohm-m. This interval correlates with the altered argillite and marble observed in the drill hole. Electric logs run below the static water table (Daniels and Scott, 1980; Maldonado and others, 1979) show an average resistivity for the Eleana argillite about 250 ohm-m and the carbonates variable but generally higher in value. Sounding 6A was expanded to 2440 m (8000 ft) so as to obtain information from greater depth. The interpreted resistivities below the 450 ohm-m interval then decrease to 130 ohm-m at 1300 m depth, the approximate limit of the sounding. This deep lower resistivity unit cannot reliably be associated with particular lithologies. The resistivity is an order of magnitude too low for a tight unaltered intrusive body. If this sounding is sensing the intrusive then significant alteration and fracturing has taken place.

An electrical cross-section (figure 11) is presented along the line of soundings 79-11, 6A, 7, 12, 13, 14, 15, and 20, (figure 9). This is essentially along the long axis of the dome extending to the upper end of Topopah wash at sounding 20.

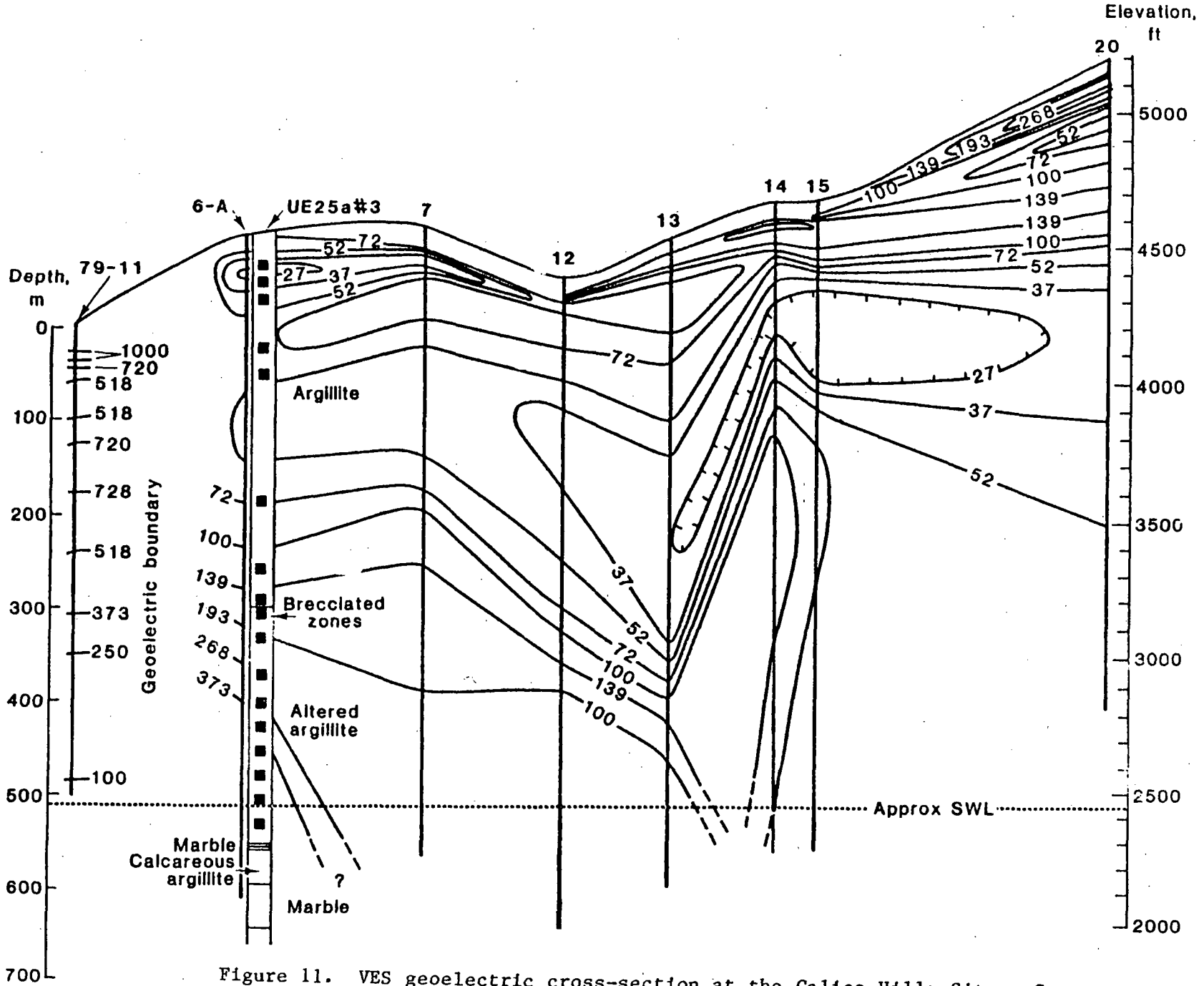

Figure 11. VES geoelectric cross-section at the Calico Hills Site. Contour interval is logarithmic and resistivities are in ohm-meters. Breccia zones observed in drill-hole UE 25a3 are shown as black boxes.

The cross-section shows that between VES 6A and 79-11 a major boundary must exist. The inversion of 79-11 doesn't show any interval of the geoelectric section that can be identified with the Eleana Formation. The Eleana is either missing entirely, is too deep or too thin to be identified, or is altered to much higher resistivities. VES 79-11 was sited on shallow Quaternary alluvium underlain by Tertiary volcanics. The high resistivities (200 ohm-m and greater) seen in the inversion of 79-11 are assumed to be typical of the unaltered volcanics in this area. No attempt was made to contour between VES 6A and 79-11. Faulting is inferred between these two soundings along which uplift of the dome has occurred.

From sounding 6A to the northeast, the resistivities seen in the geoelectric section are generally less than 50 ohm-m. Based on the lithology of drill hole UE25a-3, Eleana argillite, both altered and unaltered, is inferred to be present at least to a depth of 600 m. The higher resistivities (above 100 ohm-m) seen at shallow depth on the northeast end of the section may in part be attributed to Tertiary volcanics overlying the Eleana Formation. Between VES 13 and 14 faulting is inferred from the vertical offset seen in the section contours. Based on the 27 ohm-m contour displacement of 200 m may be present. Mapped north-trending faults that are exposed south of the section may extend under alluvial cover in Topopah Wash.

From sounding 6, at a depth of 400 m corresponding to the interface between altered and unaltered argillite, an arcuate (concave downward) resistivity gradient can be seen in the geoelectric section extending to sounding 13. Higher resistivities associated with the altered argillite become deeper northeast of VES 7. This pattern is inferred to reflect the thermal alteration halo in the argillite. A similar pattern was noted in seismic refraction data along this same line of section (L. W. Pankratz,

oral communication, 1980). All the VES soundings and inversions are shown in appendix 1.

Because of the complex structure in the Calico Hills area, a more detailed examination of the individual VES data will not be made. However A few additional results will be mentioned. Low resistivities over a thick vertical interval were not identified on soundings 1, 2, 10, 11, and 28. Soundings 16 and 17 showed what is inferred to be Eleana argillite at relatively great depth, 200 to 600 m. All other soundings showed the top of the Eleana at relatively shallow depth with Nos. 3, 4, 5, and 6 showing it at the surface consistent with the mapped geology. Sounding 28 was positioned near some old mining prospects and on outcrop of Eleana. Interpreted resistivities were in the range of 100 to 300 ohm-m suggesting that altered Eleana argillite is near the surface.

Dipole-dipole induced polarization data and results

Six IP traverses were run across the Calico Hills area, three near the central part of the dome and three profiles crossing Topopah wash (fig. 8). The three profiles that ran across the central part of the dome TR-1, TR-2, and CH1 used 500-, 1000-, and 1000-ft dipole separations respectively and expanded only to an "n" of four. The other three (CH 4, 5, and 6) each used 500-ft dipoles expanded to an "n" of six. Lines TR-1, TR 2 and CH 1 were modeled by the University of Utah (Ross and Lunbeck, 1978). The results are summarized below along with the derived models.

Ross and Lunbeck (1978), by correlating modeled intrinsic electrical parameters with known and inferred geologic units, presented a table of probable bulk electrical properties for the lithologies present at the Calico Hills site. These are reproduced as table 1. They state in their report that

the Eleana argillite is 50-100 ohm-m for the most part, while the low range for the Topopah Spring Member of the Paintbrush Tuff is 60 ohm-m. From all the data presented the low range for the Topopah Spring is inferred to be associated with limited areas of extensive alteration. The results of table 1 agree well with inferences made from VES and drilling data.

Line TR-1 (fig. 12) was run near drill hole UE25a-3 along the same path used in the expansion of VES 6. More near-surface detail is given in the modeled data along TR-1 (fig. 13) because shorter dipole separations (500 ft) were used than on TR-2 and CH-1. The exploration depth however is correspondingly reduced. Drill hole UE25a-3 is adjacent to station E-7. At this position the interpretation of the IP data shows a low-resistivity unit of 45 ohm-m identified as Eleana overlying a 100 ohm-m unit at 460 m (1500 ft) below surface. This is in excellent agreement with the boundary of altered argillite at 416 m (1365 ft) and with the two corresponding VES soundings 6 and 6A (fig. 10).

Further comparison of the modeled IP and VES data give reasonable agreement. VES 3 is near position 12.5 E of TR1, the sounding interpretation is similar to 6A but the more resistive lower layer, corresponding to altered Eleana, is a bit shallower than given in the IP model. VES 2 is a short distance south of position 15.5 E of TR1 and shows a high-resistivity section about 700 ohm-m above 100 m descending to an average of about 200 ohm-m. This sounding interpretation corresponds well with the IP model near station 19E but not with that at the nearer position (15 1/2E). It would appear that a major interface occurs between IP station 15 and VES 2. VES 10 close to IP station 21 E does not see the modeled low resistivity unit (50 ohm-m) but otherwise is in good agreement. We suggest that the lower resistivity units seen in the modeled IP data within zones of known volcanics are zones of

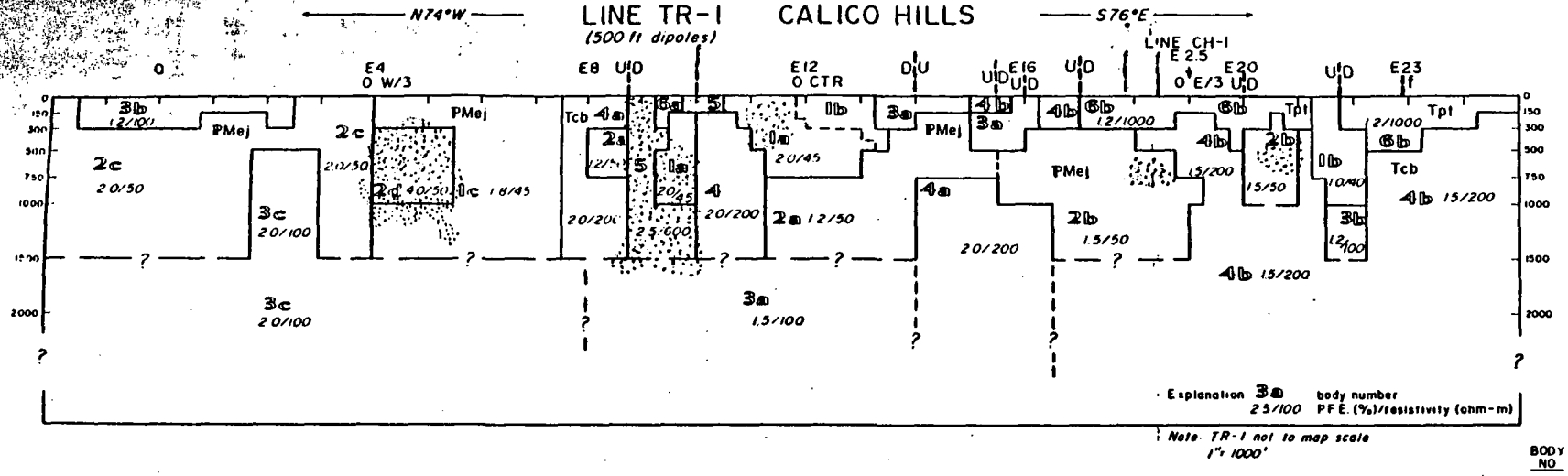

BODY NO	RESISTIVITY ρ (ohm-m)	PFE φ(%)
1a		2.0
1b	45	1.0
1c		1.8
2a		1.2
2b	50	1.5
2c		2.0
2d		4.0
3a		1.5
3b	100	1.2
3c		2.0
4a	200	2.0
4b		1.5
5	600	2.5
6a	1000	1.0
6b		1.2

Stratigraphic zone of high PFE, PFE >20%

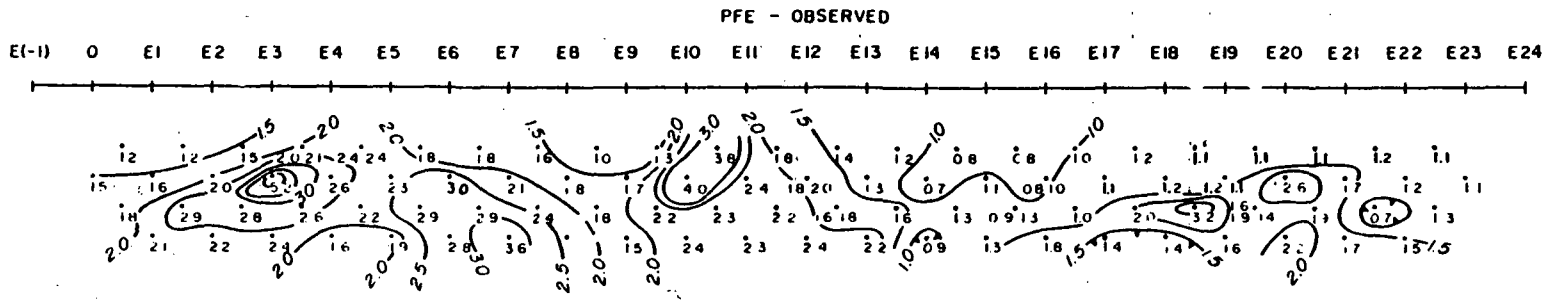

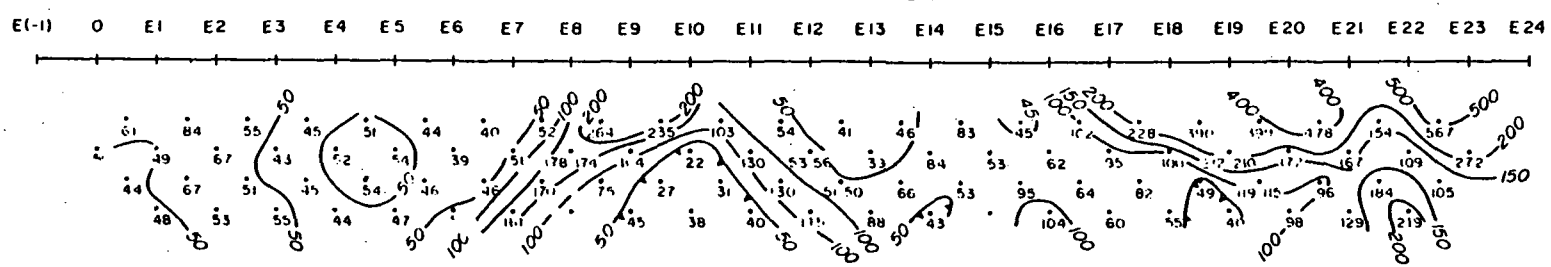

EARTH SCIENCE LABORATORY
UNIVERSITY OF UTAH RESEARCH INSTITUTE

Figure 13. Induced polarization line TR 1 showing the derived two-dimensional model and the pseudosections.

TABLE 1

STRATIGRAPHIC SECTIONS FOR CALICO HILLS WITH PROBABLE BULK ELECTRICAL PROPERTIES

		Thickness (feet)	PEE (%)	Resistivity (Ohm-m)
Qac	Alluvium and colluvium gravels and sands	0-1.025	0.5-2.0	45-200
Tpt	Piapi Canyon Group Paintbrush Tuff, Topopah Spring Member, ash flow devitrified welded tuff;	300-800	1.2-2.0	100-1000
	pervasive alteration: silicified, alunitized, kaolinized; porphyritic		3.0-4.0	60-200
Tcb	Tuffaceous beds of Calico Hills non-welded ash flows and debris; beds of rhyolitic and pumice;	1000±	1.5	100
	may be silicified, alunitized and kaolinized		4.0	200
Tci	Rhyolite intrusions silicified, kaolinized; porphyritic	?	not defined in this study	
PMaj	Eleana Formation, unit J. thin bedded argillite and thin to thick-bedded quartzite and conglomerate; forms sole of thrust fault	350±	.5-1.5	60-200
MDld	Limestone and dolomite aphanitic crinoidal limestone, thin bedded limestone and dolomite; occurs in upper plate of thrust over PMaj	100±	not well defined	
Ddn	Devil's Gate(?) Limestone fine- to coarse-grained, brecciated dolomite and limestone; occurs in faulted blocks thrust over MDld and PMaj	400±	not well defined	

alteration, fracturing and faulting, which were not readily identified in the VES data.

Associating the large units of 50 ohm-m material modeled on line TR-1 with the unaltered argillite indicates its present along the line generally from the western end to about station E 19 on the east. The surface contact between Eleana argillite and volcanics occurs at station E 17. The significance of a thick 600 ohm-m unit modeled near IP station 9E is not clear since it cannot be attributed to the thin overthrust plate of carbonates at that position. The IP model suggests geoelectric complexity, which may be due to structural complexity or to variations in alteration, but probably is a combination of both.

Line TR 2 (fig. 14) is parallel to TR 1 and 800 m to the north. Dipoles spaced 305 m (1000 ft) apart were used on this line so poorer definition of fine structure results but greater depth of investigation is achieved. The line from the west end to station E 7 crosses surface exposures of Eleana or remnants of the overthrust carbonates. The IP data indicate that low-resistivity material corresponding to unaltered Eleana is generally present to depths of 460 m (1500 ft) except for a narrow zone at E(-4) and a broad zone from E1 to E5. These two zones are modeled at 100 ohm-m and probably indicate increased alteration of those parts of the Eleana argillite. Zones of increased polarizability are indicated at E-4 and between E-7 and E-10. The eastern zone between E-7 and E-10 correlates with a large zone of increased silicification, alluvitization and kaolinization mapped in the volcanics. Strongly magnetic Eleana argillite is present at the surface between station E-5 and E-6, yet the magnetic mineralization does not appear to contribute to polarizabilities above background at this location. The lack of correlation between magnetic argillite and higher polarization values gives additional

PLATE IVa

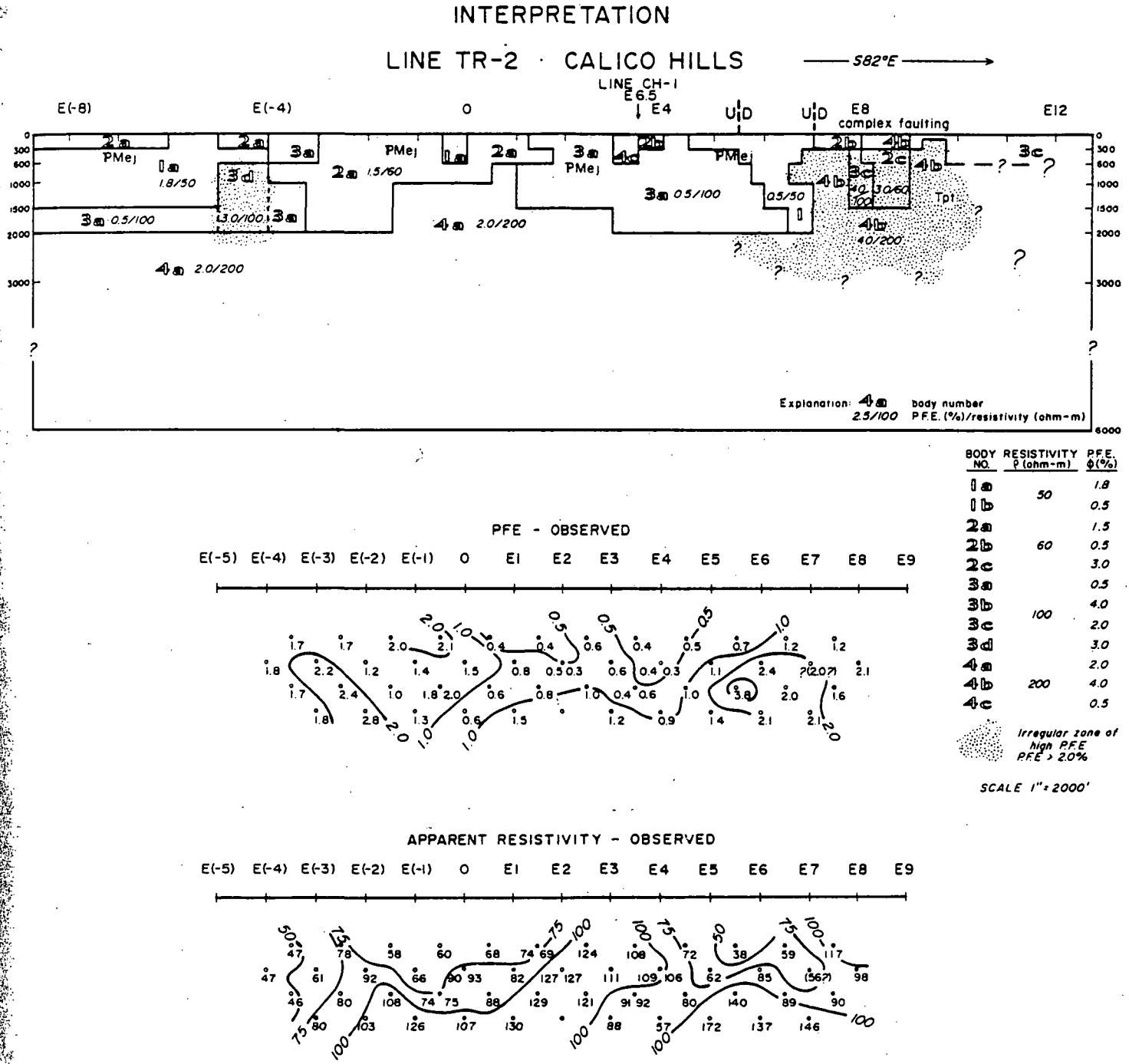

BODY NO.	RESISTIVITY ρ (ohm-m)	P.F.E. Φ(%)
1a	50	1.8
1b		0.5
2a	60	1.5
2b		0.5
2c		3.0
3a	100	0.5
3b		4.0
3c		2.0
3d		3.0
4a	200	2.0
4b		4.0
4c		0.5

Irregular zone of high P.F.E. P.F.E. > 2.0%

SCALE 1" = 2000'

EARTH SCIENCE LABORATORY
UNIVERSITY of UTAH
RESEARCH INSTITUTE

Figure 14. Induced polarization line TR 2 showing the derived two-dimensional model and the pseudosections.

evidence for disseminated sulfides as the cause of polarization anomalies in the Eleana Formation on the other IP lines. Line CH 1 (fig. 15) runs northwest-southeast in part along one of the access roads into the area. The surface contact between Eleana argillite and volcanic units is between station E3 and E4. Near the contact and throughout the surface exposure of the volcanic units, the modeling indicates a fair amount of geoelectric complexity. Also no large blocks of low resistivity, correlative with unaltered Eleana argillite, are identified as in the other two lines. Where the line runs across surface exposures of predominantly Eleana Formation the model data shows units of 100 and 160 ohm-m material. Ross and Lunbeck (1978) suggested that the deeper 100 ohm-m material may be an intrusive, but here we suggest this is more probably altered Eleana extending essentially to the surface in this region. As on TR 2, an extensive region of higher intrinsic polarizability is seen in the altered volcanics.

These three indicate a complex geoelectric section, but no through-going trends can be discerned. The central part of the dome, to the depth of exploration, is inferred to be underlain by the Eleana Formation with faulting and variations in alteration contributing to the observed complexity. The contact with the surrounding volcanics can be seen and is easily identified where alteration increases polarizability. There is no clear evidence that an intrusive is present within the depth of exploration.

Subsequent to the completion and modeling of the IP lines just discussed, three other IP lines were run across Topopah Wash (fig. 12) to give better definition of the Eleana argillite and its structural relations along the northeastern part of the area. These are lines CH 4, 5, and 6 which roughly parallel CH 1. All three lines used 500 ft dipoles. The lines are

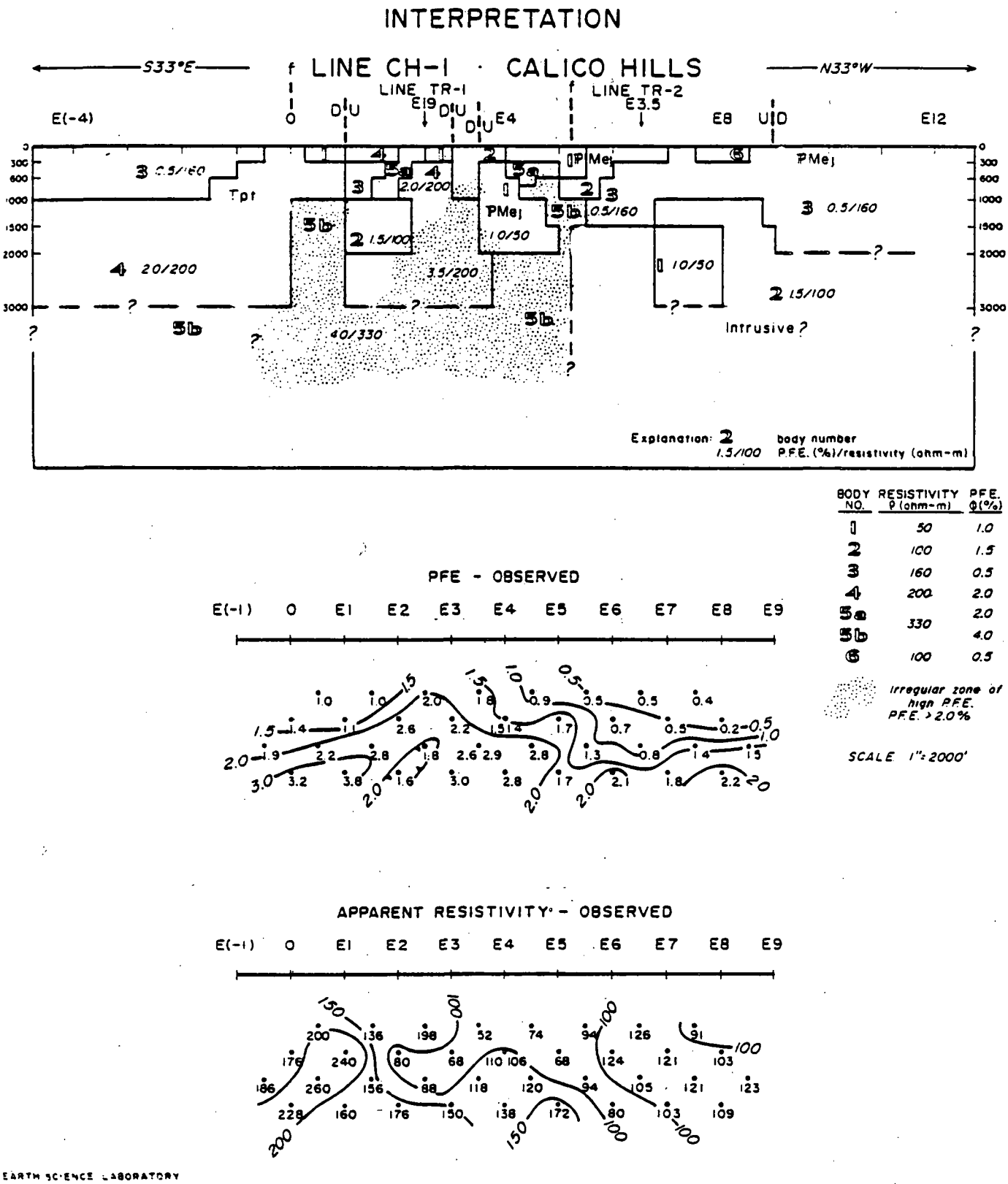

BODY NO.	RESISTIVITY ρ (ohm-m)	P.F.E. Φ(%)
1	50	1.0
2	100	1.5
3	160	0.5
4	200	2.0
5a	330	2.0
5b		4.0
6	100	0.5

EARTH SCIENCE LABORATORY

Figure 15. Induced polarization line CH 1 showing the derived two-dimensional model and the pseudosections.

not yet modeled; however, a number of conclusions can be made based on qualitative examination of the data. Line CH 4 (fig. 16) runs across the Eleana Formation either exposed or buried beneath shallow cover between stations 95W and 10E. Volcanics crop out on each end of the line. These data (fig. 16) show a distinct resistivity boundary at 45W-50W between low resistivities to the southeast (50± ohm-m) which we associate with the unaltered Eleana and higher resistivities (150± ohm-m) to the northwest. Between 80W and 85W, another resistivity boundary appears to be present, but the data is insufficient to give it adequate definition. The frequency effect pseudosection shows relatively high polarizability west of station 50W.

One prominent feature observed in the Eleana Formation is a zone of slightly higher resistivity and increased polarizability between station 15W and 25W. The feature shows most distinctly in the PFE pseudosection where it is defined by large gradients along 45-degree lines beginning at 25W and 15W. Such an anomaly would be produced by a broad near-vertical zone between 15W and 25W containing material of increased polarizability. This is believed to be the electrical expression of the inferred northeast-trending fault along Topopah Wash. From 10E to about 35E a thin, high-resistivity horizon is seen. This correlates with volcanics crossed in outcrop along this portion of the line. The low resistivities seen at greater depth in the pseudosection imply that unaltered Eleana argillite underlies the volcanics.

In a broad sense, line CH 5 (fig. 17) shows a similar picture. At 25W-30W there is a contact between low-resistivity material, on the east corresponding to unaltered Eleana argillite and higher resistivity material on the west. Faulting has been mapped in the volcanics near 35W. The frequency effect pseudosection shows increased polarizability and appears in this same region suggesting alteration and possible mineralization. The southeastern

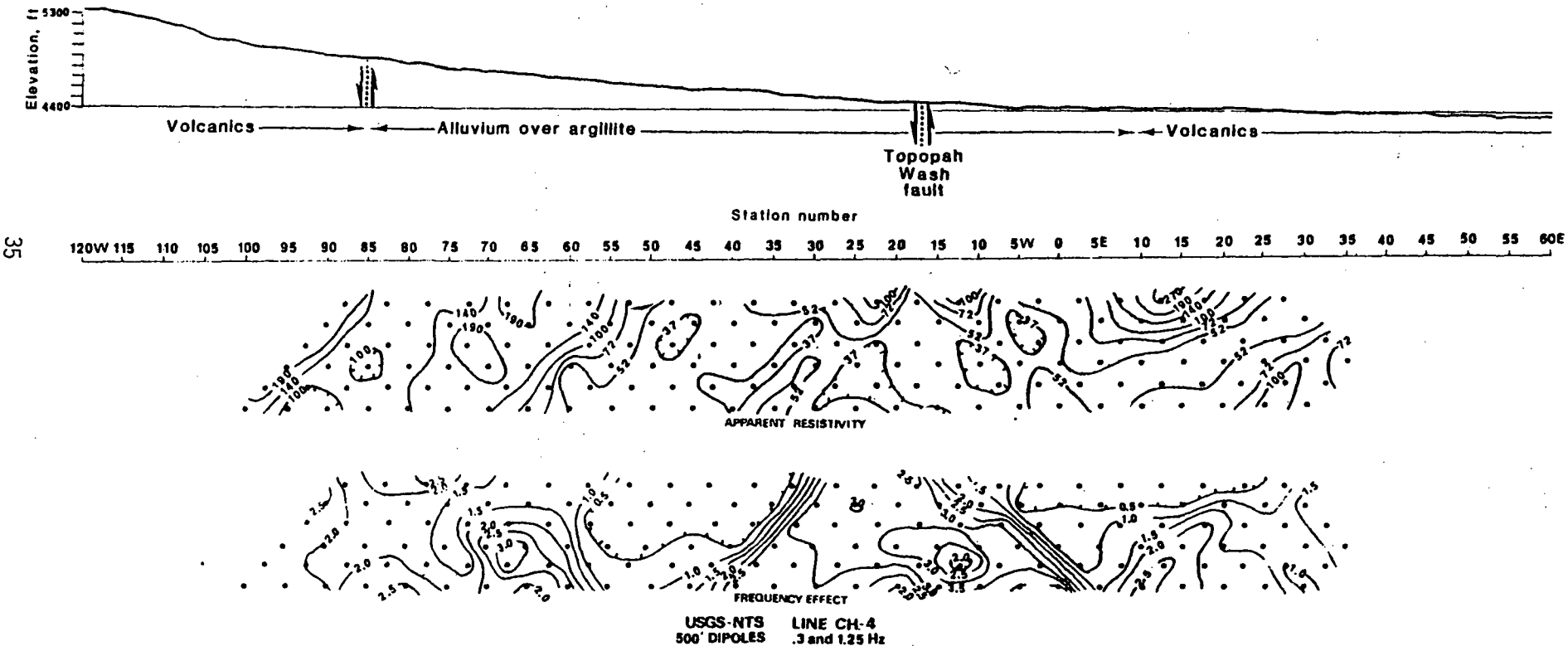

Figure 16. Induced polarization line CH 4 showing the surface lithologies and pseudosections. The resistivity pseudosection is contoured logarithmically and resistivities are in ohm-meters.

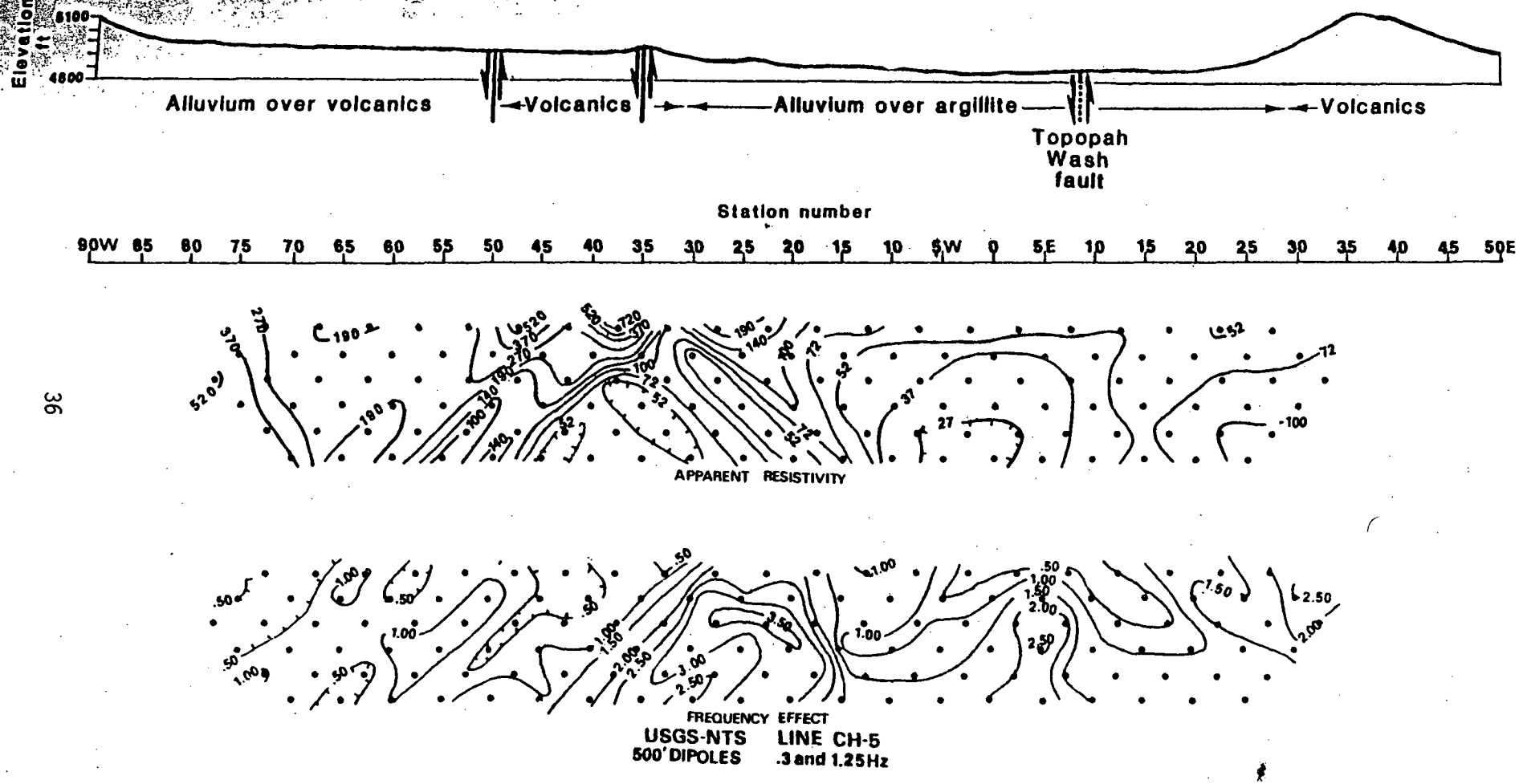

Figure 17. Induced polarization line CH 5 showing the surface lithologies and pseudosections. The resistivity pseudosection is contoured logarithmically and resistivities are in ohm-meters.

part of the line shows low resistivities (unaltered Eleana) and a narrow zone with significantly increased polarizability at about 5 E. This is believed to be the northeast extension of the fault inferred on line CH 4 at station 20 W.

Line CH 6 (fig. 18) was run across the northeastern part of Topopah Wash alluvium presumably overlying Eleana argillite is present along most of the line (25W to 80E) and Tertiary volcanics crop out on each end. Low resistivities seen in the pseudosection suggest that the subsurface consists of Eleana argillite except on the extreme southeastern end where the effect of higher resistivity, volcanic rocks appear. The central fault seen on CH 4 and 5 appears to cover a broader zone (30E to 50E) which may be due to branching of the fault. Modeling is needed to resolve some of the detail seen in the pseudosections. The zone of higher polarizability associated with the inferred central fault along Topopah Wash suggests that alteration and probably mineralization has occurred along the fault and into the surrounding rock.

Table 2 summarizes the major electrical parameters with their possible associated lithologies in the Calico Hills area. The low resistivity units (under 100 ohm-m) can with reasonable certainty be assigned to the Eleana argillite, and to narrow fault zones in the volcanics. Polarizability however for these low resistivity units can be either high or low. This suggests that local alteration and(or) mineralization has taken place that increases polarizability but not resistivity. Units of intermediate resistivity can be associated with either Eleana Formation or volcanics. The inability to distinguish these two distinct lithologies, when using electrical methods places a severe constraint on interpretation without the use of other geophysical data. The high-resistivity units can reliably be associated with volcanics at Calico Hills.

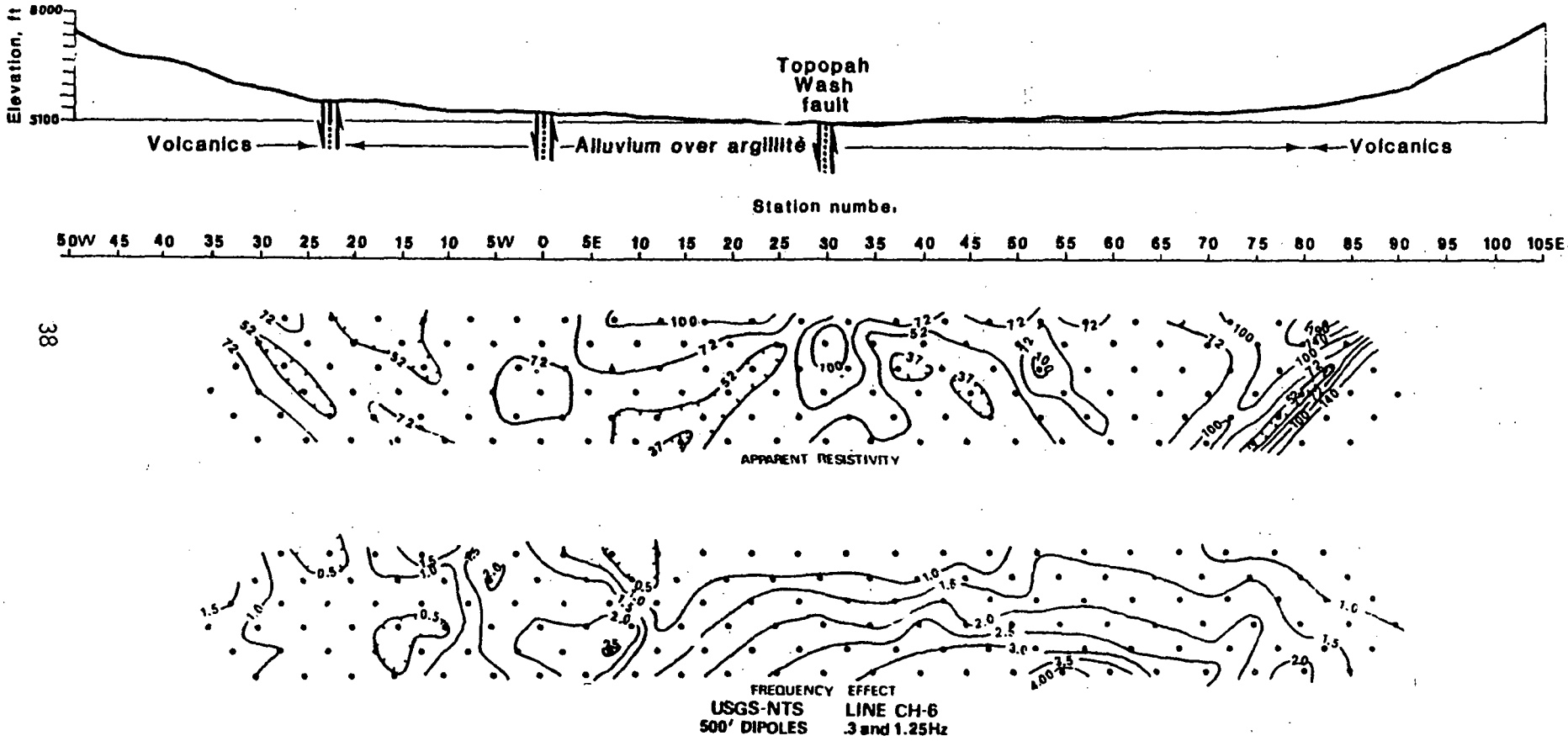

Figure 18. Induced polarization line CH 6 showing the surface lithologies and pseudosections. The resistivity pseudosection is contoured logarithmically and resistivities are in ohm-meters.

Table 2.--General geoelectric parameters and possible correlative lithologies

Polarizability less than 1.5% is considered low

and greater than 1.5% is considered high

Resistivity (ohm-m)	Polarizability	Lithology
Low (less than 100, average 50)	low	Eleana argillite
Low	high	Eleana argillite with hydrothermal? alteration
Intermediate 100-250	low	Thermally altered Eleana, argillite, or fractured, partially altered Tertiary volcanics
Intermediate	high	Fractured and altered volcanics, altered Eleana argillite
High 500 and greater	low	Volcanics relatively unfractured and unaltered Devonian limestone, or Tertiary intrusive dikes

Magnetotelluric Data

Sixty magnetotelluric (MT) soundings within the NTS area provide information on the variation in the geoelectric section within the crust and upper mantle. The frequency range used was 25 Hz to 0.003 Hz. The complete results are given in a report submitted to the USGS (Williston McNeil and Assoc. 1979). Five stations were occupied on or near the Calico Hills dome (fig. 12.); the results of the one-dimensional inversion of these data are on figure 19. Owing to known data distortions and geologic complexity the results should be considered in a semi-quantitative sense.

The results support the existence of a deep and thick, high-resistivity body beneath stations 14, 13, and 19. The modeled intrinsic resistivities are in the range of 3500-6200 ohm-m, an appropriate range for dense igneous rocks or metamorphic basement. The top of the resistive body given by the one-dimensional inversion at stations 13 and 19 is 2.7 km (9000 ft) and the bottom at 100 km. It is possible that the top of the resistivity body seen in this geoelectric model represents the buried intrusive, which was responsible for the uplift and alteration of the overlying units.

Conclusions

The inferences made from the present electrical data have not been adequately constrained by other geophysical data. The electrical data however do suggest some general conclusions.

Intrusive bodies are probably present at both sites, very shallow at Wahmonie and deep at Calico Hills. At Wahmonie the inferred intrusive shows a relatively simple geoelectric picture, although at least one fault is present with significant vertical offset. At Calico Hills the geoelectric section appears significantly more complex and probably comprises principally the Eleana Formation and various Tertiary volcanic units. The complexity is due

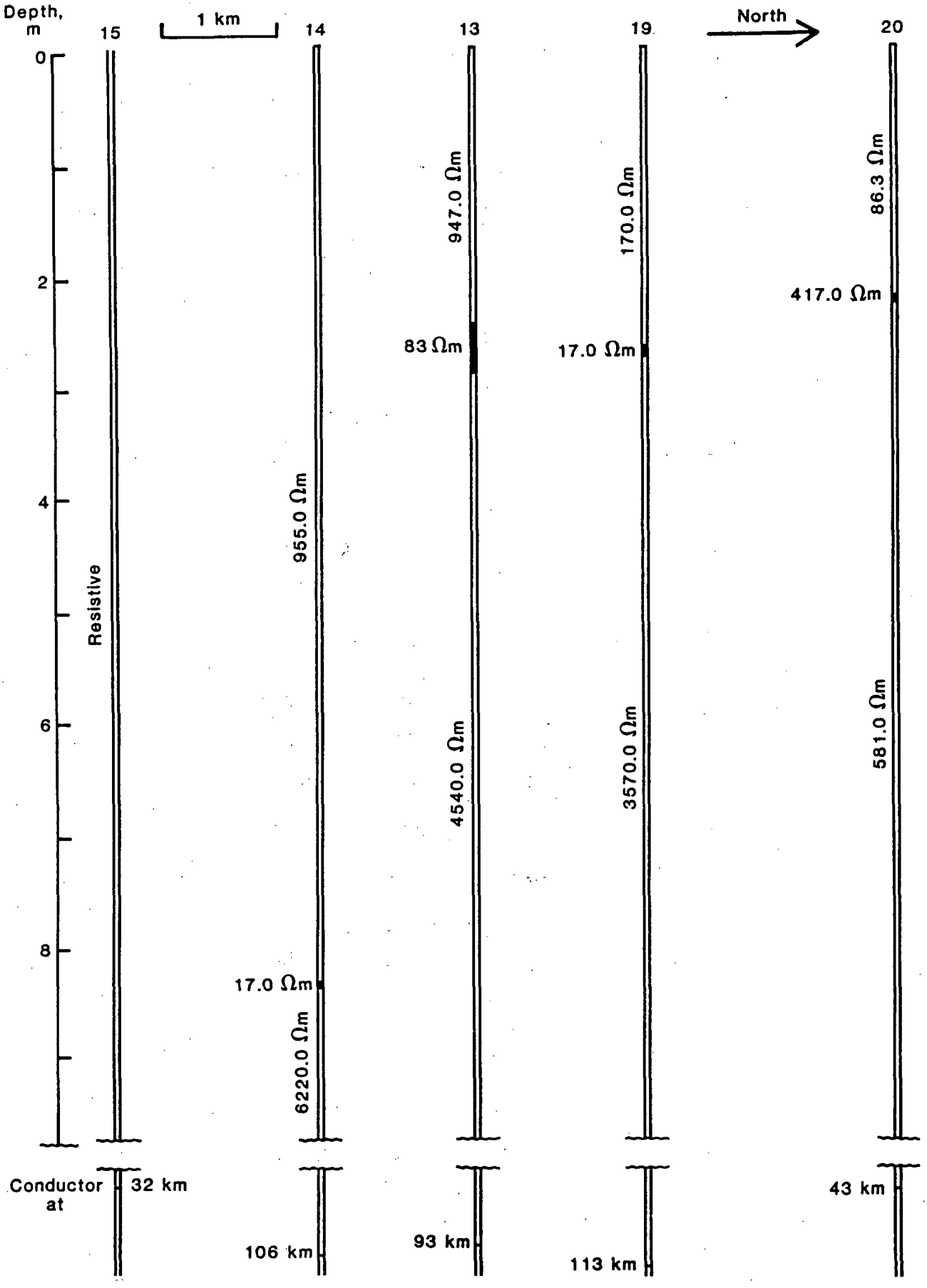

Figure 19. Geoelectric cross-section derived from one-dimensional inversion of magnetotelluric data at Calico Hills.

to structure and to metamorphism. Hydrothermal processes have significantly altered the electrical properties of various rock units. There are indications that sulfide mineralization is present at both sites. The inferred extent and grade of mineralization at the Wahmonie site is such as to make it an attractive economic exploration target. These results imply that the two sites studied have serious short comings for the emplacement of nuclear waste.

References

Ball, S. H., 1907, A geologic reconnaissance in southwestern Nevada and eastern California: U.S. Geological Survey Bull. 308, 218 p.

Cornwall, Henry R., 1977, Geology and mineral deposits of southern Nye Co. Nevada: Nev. Bur. of Mines Bull. 77, 49 p.

Daniels, Jeffrey J., and Scott, James H., 1980, Borehole geophysical measurements for hole UE25a-3, Nevada Test Site, Nuclear Waste Isolation Program: U.S. Geological Survey Open-File Report 80-126, 30 p.

Ekren, E. B., and Sargent, K. A., 1965, Geologic map of the Skull Mtn. Quadrangle Nye Co. Nevada: U.S. Geol. Survey Map GQ 387, scale 1:24,000.

Flathe, H., and Leibold, W., 1976, The smooth sounding graph, a manual for field work in direct current resistivity sounding: Federal Inst. for Geosciences and Natural Resources Hanover Germany, 59 p.

Gamble, T. D. Gouban, W. H., and Clarke, J., 1979, Error analysis for remote reference magnetotellurics: Geophysics, v. 44, no. 5, p. 959-968.

Killpack, T. J., and Hohmann, G. W., 1979, Interactive dipole-dipole resistivity and IP modeling of arbitrary two-dimensional structures (IP2D users guide and documentation): Earth Sci. Lab., Univ. of Utah Rept. ESL/UURI-15.

Maldonado, F., Muller, D. C., and Morrison, J. N., 1979, Preliminary geologic and geophysical data of the UE 25a-3 exploratory drill hole, Nevada Test Site Nevada: U.S. Geological Survey Rept. Open-File report 81-522, 47 p.

McKay, Edward, J., and Williams, W. P., 1964, Geology of the Jackass Flats quadrangle Nye Co. Nevada: U.S. Geological Survey Map GQ 368, scale 1:24,000.

McPhar Geophysics Corp., 1966, Induced polarization and drilling results from zone of disseminated mineralization Quartzite, Arizona: Case History series 23, 139 Bandque Don Mills, Ontaria, Canada, 3 p.

Nuclear Regulatory Commission, 1980, Technical Criteria for Regulating Geologic Disposal High Level Radioactive Waste 10 CFR Part 60: Federal Register vol. 45, no. 94, p. 31393-31408.

Orkild, Paul P., and O'Connor, J. T., 1970, Geologic map of the Topopah Spring quadrangle Nye. Co. Nevada: U.S. Geological Survey Map GQ 849, scale 1:24,000.

Rijo, Luiz, 1977, Modeling of electric and electromagnetic data: unpub. Ph.D. thesis Dept. of Geol. and Geoph., Univ. of Utah.

Ross, Howard P. and Lunbeck, J., 1978, Interpretation of resistivity and induced polarization profiles, Calico Hills and Yucca Mountain areas Nevada Test Site: Earth Sci. Lab., Univ. of Utah Rept. ESL/UURI-8, 17 p.

Sass, J. H., Lachenbruch, Arthur H., and Mase, C. W., 1980, Analysis of thermal data from drill holes UE25a-3 and UE25a-1, Calico Hills and Yucca Mountain, Nevada Test Site: U.S. Geological Survey Open-File Report 80-826, 25 p.

Smith, Christian, Ross, Howard P., and Edquist R., 1981, Interpreted resistivity/IP section line U1 Wahmonie area Nevada Test Site: U.S. Geological Survey Open-File Report 81-1350, 6 p.

Snyder, D. B., and Oliver, H. W., 1981, Preliminary results of gravity investigations of the Calico Hills, Nevada Site, Nye County, Nevada: U.S. Geological Survey Open-File Report 81-101, 42 p.

Sumner, John S., 1976, Principles of induced polarization for geophysical exploration: Amsterdam, Elsevier Publ., 277 p.

Vozoff, K., 1972, The magnetotelluric method in the exploration of sedimentary basins: Geophysics, vol. 37, no. 1, 43 p.

Williston, McNeil and Associates, 1979, Nevada National Test Site magnetotelluric survey: Irongate 2 Executive Plaza 777 S. Wadsworth Blvd., Lakewood, Colo., 120 p.

Winograd, Isaac and Thordarson, W., 1975, Hydrogeologic and hydrochemical framework south-central Great Basin Nevada-California, with special reference to the Nevada Test Site: U.S. Geological Survey Prof. Paper 712-C, 126 p.

Zohdy, A.A.R., and others, 1974, Application of surface geophysics to ground water investigations: U.S. Geological Survey Techniques of Water Resources Investigations, Chapter D1., 116 p.

Zohdy, A.A.R., 1974, A computer program for the automatic interpretation of Schlumberger sounding curves over horizontally layered media: National Technical Information Service PB-232 703/AS, U.S. Department of Commerce, Springfield, Va. 22161, 25 p.

_____1975, Automatic interpretation of Schlumberger sounding curves using modified Dar Zarrouk functions: U.S. Geological Survey Bull. 1313-E, 39 p.

Open-File Report 82-1043

UNITED STATES DEPARTMENT OF THE INTERIOR

GEOLOGICAL SURVEY

Resistivity sounding investigation by the Schlumberger method in the Yucca Mountain and Jackass Flats area, Nevada Test Site, Nevada

by

R. M. Senterfit[1], D. B. Hoover[1], and M. Chornack[2]

This report is preliminary and has not been edited or reviewed for conformity with U.S. Geological Survey standards.

[1]U.S. Geological Survey, Denver, CO.

[2]Fenix and Scisson, Inc., Mercury, NV.

Contents

Introduction

A Schlumberger resistivity survey was made in the west-central sector of the Nevada Test Site (fig. 1) as part of an extensive program to assess and identify potential repositories for high-level nuclear waste. The survey area is located within the Topopah Spring 15-minute quadrangle, part of which is shown in plate 1. The intent of the survey was to determine the geoelectric characteristics of the area and to relate them to the thicknesses and horizontal continuity of lithologic units in the Yucca Mountain and Jackass Flats area, and to locate faulting within the survey area. A total of 29 soundings is included in this report. The field data were interpreted in terms of rock layer resistivity and thickness by computer methods (Zohdy, 1973), and cross-sections were constructed to illustrate lateral resistivity variations within the near-surface rock.

Schlumberger vertical electrical sounding

Vertical electrical soundings (VES) were made with a four electrode configuration commonly referred to as the Schlumberger array (Keller and Frischknecht, 1966). The method uses four in-line electrodes; the inner pair for recording electrical potential as a current is passed through the outer pair. Measurements are made in a series of readings involving successively larger current electrode separations. The data are plotted on a logarithmic scale (see Appendix) to produce a sounding curve representing apparent resistivity variations as a function of half current-electrode separation (AB/2). For Schlumberger soundings, the greater the current, or outer electrode separation, the greater the depth of exploration. Sounding curves numbered YM-1 through YM-3, 24 through 27, 29 through 45, 47 through 50, and 79-3 show the results of these measurements. All the soundings used in this report are contained in the Appendix. The locations of the Schlumberger soundings are shown on plate 1. Each sounding curve has been inverted by use of a computer program to give a one-dimensional layered model (Zohdy, 1973). Interpretation of the sounding data assumes homogeneous, horizontal layering, therefore, where lateral heterogeneities in resistivity exist within the influence of the energizing current field, the sounding may exhibit distortions which, when present, the computer will model as horizontal layering. Data distortion resulting from lateral variations in rock resistivity are not always recognizable from the shape of the field curve.

Vertical geoelectrical sections

Three geoelectric cross sections were prepared from the computer derived one-dimensional layered models to illustrate resistivity variations within the sectors of the study area. The locations of the cross sections are shown on plate 1. The sections were compiled with a vertical exaggeration of 14.5 and contoured with seven logarithmically scaled intervals per decade. Each cross section includes at least one litholgoic log on-line with the Schlumberger soundings in that cross-section to provide comparison of geoelectric and lithologic data.

Resistivity cross section A-A′ is shown on figure 2. This cross section is constructed in a northwest-southeast direction across the northern part of Jackass Flats. Lithologic data from drillholes J-11 and J-13 are included. Resistivity values show a general decrease with depth, beginning at about 250

meters, which indicates that more conductive rocks are being sensed at increasing depths. Between VES 24 and 25, an abrupt change in depth to the conductive zone is shown. The Mine Mountain fault, mapped by Ekren and Sargent (1965) as a left-lateral strike-slip fault, striking northeast and down-dropped to the southeast, is mapped approximately 6 kilometers to the northeast of VES 25 and 24 (Orkild, 1968) and is inferred to pass between those two stations (D. L. Hoover, USGS, oral commun., 1981). From depths of about 150 meters and continuing downward through the section between VES 25 and 27, the resistivity contours have an apparent dip to the northwest. At VES 24, the apparent dip of the resistivity contours is more gradual to the southeast. These changes in apparent dip of the resistivity contours from VES 25 to the northwest and from VES 25 to the southeast support geologic evidence placing the Mine Mountain fault between VES 25 and 24 (Ekren and Sargent, 1965). At VES 25, beginning at a depth of about 150 meters, the resistivity contours show a gradient decreasing in value with depth, indicating the sensing of a more conductive zone. At VES 24, a similar gradient is seen beginning at a depth of about 280 meters, which supports evidence that the Mine Mountain fault is down-dropped to the southeast (Ekren and Sargent, 1965).

The two areas of low resistivity seen on cross section A-A′ at depth intervals of 50 to 150 meters are probably caused by an increase in amounts of clay and other fine-grained material within alluvial fill (see lithologic data for drillholes J-11 and J-13, cross section A-A′). The area of high resistivity seen at a depth interval of 100 to 160 meters beneath VES 26 may be due to the presence of local basalts which occur throughout this area (McKay and Williams, 1964). The water table, at a depth of about 300 meters, does not appear to have been detected by the soundings in this area.

Cross section B-B′ (fig. 3) runs from the top of Yucca Wash to Fortymile Wash. Lithologic information from drillhole J-13 is included. Geologic mapping of this area (Lipman and McKay, 1965; Christiansen and Lipman, 1965) indicates a thick section of volcanics dipping gently to the east. The geoelectrical data shows a general decrease in resistivity beginning at a depth of about 300 meters and continuing downward through the section, which indicates the presence of a more conductive layer within the tuffs. Several areas of high or low resistivity are seen along cross section B-B′ from the surface to a depth of about 200 meters, indicating significant lateral variations in rock resistivity within this depth range. These lateral changes are attributed to differences in fracturing, faulting, and lithology of the tuffs throughout the area, and to varying amounts of clay and other fine-grained materials in the alluvium.

Cross section C-C′ (fig. 4) runs from the northeast end of Drillhole Wash to the north-south road along Fortymile Wash. Lithologic data from drillhole Ue 25a-1 is included with the cross section. The deeper ranges sensed show a decrease in resistivity with depth, indicating the presence of more conductive rock in the lower part of the section. The variations in resistivity within the upper 100 meters of the section are associated with volcanic rocks, principally the Tiva formation mapped by Lipman and McKay as outcropping throughout the area. The area of high resistivity seen from VES 39 to VES 37, at a depth interval of 100 meters to about 450 meters, is probably a reflection of the Topopah Spring member of the Paintbrush Tuff (Spengler and others, 1979). In the vicinity of VES 37 and 36, sharp changes in resistivity

values are shown in the depth interval of 80 to about 350 meters. These changes could be a reflection of vertical displacement caused by faults crossing the line of the cross section.

Conclusions

The interpreted results of some of the 29 Schlumberger resistivity soundings, as shown in the cross sections of figures 2, 3, and 4, indicate some lateral discontinuities which appear to be caused by vertical displacement due to faulting. Because the lithologic section in this survey area is composed primarily of ash-flow tuffs beneath alluvium (Lipman and McKay, 1965), many of the lateral resistivity variations are probably caused by differences in amounts of clay and other fine-grained materials within the alluvium, variations of lithology within the volcanic rocks, and the effects of fracturing within the rock types.

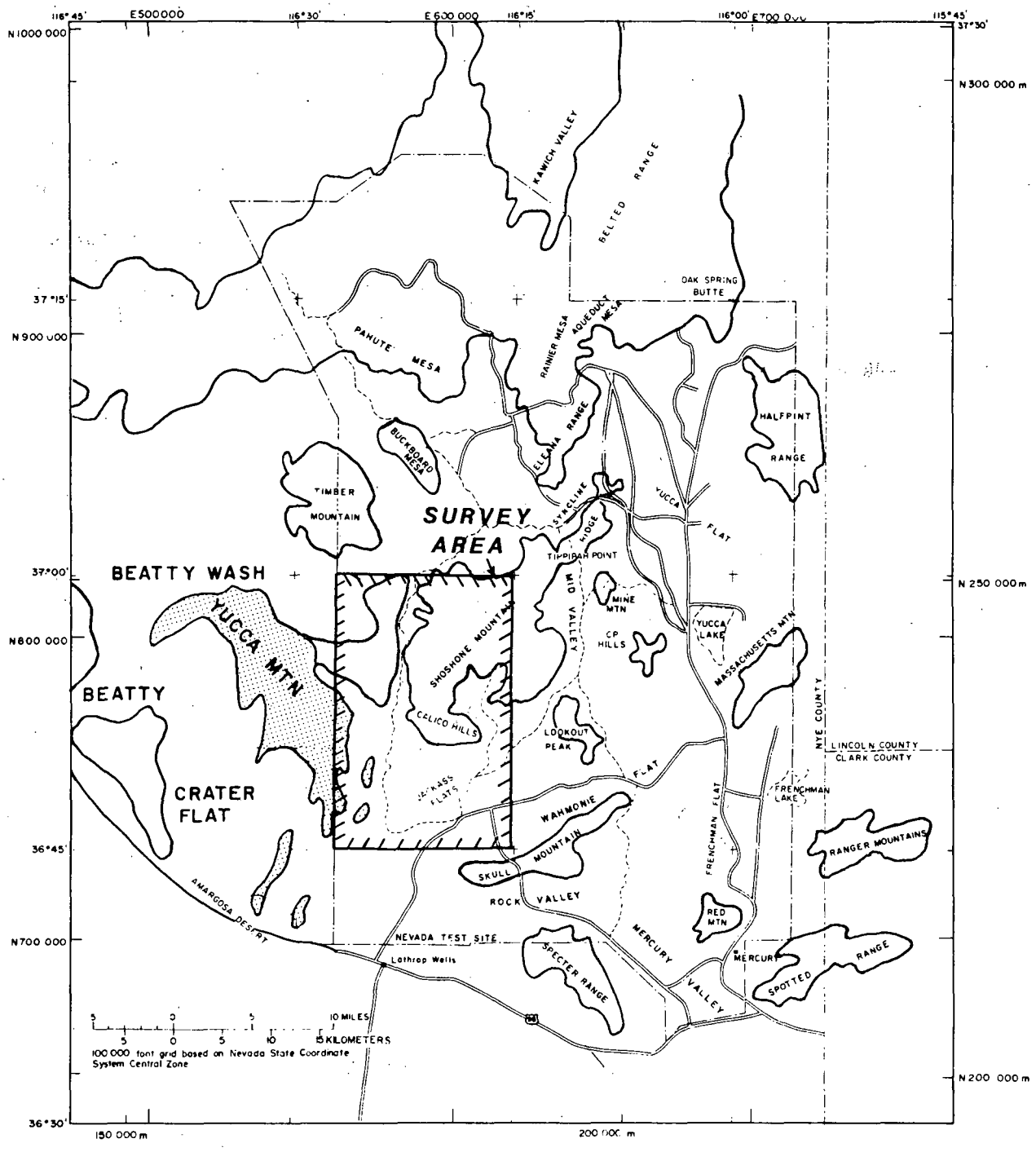

Figure 1. Index map of the Nevada Test Site and vicinity showing the location of the Topopah Spring quadrangle.

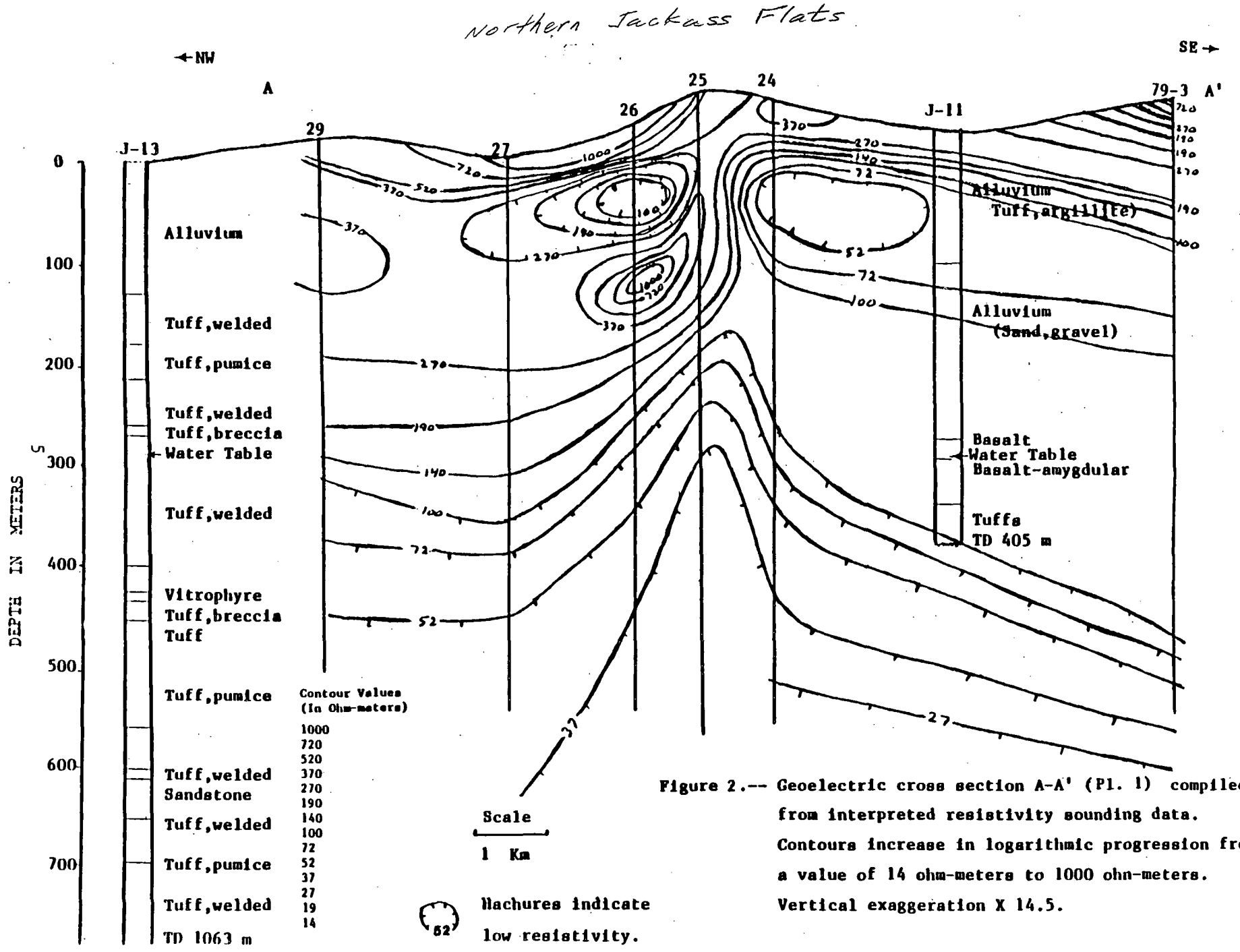

Figure 2.-- Geoelectric cross section A-A' (Pl. 1) compiled from interpreted resistivity sounding data. Contours increase in logarithmic progression from a value of 14 ohm-meters to 1000 ohm-meters. Vertical exaggeration X 14.5.

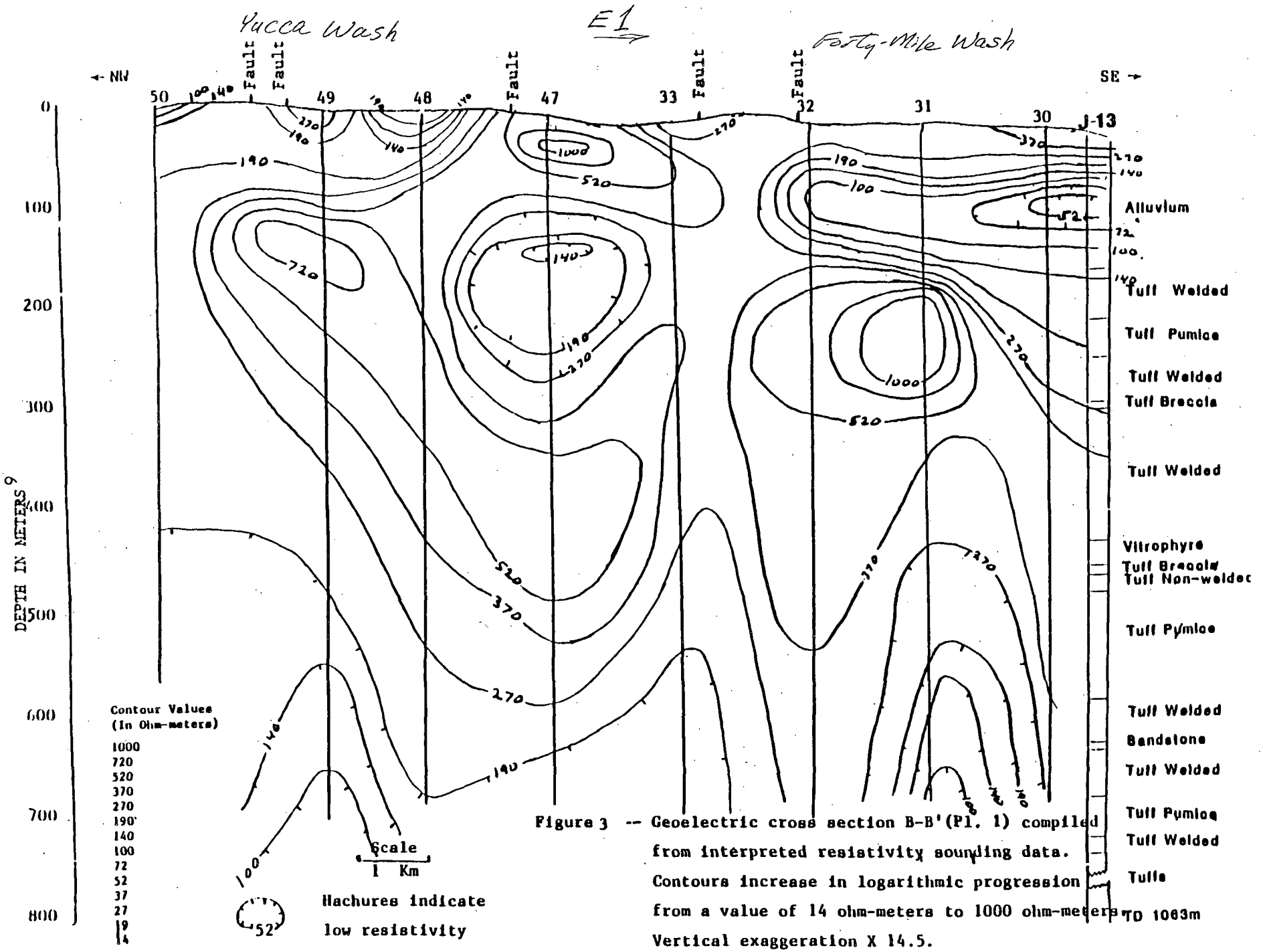

Figure 3 -- Geoelectric cross section B-B'(Pl. 1) compiled from interpreted resistivity sounding data. Contours increase in logarithmic progression from a value of 14 ohm-meters to 1000 ohm-meters. Vertical exaggeration X 14.5.

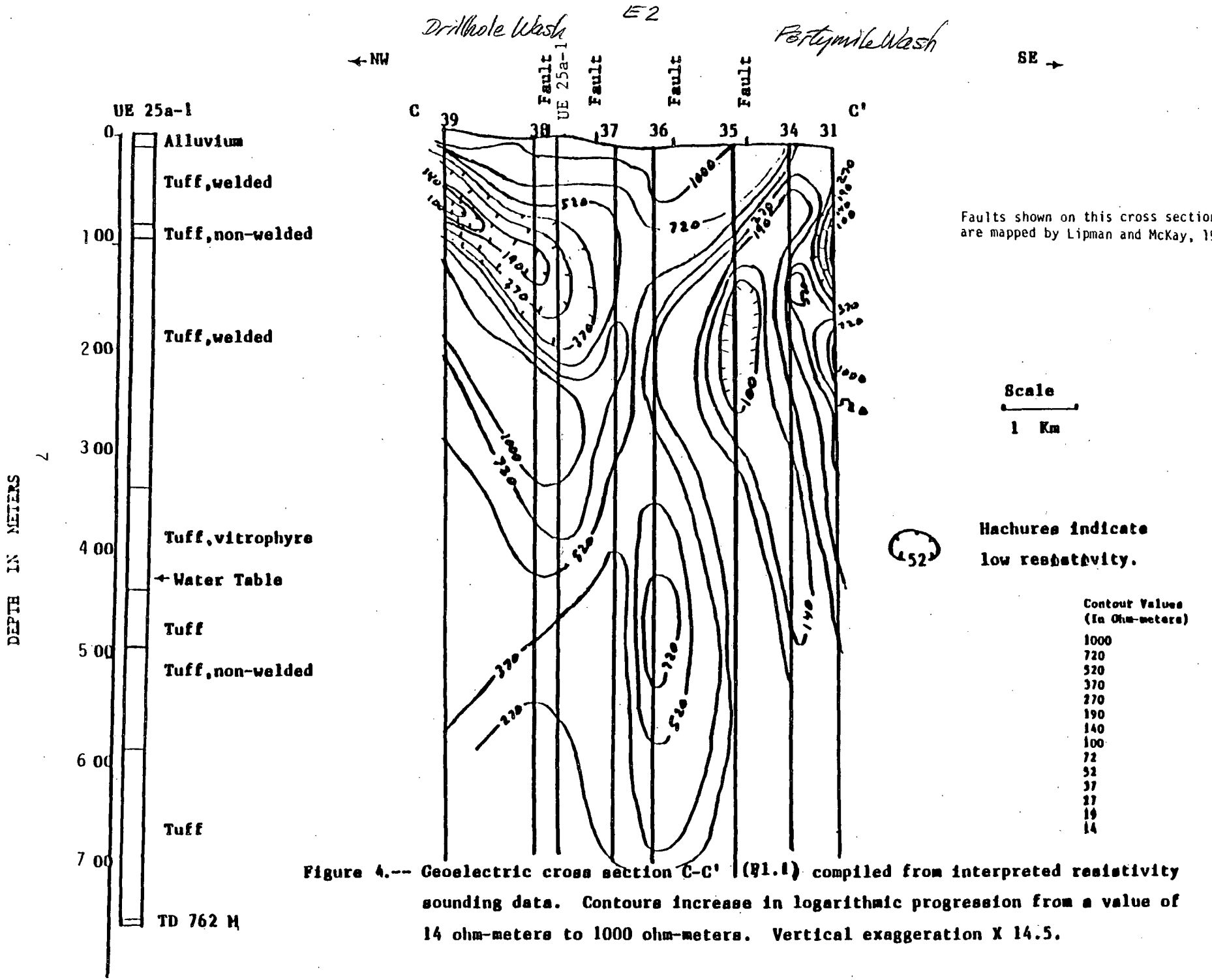

Figure 4.-- Geoelectric cross section C-C' (Fig.1) compiled from interpreted resistivity sounding data. Contours increase in logarithmic progression from a value of 14 ohm-meters to 1000 ohm-meters. Vertical exaggeration X 14.5.

References

Anderson, W. L., 1971, Application of bicubic spline functions to two dimensional gridded data: NTIS (National Technical Information Service), PB-203 579, available only from NTIS, Springfield, Va., 22161.

Christiansen, R. L., and Lipman, P. W., 1965, Geologic map of the Topopah Spring NW quadrangle, Nye County, Nevada: U.S. Geological Survey GQ-444, 1 p.

Classen, H. C., 1973, Water quality and physical characteristics of Nevada Test Site water-supply wells: U.S. Geological Survey NTS Report 474-158.

Ekren, E. B., and Sargent, K. A., 1965, Geologic map of the Skull Mountain Quadrangle, Nye County, Nevada: U.S. Geological Survey GQ-389, 1 p.

Keller, G. V., and Frischknecht, F. C., 1966, Electrical methods in geophysical prospecting: Pergamon Press, London, New York Toronto, 517 p.

Lipman, P. W., and McKay, E. J., 1965, Geologic map of the Topopah Spring SW Quadrangle, Nye County, Nevada: U.S. Geological Survey GQ-439, 1 p.

McKay, E. J., and Williams, W. P., 1964, Geologic map of the Jackass Flats Quadrangle, Nye County, Nevada, U.S. Geological Survey GQ-368, 1 p.

Orkild, P. P., 1968, Geologic map of the Mine Mountain Quadrangle, Nye County, Nevada, U.S. Geological Survey GQ-746, 1 p.

Spengler, R. W., and Rosenbaum, J. G., 1980, Preliminary interpretatons of geologic results obtained from boreholes UE 25a-4, -5, -6 and -7, Yucca Mountain, Nevada Test Site: U.S. Geological Survey Open-File Report 80-929, 33 p.

Spengler, R. W., Muller, D. C., Livermore, R. B., 1979, Preliminary report on the geology and geophysics of drillhole UE 25a-1, Yucca Mountain, Nevada Test Site: U.S. Geological Survey Open-File Report 79-1244, 43 p.

Young, R. A., 1972, Water supply for the Nuclear Rocket Development Station at the U.S. Atomic Energy Commission's Nevada Test Site, Nevada: U.S. Geological Survey Water-Supply Paper 1938 19 p.

Zohdy, A. A. R., 1973, A computer program for the automatic interpretation of Schlumberger sounding curves over horizontally layered media: NTIS (National Technical Information Service), PB-232 703/AS, 25 p., available from NTIS, Springfield, Va., 22161.

Seis, Grav, Mag, ER

Open-File Report 82-145

UNITED STATES DEPARTMENT OF THE INTERIOR

GEOLOGICAL SURVEY

40Km NE of Yucca Mtn.

Geophysical studies of the Syncline Ridge area Nevada Test Site, Nye County, Nevada

by

D. B. Hoover, W. F. Hanna, L. A. Anderson,

V. J. Flanigan and L. W. Pankratz

Open-File Report 82-145

1982

Prepared by the U.S. Geological Survey

for the

Nevada Operations Office
U.S. Department of Energy
(Interagency Agreement DE-A108-78ET44802)

Contents

List of Figures

13.--Map of the study area showing the location of Schlumberger soundings, the generalized geology and line of geoelectric sections, from Anderson and others (1980).

14.--Geoelectric cross-section A-A′ from Anderson and others (1980).

15.--Geoelectric cross-section B-B′ from Anderson and others (1980).

16.--Geoelectric cross-section C-C′ from Anderson and others (1980).

17.--Location map showing slingram traverses run over alluvium on the eastern side of Syncline Ridge.

18.--Contour map in the southern block of Syncline Ridge showing slingram real and imaginary response at 444 Hz from Flanigan (1979).

19.--Contour map in the central block of Syncline Ridge showing slingram real response at 1777 Hz from Flanigan (1979).

20.--Magnetotelluric geoelectric section at Syncline Ridge.

21.--Contour map of the relative electric field at 20-40 sec periods in the Syncline Ridge study area.

List of Tables

Abstract

A wide variety of geophysical methods were employed to study a proposed nuclear waste site at Syncline Ridge on the Nevada Test Site, Nev. The proposed site was believed to be a relatively undisturbed synclinal structure containing a thick argillite unit of Mississippian age, the Eleana Formation unit J, which would be the emplacement medium. Data acquisition for the geophysical studies was constrained because of rugged topography in a block of Tippipah Limestone overlying the central part of the proposed site.

This study employed gravity, magnetic, seismic refraction and reflection, and four distinct electrical methods to try and define the structural integrity and shape of the proposed repository medium. Detailed and regional gravity work revealed complex structure at the site. Magnetics helped only in identifying small areas of Tertiary volcanic rocks because of low magnetization of the rocks. Seismic refraction assisted in identifying near surface faulting and bedrock structure. Difficulty was experienced in obtaining good quality reflection data. This implied significant structural complexity but also revealed the principal features that were supported by other data. Electrical methods were used for fault identification and for mapping of a thick argillaceous unit of the Eleana Formation in which nuclear waste was to be emplaced.

The geophysical studies indicate that major faults along the axis of Syncline Ridge and on both margins have large vertical offsets displacing units so as not only to make mining difficult, but also providing potential paths for waste migration to underlying carbonate aquifers. The Eleana Formation appeared heterogeneous, which was inferred to be due to structual complexity. Only a small region in the northwest part of the study area was found to contain a thick and relatively undisturbed volume of host rock.

Deep electrical soundings identified a very conductive region in the crust below Syncline Ridge at depths shallower than 10 km. Similar conductive regions have been observed associated with geothermal systems in the western United States and imply the potential for a blind geothermal system below Syncline Ridge.

The geophysical studies provided negative evidence for the suitability of the site for a nuclear waste repository. This evidence was a significant factor in the decision on April 20, 1978 to discontinue most work in the Syncline Ridge area and actively pursue exploration of alternate sites on NTS.

Introduction

In late November of 1977 surface geophysical work was started within the Syncline Ridge area of the Nevada Test Site (NTS, fig. 1) as one phase of investigations of a potential repository for nuclear waste. The targeted host medium for the repository was a thick unit of Mississippian argillite belonging to the Eleana Formation of Devonian and Mississippian age. Previous geological work and 14 drill holes in the site area had defined a relatively simple synclinal structure in the Eleana Formation. Objectives of the geophysical activity were to help determine the structural integrity and the available mass of the argillite.

The geophysical work described in this paper revealed significant structural complexity in the site area. This structural complexity was an important factor in a decision on April 20, 1978, to discontinue most efforts at Syncline Ridge and to pursue more favorable appearing sites. This report summarizes the surface geophysical work which was done at the site.

Geography and Geology

Syncline Ridge is located on the western edge of Yucca Flat, one of the Basin and Range valleys situated in the northeastern part of NTS about 97 km (60 miles) northwest of Las Vegas, Nev. (fig. 1). Syncline Ridge is a north-northeast trending topographic high extending from the northeast flank of Shoshone Mountain. The ridge is quite rugged with about 365 m (1200 ft) of topographic relief in the area of investigation. To the east of the ridge is Yucca Flat and to the west, separated by a narrow valley, is the Eleana Range. The rugged topography of the ridge proper limited the acquisition of extensive geophysical data to the surrounding pediment slopes and valleys.

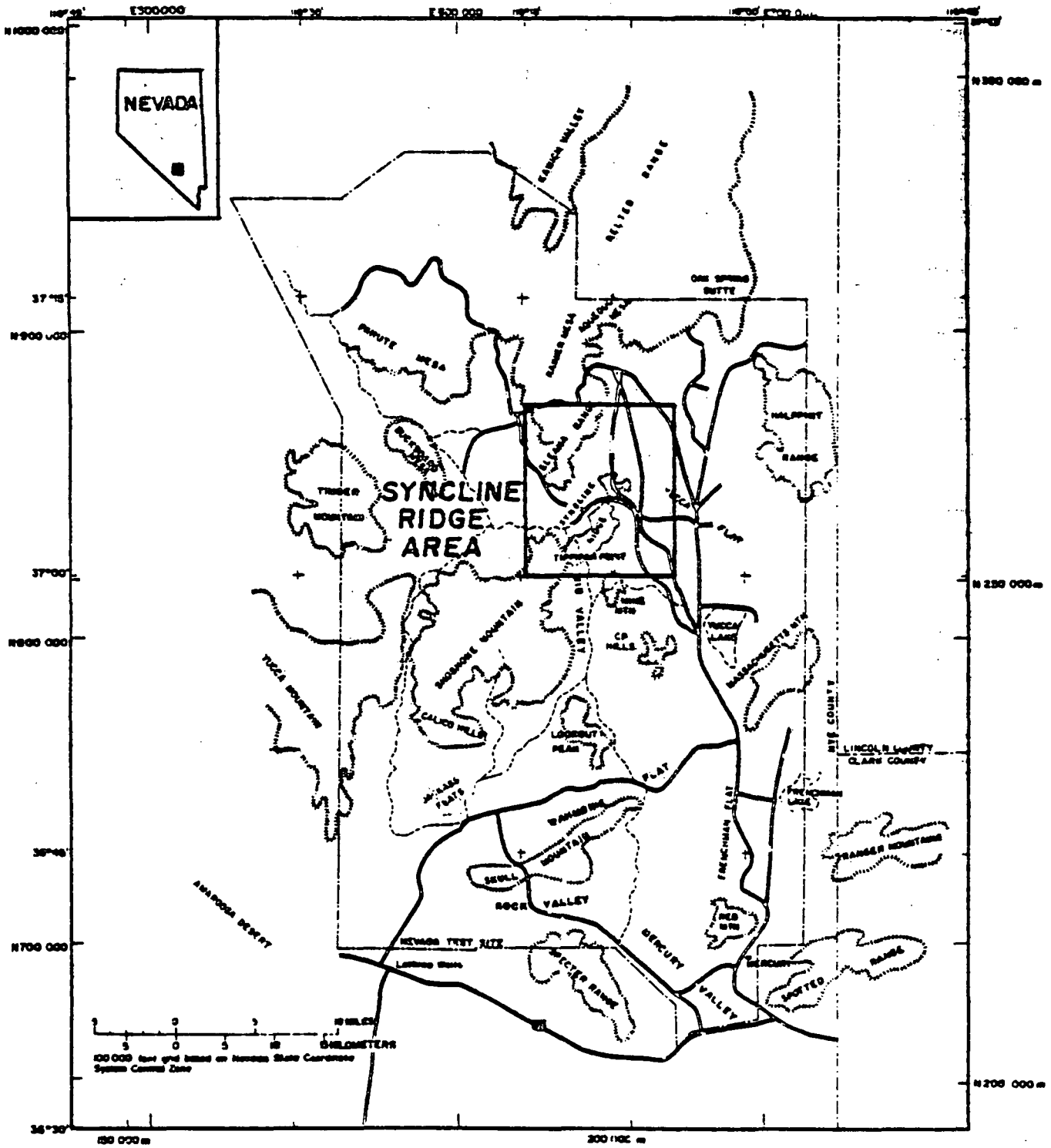

Fig. 1.--Index map showing the location of the Nevada Test Site and the Syncline Ridge area.

The geology of Syncline Ridge has been well described by Hoover and Morrison (1980) and will only be briefly summarized here. A summary geologic map from Hoover and Morrison (1980) is shown in figure 2. Structurally the Ridge is a northeast-plunging syncline with an axial fault mapped just southeast of the ridge crest. This axial fault where exposed is tight, narrow, and shows only minor displacement. The ridge is divided into a southern, central and northern block by two southeast-trending Mesozoic lateral faults (fig. 2). One originates in Gap Wash in the Eleana Range dividing the main part of Syncline Ridge in half. The other originates in the Eleana Range south of Pediment Wash cutting the ridge near the junction of Canyon and Gap Washes. The central block was of principal concern in this investigation because it was believed to contain the largest volume of relatively undisturbed argillite.

The principal lithologies in the study area are the Tippipah Limestone and the Eleana Formation. The Tippipah makes up the bulk of the ridge proper. Its outcrop pattern will be used as a reference in some of the following discussion.

In figure 2 the Tippipah is mapped as lying conformably on the Eleana Formation although drill hole and stratigraphic evidence suggests that the Tippipah may be in thrust contact in this area (Hoover and Morrison, 1980). The majority of the Tippipah exposed in the area consists of relatively pure light-grey to medium-grey limestone. Unit J of the Eleana Formation crops out or is present beneath shallow alluvium surrounding the ridge and is the potential repository medium. Unit J has a stratigraphic thickness of about 110m. It is divided into three subunits, a lower of 300 m thickness consisting of black siliceous argillite and siltstone; an argillite subunit 700 m thick 98% made up of argillite and an upper quartzite subunit 100 m

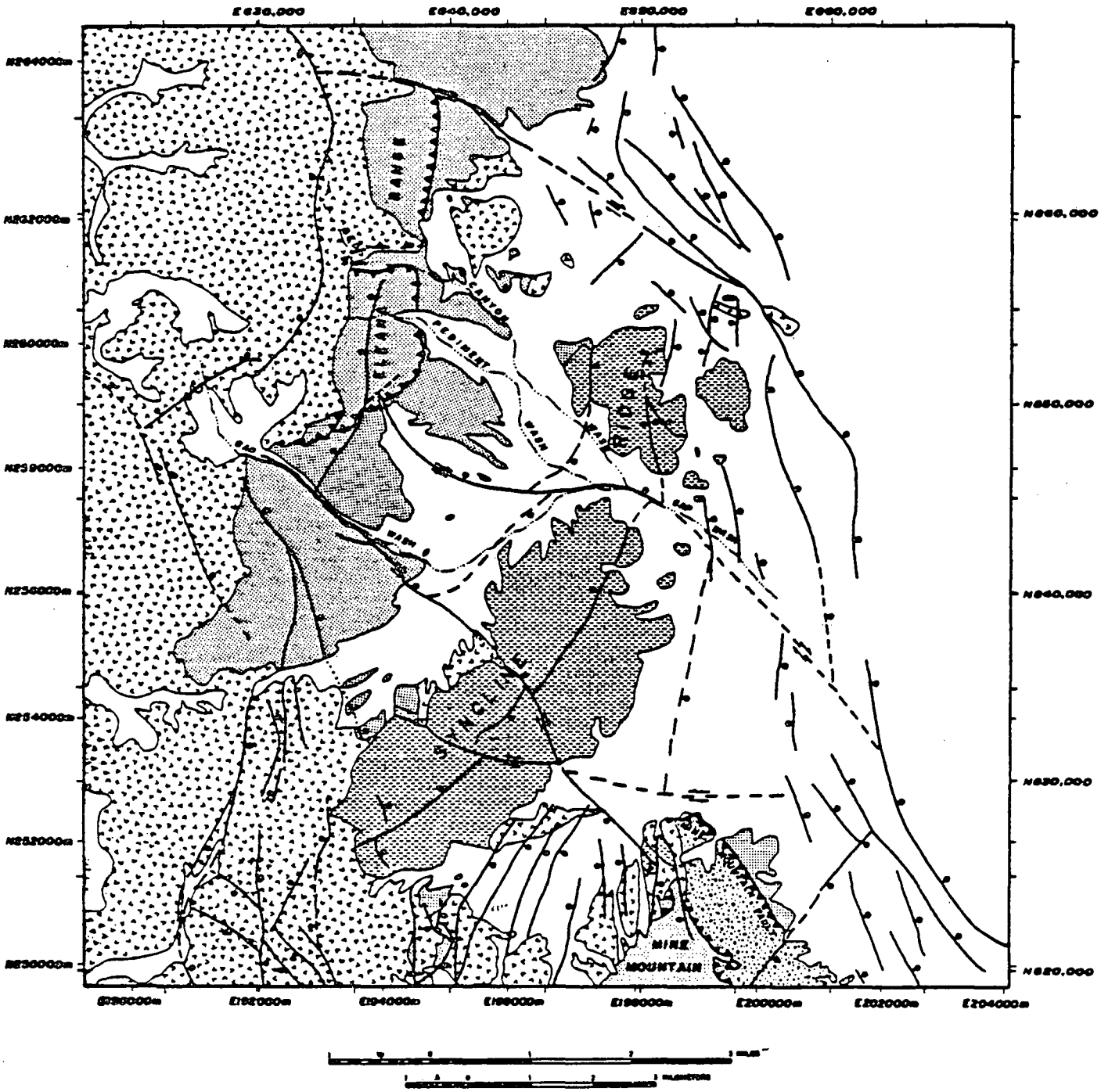

Figure 2.--Geologic map of the Syncline Ridge Area showing principal stratigraphic units and major structures, from Hoover and Morrison (1980).

thick consisting of about 30% argillite. The underlying unit I of the Eleana Formation is at least 2000 m below the surface in the central part of the area (Hoover and Morrison 1980). Limited exposures of Tertiary volcanics crop out adjacent to the Tippipah in the southern block. Tertiary and Quaternary alluvial deposits overlie the Eleana surrounding the ridge and are generally less than 50 m thick. One drill hole near the confluence of Pediment and Gap Washes encountered 122 m of alluvium. Prior gravity work has identified a small graben between the southern block and Mine Mountain where the alluvium may reach 300 m in thickness (Orkild, 1963).

Geophysical Investigations

A wide variety of geophysical investigations were made in an attempt to define the size and shape of the argillite subunit of unit J and to address the question of structural integrity of the Eleana. The presence of faulting was a major concern because it could provide paths for the escape of radio nuclides and disrupt the continuity of the repository. Some of the studies were designed to address principally the question of faulting. Shallow electrical investigations also were conducted on the east side of the ridge looking for evidence of Quaternary faulting which might have disturbed the alluvium.

This report will summarize the results of the various investigations discussing each method separately before integrating the results. Primary responsibility for the gravity and magnetic studies belongs to W. F. Hanna, for the seismic work, L. W. Pankratz, the slingram work V. J. Flanigan, the Schlumberger soundings (VES) L. A. Anderson, while the remaining work and general coordination fell to D. B. Hoover.

Previous Work

D. L. Healey (1978) had made a thorough regional gravity survey which was available and identified the principal faults bounding the site and information on alluvium thickness particularly on the eastern side of the site. Fourteen drill holes up to 1414 m deep in the central and northern block also provided important lithologic and physical property information for control of the surface geophysical studies (Hoover and Morrison, 1980; Hodson and Hoover, 1979). An unpublished report (Word and others, 1977) on a magnetotelluric survey in northern Yucca Flat for Lawrence Livermore Laboratories was generously made available by Dr. P. Kassameyer. Based on one-dimensional modeling the survey showed a conductive geoelectric section with resistivities decreasing with increasing depth to values of 2 to 10 ohm-meters at 10 km. Three cross-sections each showed that the conductive material became much shallower than 10 km on the west end of Yucca Flat. The most anomalous station was closest to Syncline Ridge 3 km due east of the northern block which showed resistivities less than 1 ohm-meter below a depth of 3 km.

In addition to the above, an 8.5 mile vibroseis reflection survey run in 1972 as part of the Yacht Prospect was available (Mossman and Garrette 1972). Two lines were run, one normal to the structure and through Gap Wash between the northern and central block and a second parallel to the structure on the east flank of the central block. The purpose of the survey was to define the geologic structure of the Eleana Formation to 1800 m depth (6000 ft). The results of the survey were ambiguous due to discontinuous reflection events. However the unpublished report concludes that the structure east of the ridge is more complex than to the west, that major faulting may exist just east of the synclinal axis with additional faulting or severe folding east of this.

Acknowledgments

Much of the work was done with the assistance of the geologists of Fenix and Scisson, Inc. whose assistance is gratefully acknowledged. The large amount of work that was done in a short time would not have been possible without the active support of many people of the USGS whose extensive knowledge of NTS made our job considerably easier. In particular thanks go to D. C. Mueller, G. D. Bath, R. D. Carroll and D. L. Healey for making their knowledge of previous geophysical studies available, and to Dave Hoover, the principal investigator for geologic studies, who contributed much to developing our models.

Geophysical Studies

Gravity and Magnetics

The important question of the subsurface distribution of unit J argillite of the Eleana Formation can best be analyzed by first establishing the regional geologic and geophysical framework upon which more detailed surveys can later be built. Two basic regional geophysical surveys have been made, one delineating Bouguer gravity anomalies and the other aeromagnetic anomalies. These surveys have as their chief function the identification of the principal subsurface contrasts of rock density or magnetization which may mark important structural features or changes in lithology.

Gravity Data

Gravity data in the study area, shown in figure 3, are derived from two independent surveys: a regional survey of D. L. Healey (1978) and a local survey by W. F. Hanna and H. E. Kaufmann in the central block. Most of the stations in both surveys were measured using LaCoste-Romberg meter G-177. All of the data have been corrected for combined tidal attraction and referenced to station Wa-128 at the Las Vegas, Nev., airport (Wollard and Rose, 1963). Bouguer gravity values were computed using a reduction density of 2.67 g/cm^3 and include terrain correction to a radius of 166.7 km.

The principal source of error in the gravity contour map is in the determination of station elevations. Although elevations on the margin of the area were obtained by precise leveling surveys (Healey, 1978) those in the central part of the trapezoidal shaped area (figure 3) were determined by interpolation between contour lines on the USGS Tippipah Spring, Nev., 7 1/2 minute topographic map. Because of this, interpolated elevation accuracy is estimated to be 3 m (10 ft), giving an uncertainty in Bouguer gravity of about 0.6 mgal.

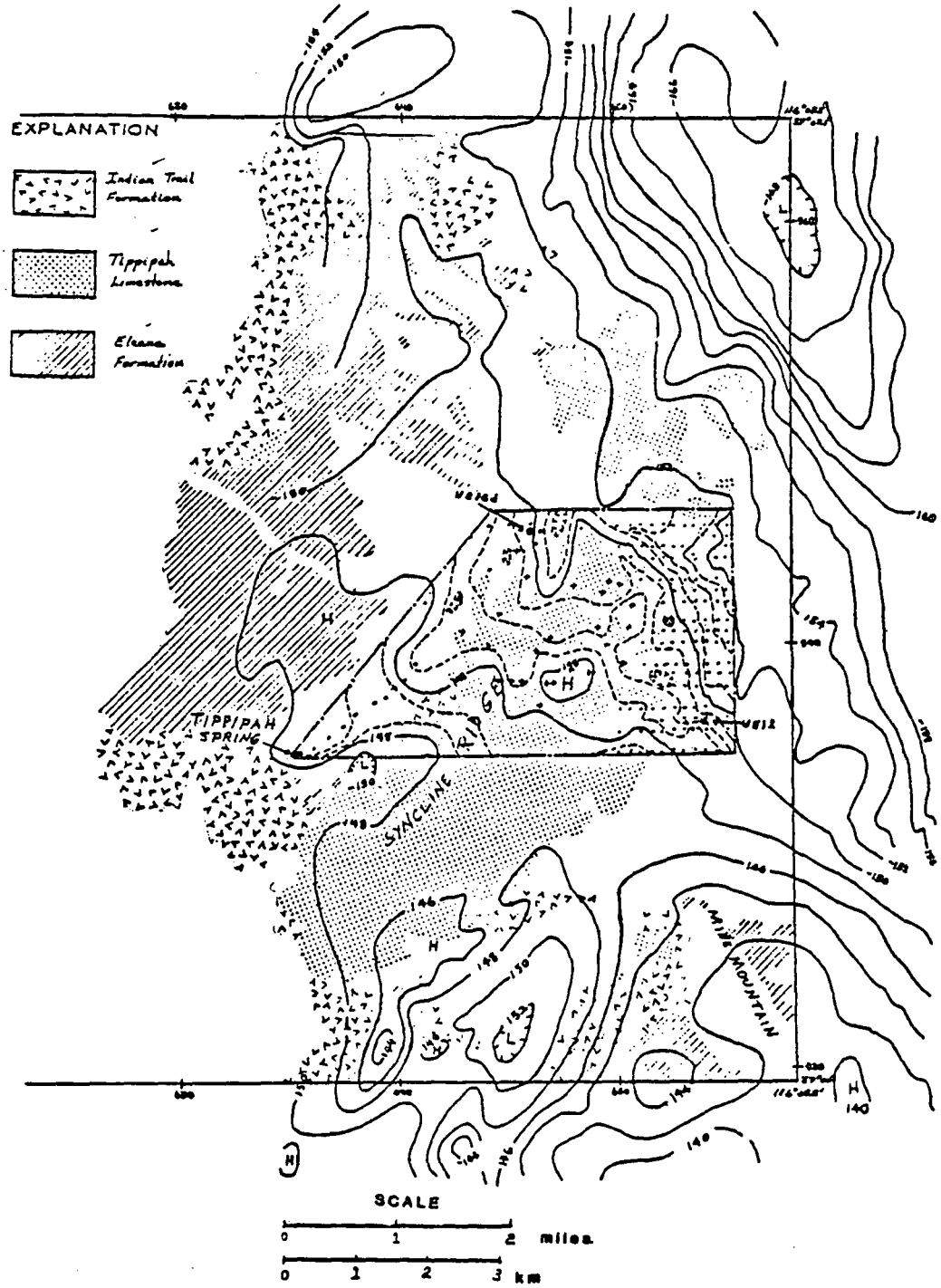

Figure 3.--Bouguer gravity anomaly maps, showing geologically mapped Eleana Formation, Tippipah Limestone, and Indian Trail Formation (Orkild, 1963) and boreholes UE16d and UE11 from which rock density data were obtained. Contour interval: 1/2 and 2 mgal. Cross: Station of W. F. Hanna and H. E. Kaufmann; Dot: Station of D. L. Healey (1978). Reduction denisty: 2.67 gm/cm^3. Terrain corrections made to a station radius of 166.7 km "H" indicates a relative high; hachures denote relative lows. Trapezoidal boundary delineates study area.

The principal source of rock density information are gamma-gamma logs from boreholes UE16d and UE11 (fig. 3) in the central block. These logs provide density information to depths of 808 m and 1606 m respectively in each hole. These logs show that there is no significant density contrast between subunits of the Eleana or between the Eleana and the Tippipah Limestone. The only appreciable density contrast occurs between Quaternary alluvium and the underlying Paleozoic rocks. Table 1 lists results from the gamma-gamma logs run in the boreholes.

Table 1.--Rock density data from gamma-gamma well logs. Depth intervals and rock units Hoover and Morrison (1980).

Depth Interval m below ground	Rock Unit	Rock Density, g/cm^3 N	Mean	Standard Deviation
Borehole UE16d				
0 - 27	Qal		Not determined	
27 - 539	PPt	148	2.50	±0.09
539 - 782	Mejuq	65	2.45	±0.23
782 - 911	Mejua	47	2.53	±0.06
Borehole UE1ℓ				
0 - 61	Qal	3	1.98	±0.04
61 - 302	Mejuq		Not determined	
302 - 396	Mejua		Not determined	
396 - 606	Mejuq	48	2.48	±0.05
606 - 1,414	Mejua	119	2.42	±0.30
1,414 - 1,615	Mejl	11	2.42	±0.07

Qal: Quaternary alluvium

PPt: Tippipah Limestone

Mejuq: Eleana Formation, unit J: upper quartzitic subunit

Mejua: Eleana Formation, unit J: argillite subunit

Mejl: Eleana Formation, unit J: lower quartzitic subunit

The Bouguer gravity anomalies within the trapezoidal study area have three principal characteristics: (1) the regional gravity contours have a distinctly northwest trend, nearly perpendicular to the mapped structure at Syncline Ridge, (2) the regional gradient is gentle compared to gradients outside of the area, and (3) superposed on the regional gradient are low amplitude anomalies having north to northeast trends, oblique to the regional trend and subparallel to the mapped structure. Anomaly values range from about -152 mgal near the northeast corner of the area to about -148 mgal near the southwest corner, the low amplitude anomalies having magnitudes of about 1 mgal. Because this amplitude is close to the estimated data error, individual anomalies probably do not accurately reflect the subsurface structure. The general trends however are believed to be significant. The predominant regional gradient represents the common flank of a high amplitude negative anomaly centered about 5 km northeast of the central block and a lower amplitude positive anomaly in the southwest part of the area. The superposed low amplitude anomalies have been isolated by constructing a residual anomaly map based upon an assumed regional background field. The residual anomaly map of figure 4, based upon a visually estimated regional field, highlights the northerly trends of the anomalies and more accurately indicates the location of the main positive anomaly contour closure, about 1.5 km northeast of the corresponding closure on figure 3.

The northeast trend of the regional gradient reflects a broad northeast to southwest lateral increase to subsurface rock density not related to the mapped structure of Syncline Ridge but related to a deeper regional density contrast. In the northeast part of the trapezoidal area (figure 3), this gradient appears as the continuation of the flank of a major gravity low (Healey, 1978) centered over Quaternary alluvium of Yucca Flat about 5 km to

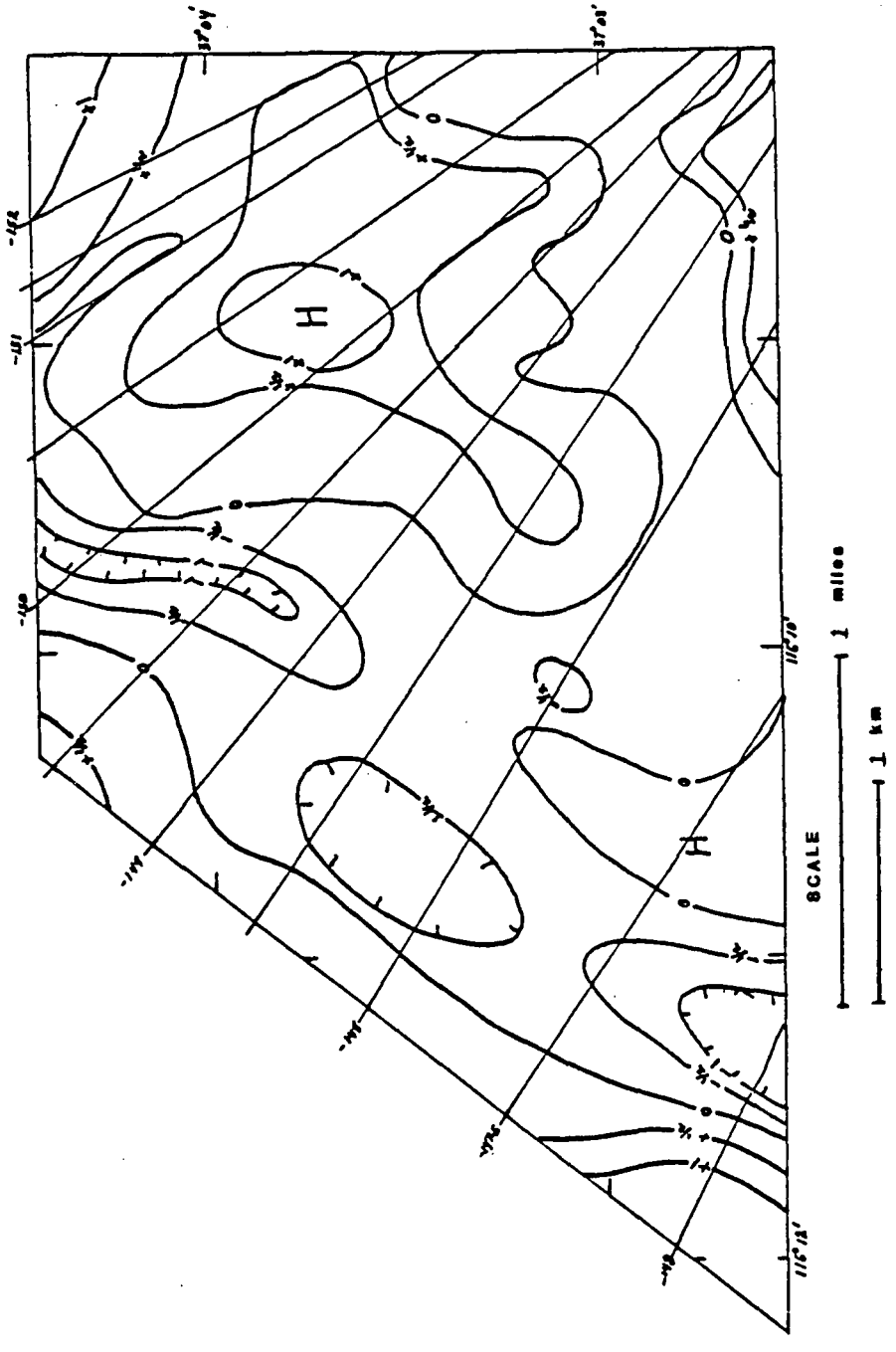

Figure 4.--Residual Bouguer gravity anomaly map of the study area showing the visually estimated regional field. H indicates relative high; hachures denote relative lows.

the north-northwest. In the southwest part of the area, the gradient forms part of a positive anomaly which extends from Mine Mountain northwestward to a broad tract of mapped Eleana Formation 2 km north of Tippipah Spring (Healey, 1968, 1978). It may be noted that a major lobe of the positive anomaly is developed over much of the southeastern part of Syncline Ridge just south of the trapezoidal study area. This positive anomaly lobe points to a sharp contrast of the rock density between the terranes underlying the northeast and southwest parts of Syncline Ridge.

The gentleness of the regional gradient is not surprising in light of the gamma-gamma log information, which indicates that there is no significant density contrast at depth between members of the Eleana Formation or between the Eleana Formation and the Tippipah Limestone. The low inclination of the gradient indicates that low density Quaternary alluvium is relatively thin, probably less than 100 m thick, and is in accord with existing borehole data.

Assuming that the residual anomalies shown in figure 4 are not entirely due to data error, they outline local regions of near-surface rocks having density contrasts which are small, on the order of 0.10 g/cm^3. Three north- to northeast-trending negative anomalies lie along the western contact between Tippipah Limestone and Quaternary alluvium. Because negative anomalies are not centered over Quaternary alluvium between Syncline Ridge and the Eleana Range the alluvium is inferred to be thin. The negative residual anomalies therefore may mark a local thickening of several 10's of meters in the alluvium adjacent to its contact with the limestone. The positive residual anomaly within the ridge may indicate a local region of relatively high density rock. This high is terminated by a northwest-striking discontinuity, which probably reflects effects of the lateral fault separating the northern and central blocks. In summary, the gravity data suggest that the

stratigraphic section underlying Syncline Ridge is lithologically variegated and structurally complex.

Magnetic data

Aeromagnetic anomaly data in the study area (fig. 5) were obtained by private contract as part of a regional survey of the Timber Mountain area to the west. Total intensity data were obtained 400 ft (122 m) above ground with a one-quarter mile (0.4 km) spacing in an east-west direction. The anomaly producing rocks within or immediately adjacent to the study area are tuffs of Miocene age which are in contact with Tippipah Limestone. These rocks, according to the description of Orkild (1963), include nonwelded ash-flow and ash-fall tuffs, similar to those for which total magnetizations have been determined by Bath (1968). On the basis of the work of Bath (1968), the lower member tuffs are estimated to have magnetic susceptibilities within the range 1 to 5 x 10^{-4} emu/cm^3, normally polarized remanent magnetization intensities within the range 1 to 5 x 10^{-4} emu/cm^3, and normally polarized total magnetization intensities within the range 2 x 10^{-4} to 1 x 10^{-3} emu/cm^3.

The survey area is magnetically quiet, containing one distinct, positive 20-gamma anomaly, and a number of vague 5-gamma flexures in the threshold of the background noise level. The lone anomaly is associated with outcrops of tuff of the lower member of the Indian Trail Formation; an anomaly comparable in amplitude is associated with similar rocks 2 km to the southwest. The aeromagnetic map does not contribute to an understanding of the geologic terrane underlying Syncline Ridge but does shed information on the patches of Tertiary tuff which abut or overlap the Tippipah Limestone. Using approximate calculations for subhorizontal sheet-like models successfully applied by Bath (1968, p. 140) to lava and ash flows elsewhere in the Nevada Test Site, we may

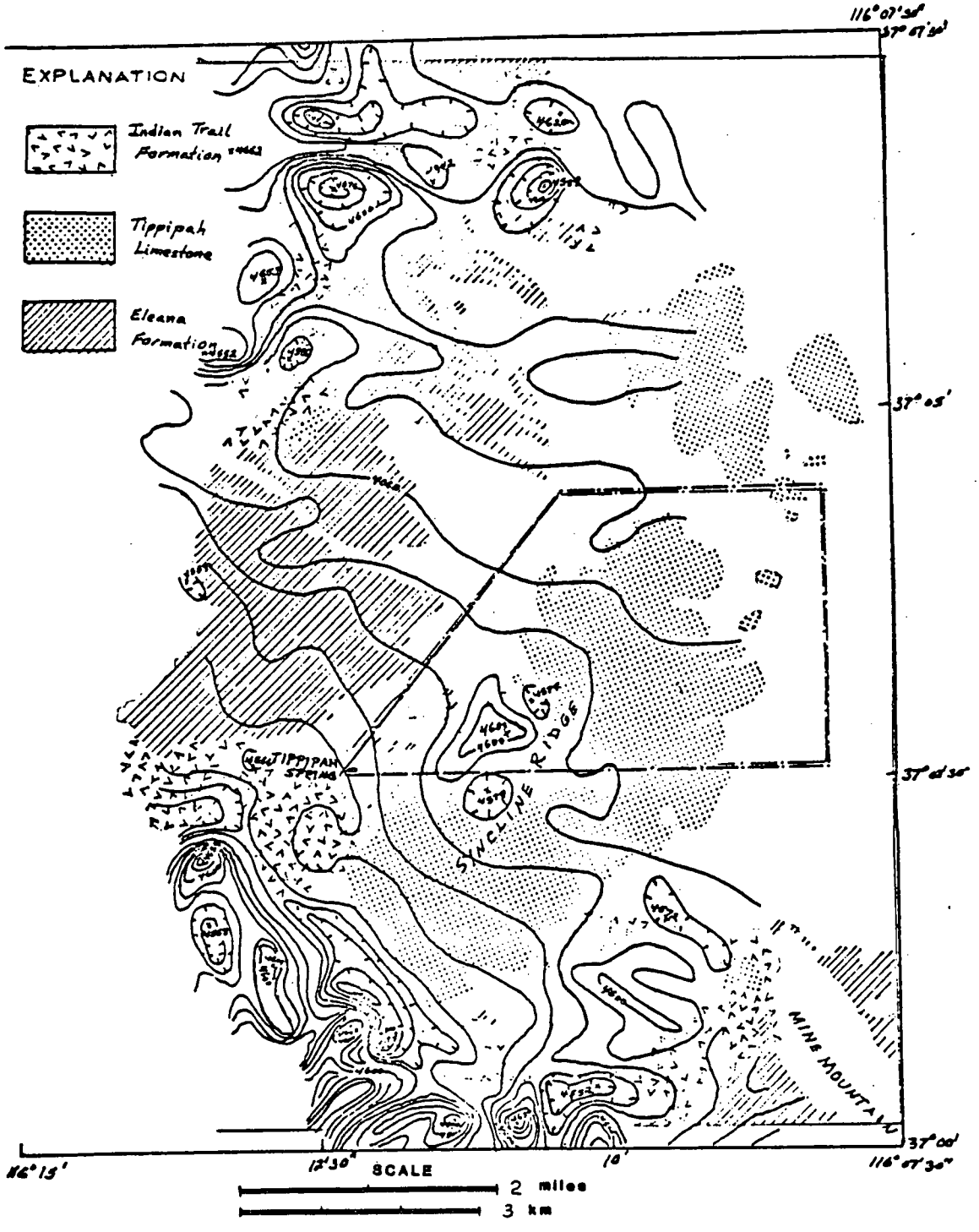

Figure 5.--Aeromagnetic anomaly map showing geologically mapped Eleana Formation, Tippipah Limestone, and Indian Trail Formation (Orkild, 1963). Survey flown 400 ft (122 m) above ground along east-west lines spaced one-quarter mile (402 m) apart. Contour interval; 10 gammas.

infer a tuff thickness of 10 to 50 m corresponding to an assumed range of total magnetizations of 2 x 10^{-4} to x 1 x 10^{-3} emu/cm^3. It may be noted that the gently inclined, northwest-trending gradient throughout the area is related not to the earth's core regional field but rather to a distant flank of a high-amplitude anomaly complex associated with strongly magnetic welded tuffs and vitrophyres 2 km southwest of the study area.

Seismic Methods

The prior seismic reflection study by Seismograph Service Corp showed that significant problems existed with the acquisition of both refraction and reflection data in the Syncline Ridge area (Mossman and Garrette, 1972). In this early work a test refraction spread was measured in an attempt to obtain velocity and depth control on the near surface weathered zone. The results were negative. Because a key to obtaining useful reflection data in the future could be adequate definition of the weathered zone or zones, an extensive refraction program was undertaken in January 1978 to address this problem and to attempt to identify near surface faults and structure. U.S. Geological Survey equipment and personnel were used for this work. Additional reflection work had not been planned; however it was learned in late January 1978 that a Western Geophysical Company vibroseis crew was then operating in Yucca Flat on an unrelated program. Because of significant economies which were realized by not having to pay mobilization charges it was decided to conduct additional reflection surveys. From February 4 to 8, 9.0 km of additional reflection data were obtained.

Refraction surveys

Eleven refraction lines consisting of 17 spreads were shot in January 1978 using spread lengths of either 345 m (1130 ft) or 1380 m (4525 ft). Each spread consisted of 24 geophones equispaced at 15 m or 60 m depending on spread length. Geospace HS-1, 4.5 Hz geophones were used with an SIE Inc. PT-700 seismic data acquisition system. Normally five shots were used with each spread; at the center, each end, and offset one spread length from each end. High velocity gelatin was used as a source with charge size varying from 1 to 40 pounds.

Analysis of the refraction data was performed with an interactive computer program of H. D. Ackermann (unpub. program, 1981). When reversed coverage is available as was generally the case in this study, the computer program gives depth and velocity values on fixed distance increments for each layer observed. The derived models are normally presented as velocity cross-sections (appendix 1).

Figure 6 shows the location of the 11 refraction lines measured in the study area. The position along each line where either a 3.0 to 3.5 km/sec or a 4.0 to 6.0 km/sec layer was identified also is shown in the figure. The velocities represent different interfaces in the Paleozoic section, but we have not been able to correlate them with specific lithologic units. Arrows in figure 6 identify faults which were inferred from the seismic velocity-depth models. The velocity models for each line are shown in appendix 1.

From 2 to 6 individual layers were computed for the 11 lines with velocities increasing with depth. Table 2 summarizes the velocity layering observed on each line and the exploration depth. Some tentative correlations have been made between the observed layering and the near surface lithologies based in part on well logs. Borehole Uel-L is adjacent to the

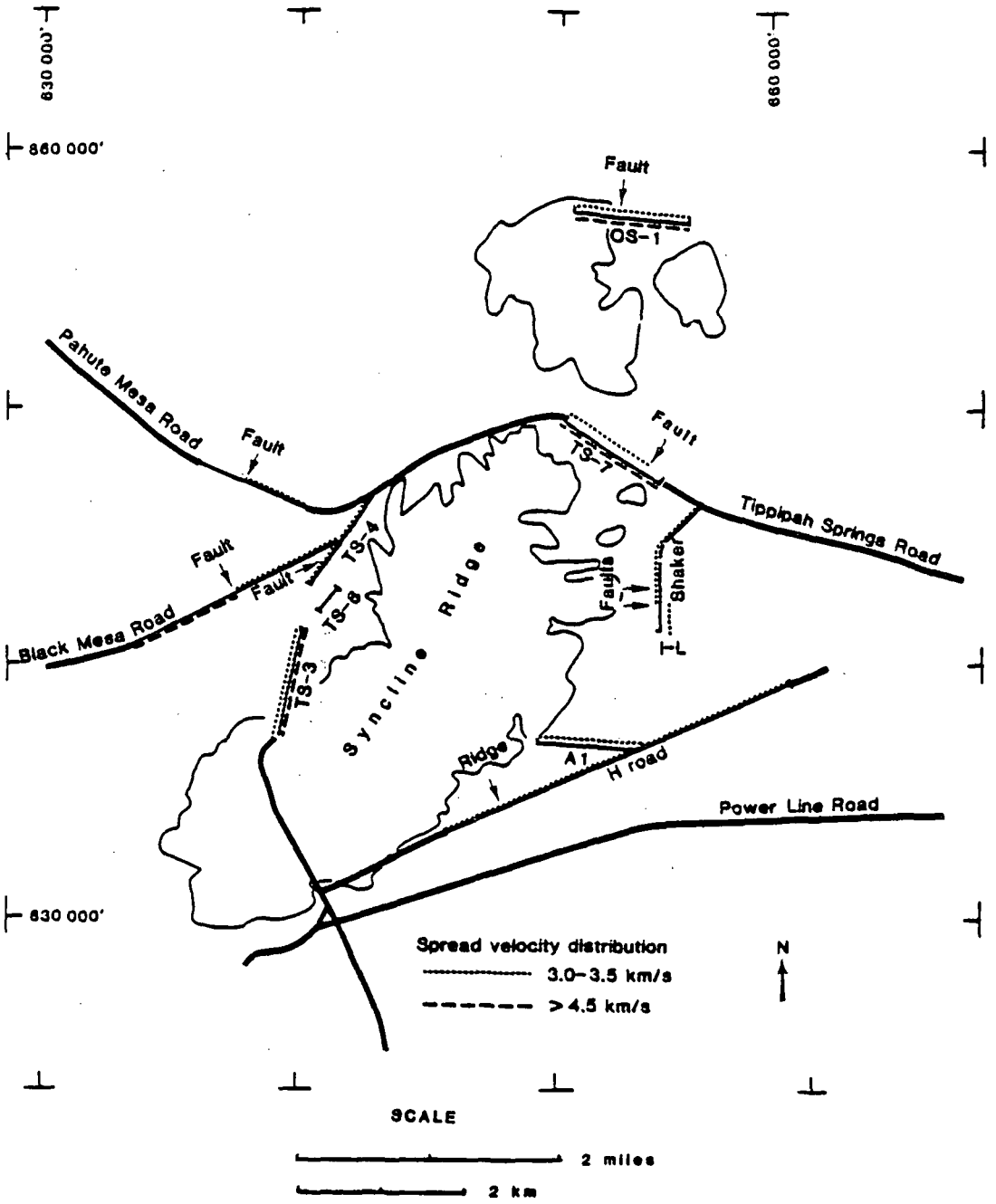

Figure 6.--Location map of 11 seismic refraction lines measured in the study area. Dotted lines above each spread show the interval over which a velocity layer of 3.0 to 3.5 km/s was observed and the dashed line the interval over which 4.5 km/s velocities and greater were found. Arrows indicate the location of faults identified on the lines.

Table 2.

Summary of observed layer velocities and depth of exploration for 11 refraction lines measured in the study area

SPREAD	TOTAL SPREAD LENGTH	MAX AVERAGE DEPTH	LAYER	VELOCITIES 1	2	3	4	5	6
A-1	1380 m	175 m		x	1.4	x	2.5	3.5	x
HROAD	4300 m	300 m		x	1.2	1.6	2.1	3.2	x
PMROAD	1380 m	160 m		0.5	1.4	x	2.45	3.2-3.5	4.5
BMROAD	2760 m	150 m		0.8	1.1	x	2.50	3.3	4.0
TS-3	1380 m	300 m		0.8	x	1.6	2.6	3.5	4.3
PM-3	345 m	150 m		0.8	1.3	x	2.2	x	x
OS-1	1380 m	400 m		0.6	x	1.6	2.2-2.5	3.4	5.0-6.7
TS-4	1380 m	150 m		0.8	1.0	1.6	2.0-2.5	3.1	4.3
TS-7	1380 m	250 m		0.85	1.1	1.5-1.7	2.4	3.0	4.1-4.6
SHAKER	2000 m	200 m		0.4	1.2	1.7	2.4-2.7	3.5	4.0-5.0
TS-6	345 m	30 m		0.4-0.8	x	1.7-1.9	x	x	x

x = indicates layer not observed

southern end of the Shaker spread and UE16-f is adjacent to the western end of spread A-1. Alluvium can be reliably correlated with velocities of 2.0 km and less. From table 2 it can be seen that some spreads identified three distinct layers in the alluvial cover. These distinct layers are probably related to different ages of the alluvial units described by Hoover and Morrison (1980). However we have been unable to correlate any of the layers with specific alluvial units and no consistent spacial pattern of these low velocity layers is evident in the seismic models. The south end of line TS-3 was on outcrop of thin Tertiary non-welded tuffs seen in the magnetic data and not over 50 m thick. This line shows about 50 m of 1.6 km/s and less velocity material at the surface. We conclude that these Tertiary units would be indistinguishable from the alluvium, as would other Tertiary alluvium known from the area (Hoover and Morrison, 1980).

Velocities above 2.0 km/sec are correlated with the Paleozoic rocks in the study area. We, however, have been unable to correlate individual layers of the seismic models with specific lithologic intervals observed in the boreholes, except possibly for a deeply weathered zone at the top of the Eleana Formation. Borehole Ue1-L showed a 58 m thick zone of weathering (Hoover and Morrison, 1980) which it is believed developed during a long, wet, stable period prior to the local Tertiary volcanism. This weathered zone correlates in part with a 2.4 km/s layer observed on the Shaker line. The weathered zone in the Eleana Formation has only been observed on the east side of Syncline Ridge so that layer velocities near 2.4 km/sec do not necessarily correlate with this weathered horizon.

Several lines, in particular OS-1, extended onto outcrop of the Tippipah Limestone. Observed velocities for this unit were quite low for limestone and indistinguishable from Eleana Formation velocities. Thus neither density nor

seismic p velocities provide a means of geophysically distinguishing these distinctive lithologies.

Based on the above correlations and lateral changes in seismic velocities the seismic sections show a number of significant structural features. Faulting or erosion is interpreted as cutting the alluvium on lines H Road and Shaker, both on the east side of Syncline Ridge. This may suggest but is not conclusive evidence for Quaternary faulting within the central block. A number of other faults were interpreted on the cross-section but appear to be restricted to Paleozoic rocks. In general those faults identified on the eastern side of the ridge correlate with mapped faults or reasonable extensions of mapped faults. On the west side the correlation is not as clear and there is insufficient data on which to infer trends from the seismic sections.

A number of lines show structural relief on top of or within the Paleozoic section. This could result from faulting, folding, or erosion, of what ever horizon is being mapped. The most significant structural feature in all of the sections is a graben-like feature and fault interpreted on line TS-7. Vertical offset of this feature is 130 m. Line TS-7 is parallel to a lateral fault projected through Gap Wash which separates the northern and central blocks. The features on this line lie east of the extension of the axial fault in the central block.

Variations in alluvial thickness identified in the seismic sections correlate in general with trends shown in the gravity map (fig. 4). Line TS-4 crosses one of the small closed gravity lows discussed earlier, which is on the western edge of the ridge. The seismic section shows the alluvium thickening from 30 meters south of the low to 65 m in the low. This confirms the earlier inference that this gravity anomaly could be the result of local alluvial thickening, which is probably true of the others.

The faulting indicated in the Paleozoic rocks shown in the velocity sections BM Road and TS-4 and the thickening of the alluvial section on the southwest end of H Road seems quite consistent with the major Northwest trending lateral fault which separates the central and southern blocks. In addition a mapped fault on the northeast side of the northern block correlates well with one in the fifth layer of OS-1.

Reflection surveys

Experience gained from the 1972 reflection survey and from the work by Western Geophysical Company in Yucca Flat was used to establish the recording parameters used in this survey. Three lines were recorded in the study area (fig. 7) which combined with the earlier SSC data provided coverage encircling the Ridge. Line W-1 starts on the western edge of an east-west line run for Southern Methodist Univ. (SMU). Line W-1 runs south-west across the central and southern blocks. Line W-2 crosses Syncline Ridge along a road in the southern block and line 3 runs north-south on the western flank of the Ridge and along the valley separating Syncline Ridge from the Eleana Range. The location of the two SSC lines are also shown in figure 7.

The recording and operating parameters used in this survey are given in table 3. A 48-channel LRS Coba recording system was used throughout the survey with Mark Products L-10A, 10 Hz geophones. The energy source was 4, Y-900 LF vibrators (Gardner, 1978). Processing of the data was done at Western Geophysical's Denver Digital Center using standard methods. As in the earlier SSC work the data quality of the record sections was marginal at best. A number of different processing parameters and techniques for improving the data quality were tried. Velocity analyses were run and various

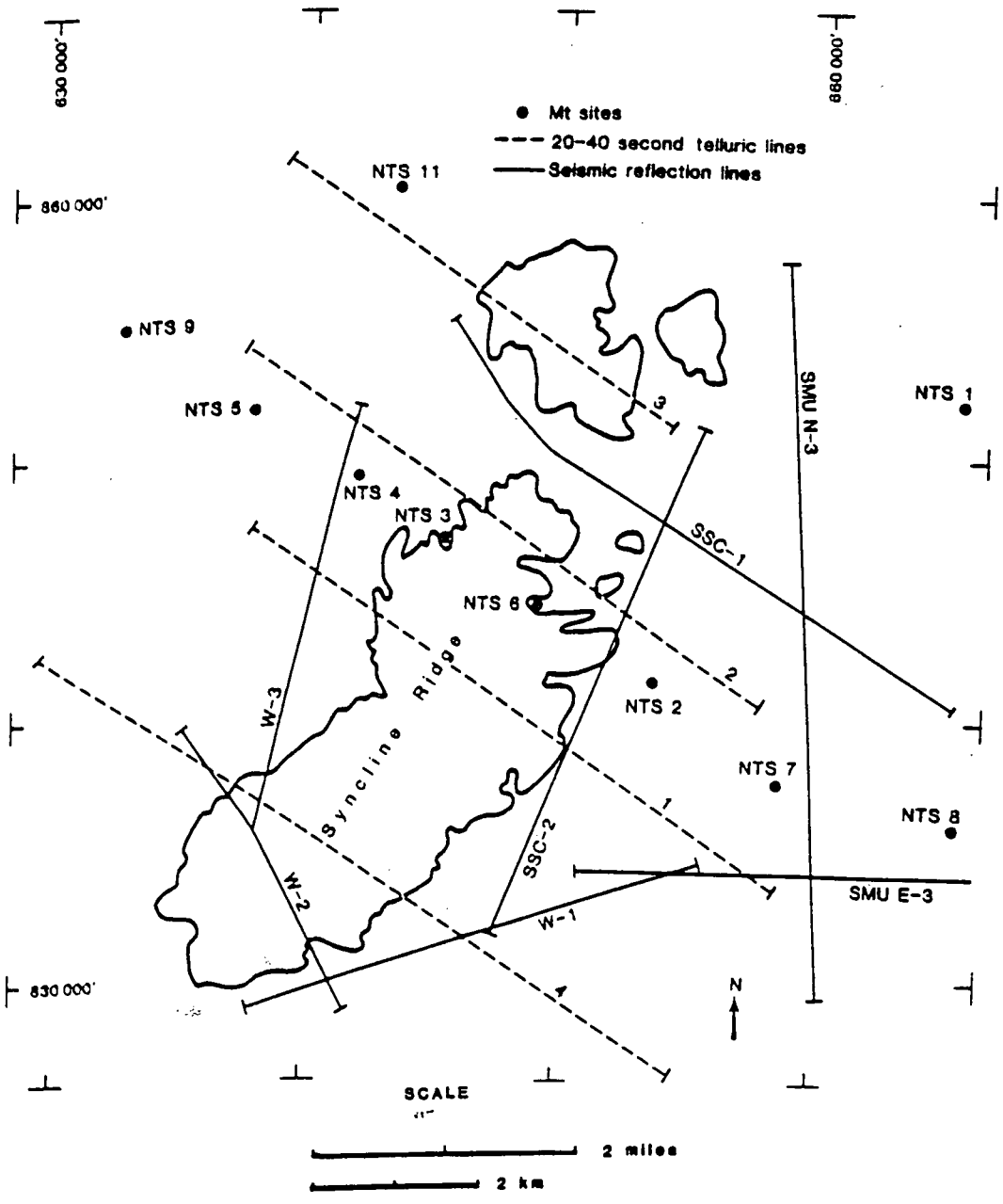

Figure 7.--Location map of five seismic reflection lines measured by Seismograph Service Corp. (SSC) and by Western Geophysical Co. (W), along with magnetotelluric sounding location and E-field ratio telluric traverse locations in the study area.

Table 3.

Operating Parameters of Reflection Survey

Recording	24 fold CDP
Sample rate	4 milliseconds
Channels	48
Group interval	220 feet
Vibrator point interval	220 feet
Spread	5720-660-0-660-5720 feet
Geophones per group	36
Number of sweeps/VP	16
Length of sweep	16 seconds
Listening time	5 seconds
Sweep frequency range	14-56 Hz
Recording filter	out-62 Hz

velocity-depth functions were tried. Deconvolution tests before and after stacking and multichannel filtering tests didn't improve the data quality (Gardner, 1978).

It should be noted that the SMU line in Yucca Flat which was tied to line W-1 revealed good reflections from the paleozoic section. The seismic data quality decreases rapidly west of the north-trending normal faults which define the eastern border of the study area. Drill hole data shows that west of this line the Eleana Formation lies below relatively shallow alluvium while to the east the alluvium thickens and a thick section of Tertiary volcanic rock overlies the Paleozoic.

A number of geologic factors could be responsible for the poor data quality. Random scattering may be occurring from faults and fractures and in steep dipping layers. Drill hole data show bedding plane dips in the Eleana Formation ranges from 0^{o} to 60^{o} at the site. The relatively low velocity argillite may be absorbing much of the energy. In addition static corrections may be in error due to a rapidly changing and variable "weathering" layer. This latter may be especially severe because as mentioned earlier there appear to have been three distinct weathering episodes which are still preserved at the site: Quaternary, Tertiary, and pre-Tertiary.

The completed seismic sections provided by both Western and SSC are shown in figures 8 through 12. The SSC sections had been marked lightly to emphasize the few reflections which could be carried for any distance and inferred faults were marked. Although the data quality is poor, SSC line 1 (fig. 11) which runs across the northern end of the central block we believe gives an accurate picture and the most detailed view possible of the structural configuration at Syncline Ridge. The other geophysical data sets are in agreement with this general picture. The only prominent reflection

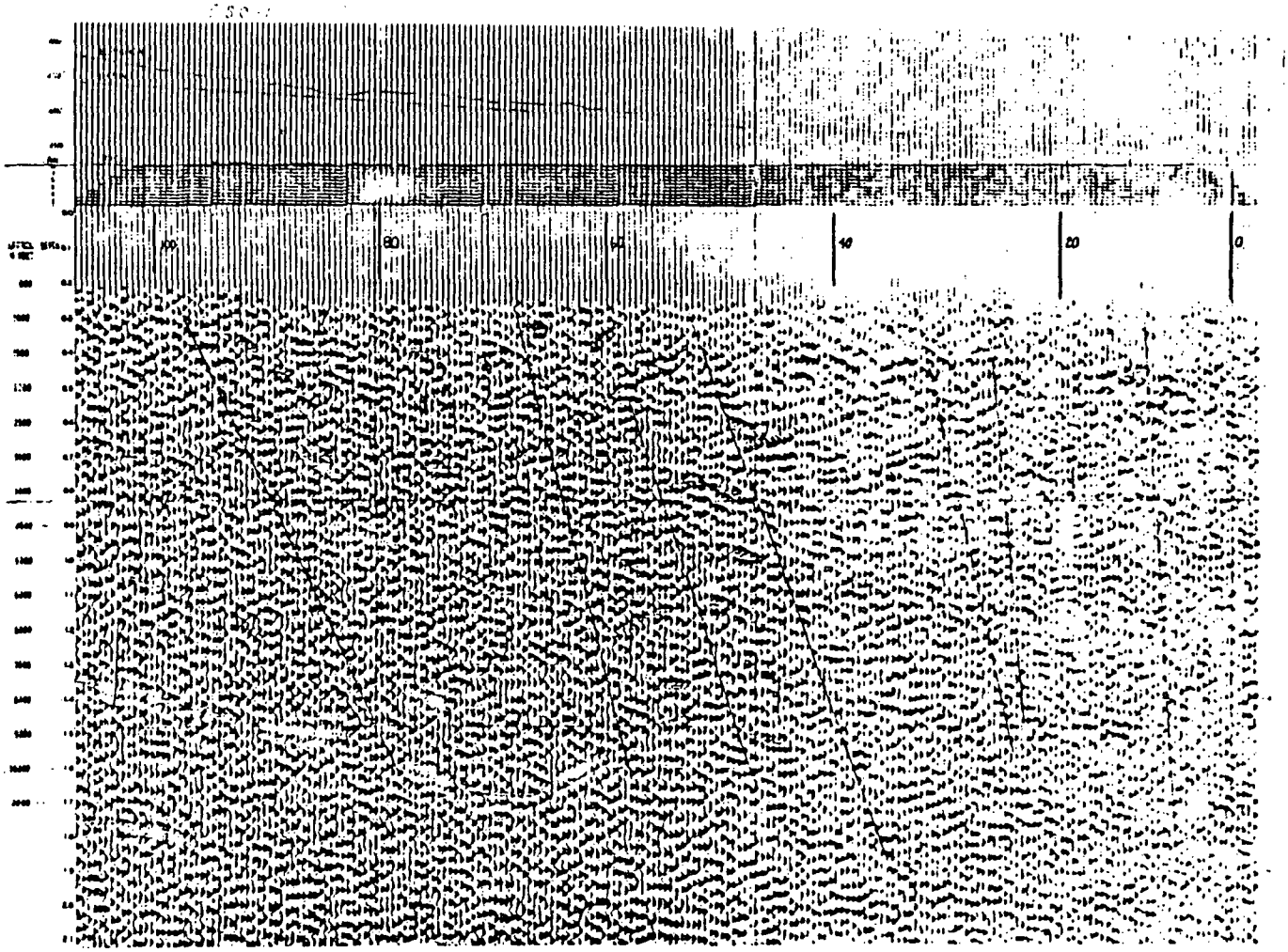

Figure 8.--Seismic reflection time section for Seismograph Service Corp. Line 1 Syncline Ridge.

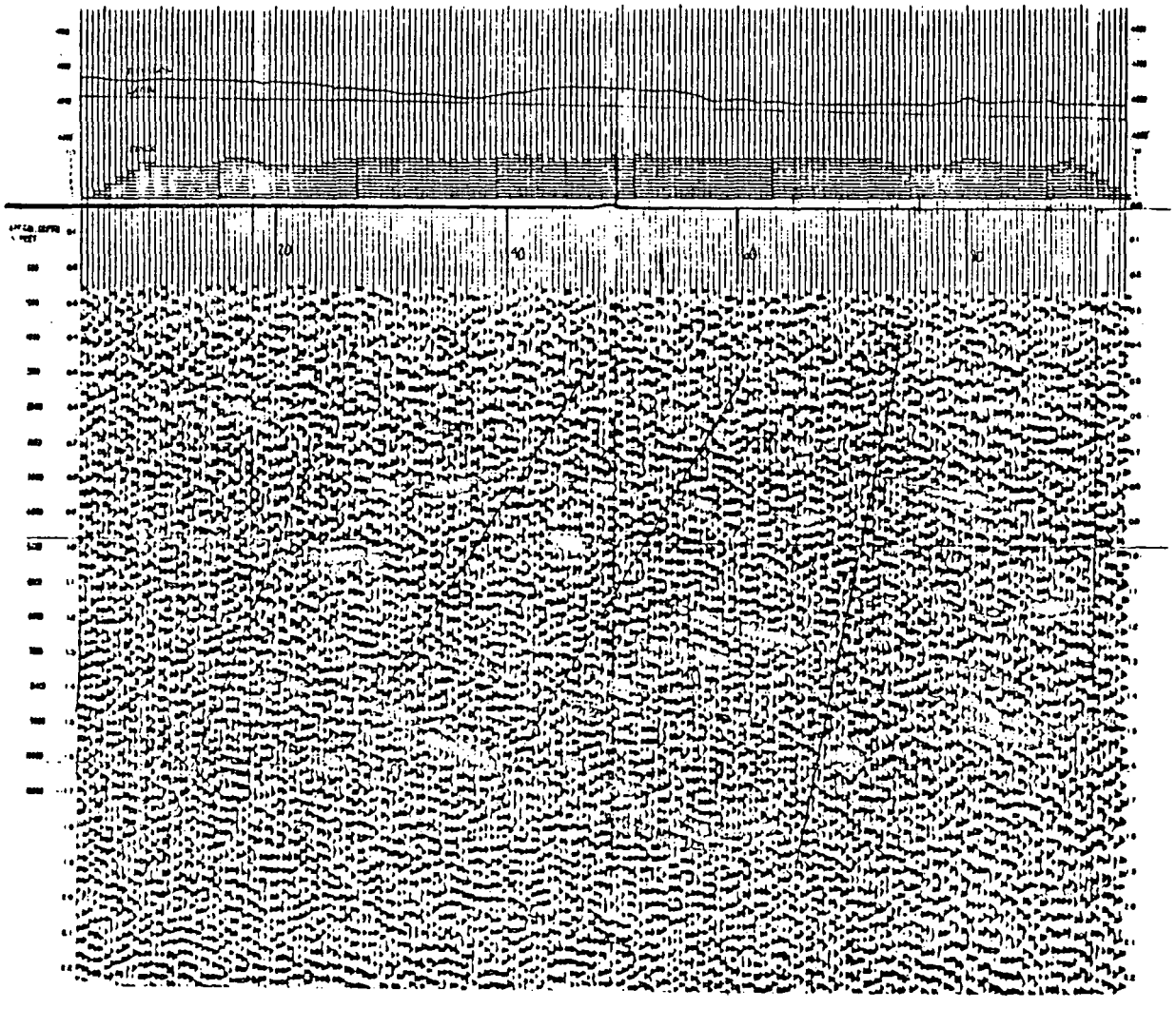

Figure 9.--Seismic reflection time section for Seismograph Service Corp. Line 2, Syncline Ridge.

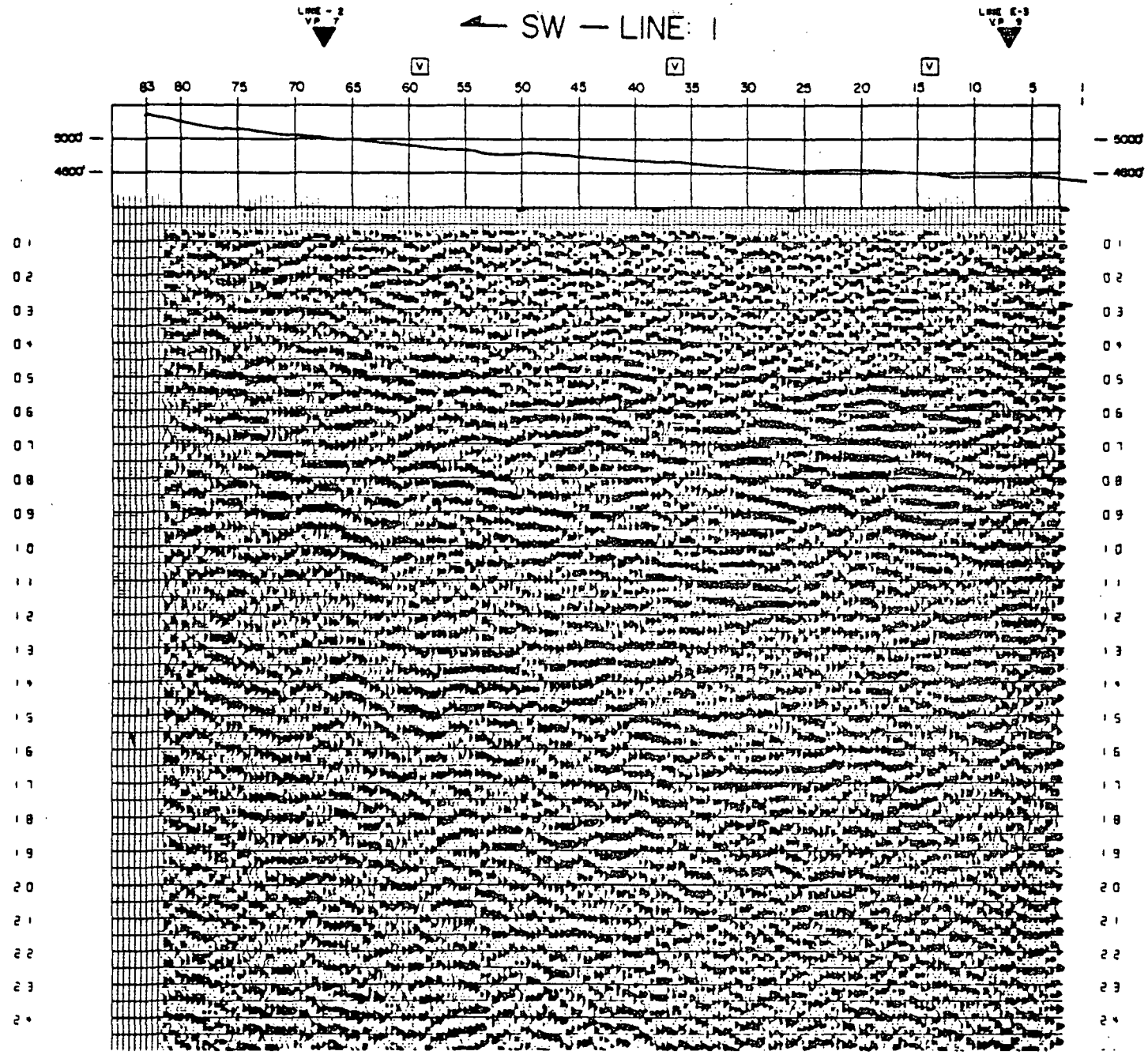

Figure 10.--Seismic reflection time section for Western Geophysical Co. line 1, Syncline Ridge.

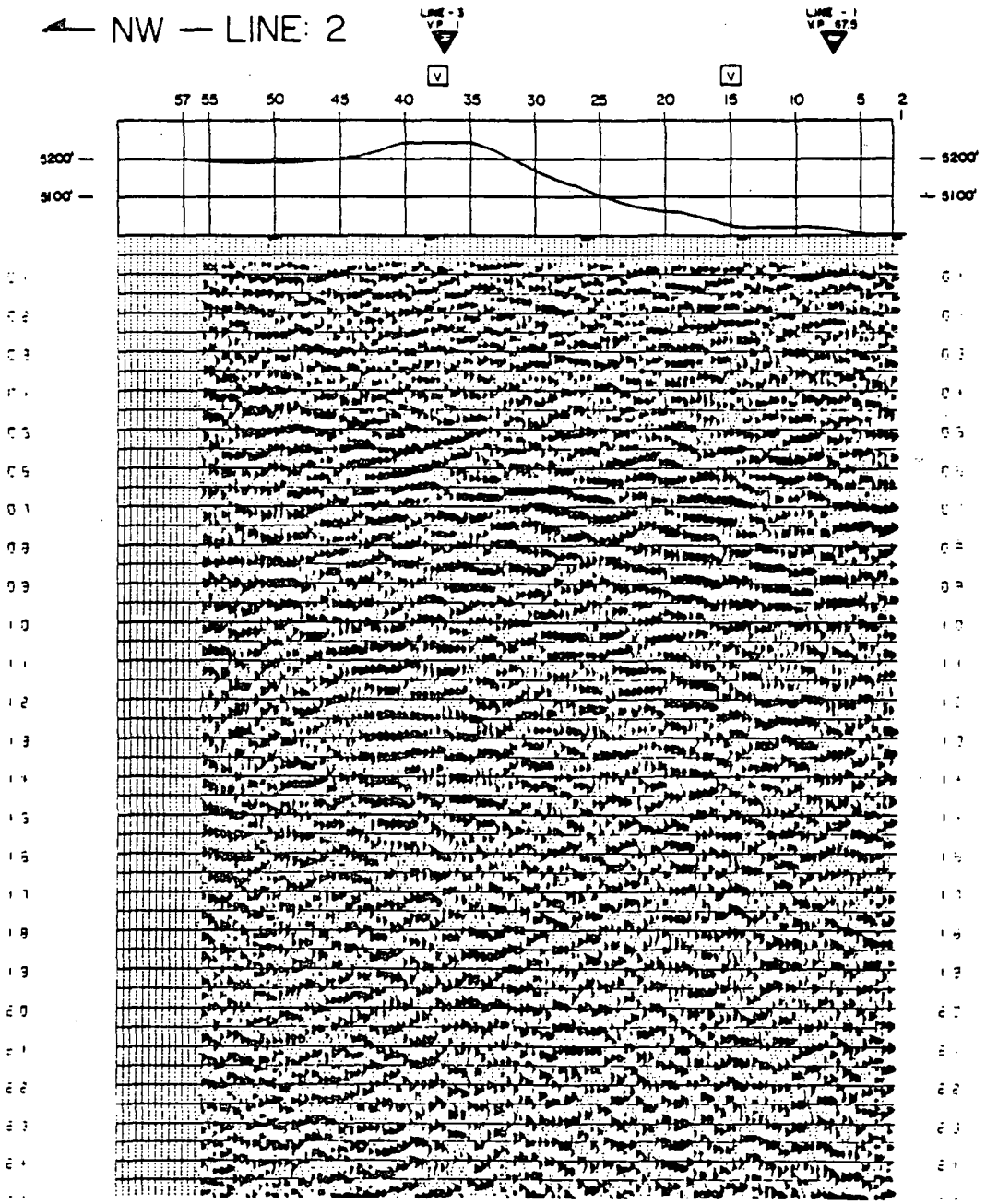

Figure 11.--Seismic reflection time section for Western Geophysical Co. line 2 Syncline Ridge.

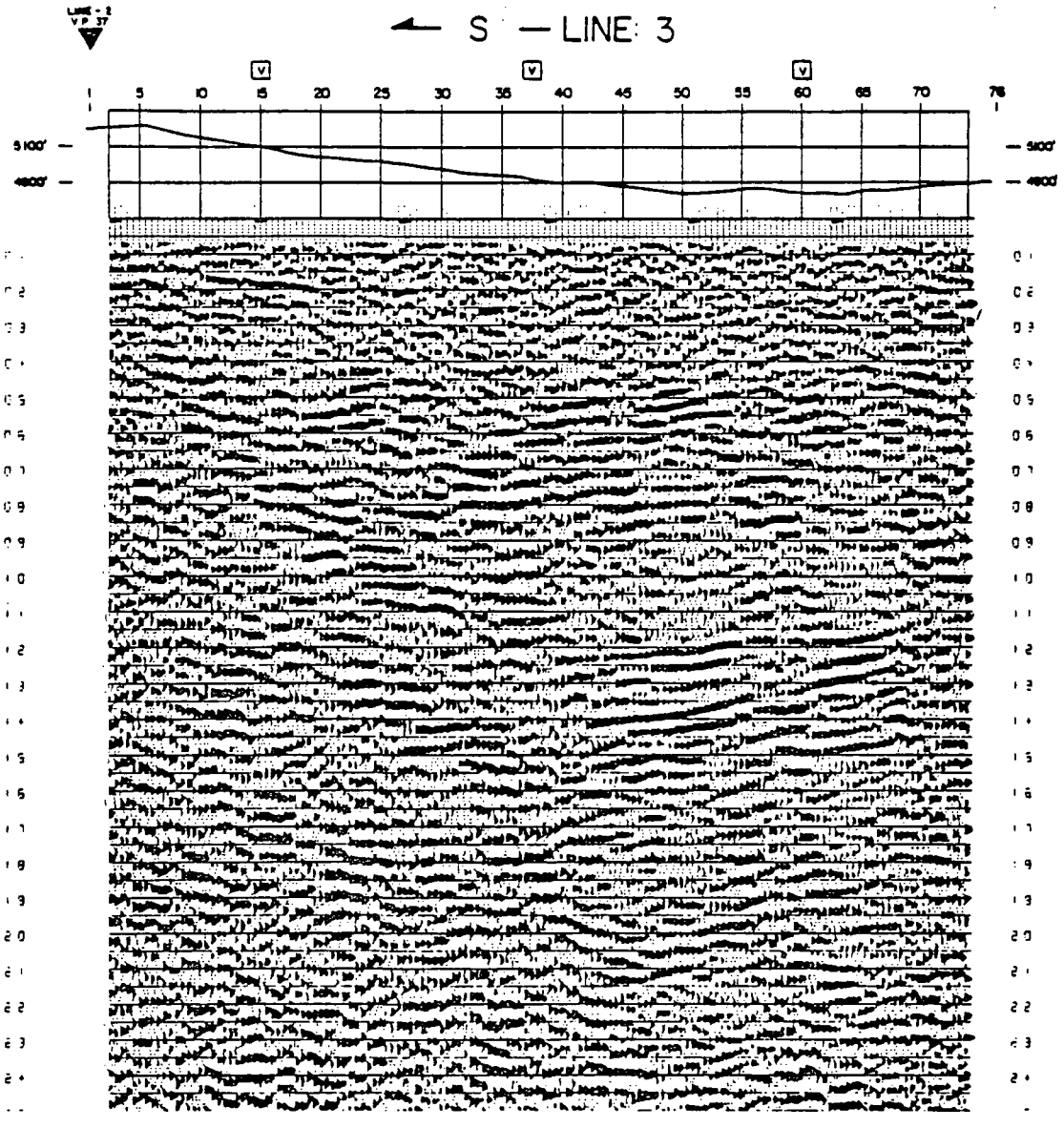

Figure 12.--Seismic reflection time section for Western Geophysical Co. line 3, Syncline Ridge.

event on these sections is seen on the northwest end of line SSC-1 (fig. 8) and the north end of line W-3 (fig. 12). These appear to be the same reflecting horizon beginning at about 1.3 seconds at the end of the respective sections. If the average velocity through the section is 4.0 km/sec this horizon is at a depth of 2.6 km (8500 ft). This may mark the base of the Eleana where older Paleozoic carbonate rocks are expected. Hoover and Morrison (1980) estimate the Eleana Formation at the site to be at least 2.0 km thick. The synclinal structure is evident on line SSC-1 but not on W-2 (fig. 11) both of which cross normal to the structural axis. Faulting which was interpreted on SSC-1 offsets what we infer to be the base of the Eleana Formation downdropping the central part of the structure. This faulting provides a potential short pathway from the repository to the underlying carbonate aquifer.

Because of the poor data quality and other data also implying structural complexity no further attempt was made to interpret the reflection data. We believe the principal cause of the poor data quality is the highly variable upper few hundred meters which prevents good stacking of the data. The structural complexity is in an area with widely varying dips. The greatest complexity is on the east side of the ridge and the least disturbed on the northwest part of the study area.

Electrical Methods

A number of electrical methods were tried because of the Eleana argillite unit and particularly the argillaceous subunit of unit J is quite conductive and should be electrically distinctive. Schlumberger vertical electrical soundings (VES) were used extensively around Syncline Ridge where access and gentle topography permitted. The principal function of the VES was to map the argillite. Slingram electromagnetic traverses, a shallow exploration method

was used on the east side to assess its applicability to defining Quaternary faulting. Magnetotelluric (MT) soundings were used to get deep structural information particularly in view of anomalous results observed in an earlier MT survey. E-Field ratio telluric traverses were employed so as to get some electrical data in and across the ridge itself. Details of the VES work have been published by Anderson and others (1980) and for the Slingram results by Flanigan (1979).

Schlumberger VES

Figure 13 shows the location of the VES and lines of section presented by Anderson and others (1980) and figures 14-16 shows their interpreted sections AA′, BB′ and CC′. A total of 44 soundings were made using a direct current source. The transmitter and receiver system are of U.S. Geological Survey manufacture. Conventional field operating methods were used in the survey (Keller and Frischknecht, 1966). The sounding curves were inverted using computer programs developed by Zohdy (1974, 1975). These programs produce a geoelèctrical cross-section based on an equivalent one-dimensional earth. The principal source of error in the derived geoelectric sections is the assumption of one-dimensionality in the inversions. The prior geophysical data and the VES data reveal extensive lateral heterogeneity which has not been accounted for in the models presented.

Electric logs from the deeper drill holes in the study area provided a means of correlating lithologies with resistivities (Anderson and others, 1980). Resistivities of 20 to 40 ohm-m generally characterize the high argillite parts of unit J, quartzite intervals go as high as 300 ohm-m, and the Tippipah Limestone is generally over 1000 ohm-m. It is interesting to observe that density and seismic velocity obtained from the well layer are

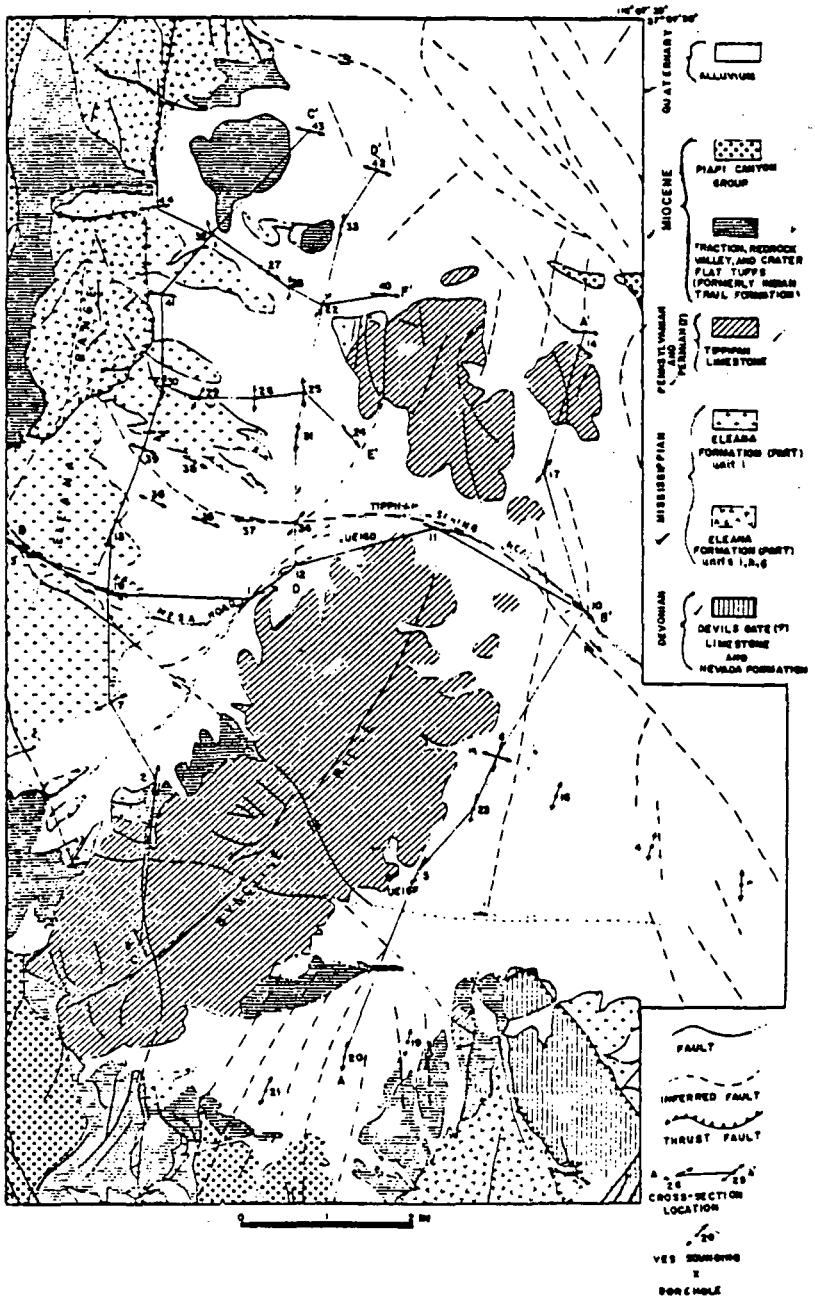

Figure 13.--Map of the study area showing the location of Schlumberger soundings, the generalized geology and line of geoelectric sections, from Anderson and others (1980).

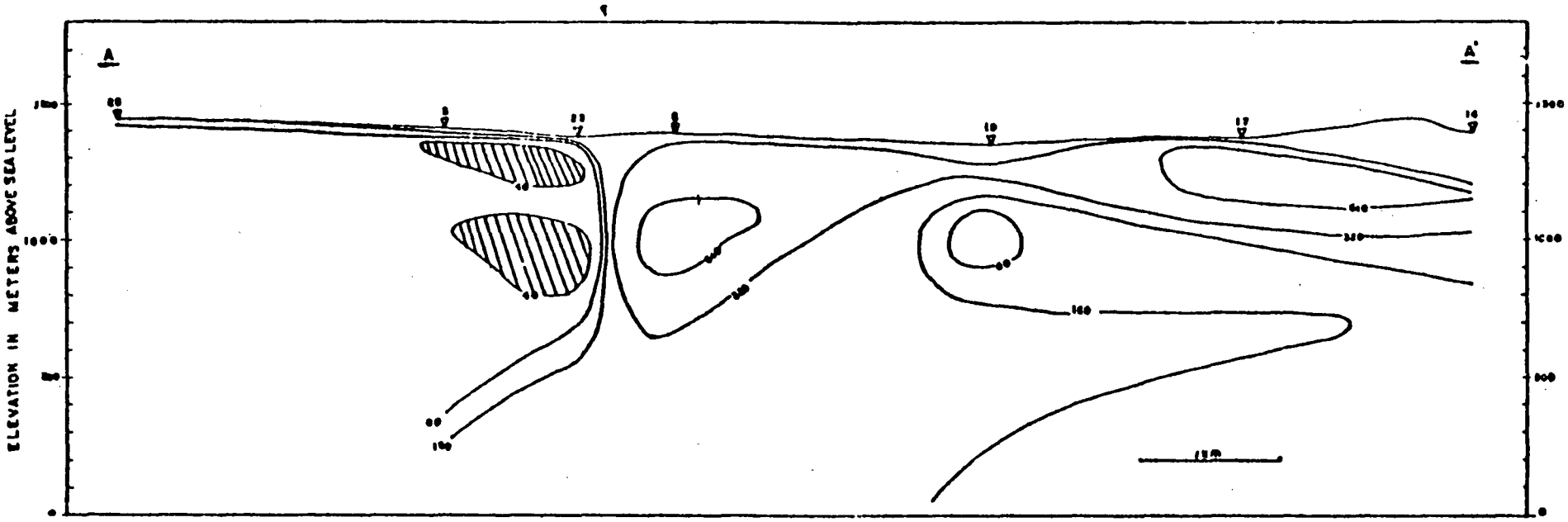

Figure 14.--Geoelectric cross-section A-A′ (fig. 13) compiled from interpreted resistivity sounding data. Contours increase in geometric progression from a value of 20 ohm-meters. Patterned areas are those intervals considered to be composed primarily of argillaceous argillite (Hoover and Morrison 1980) of the Eleana Formation. Vertical exaggeration is 2X. From Anderson and others (1980).

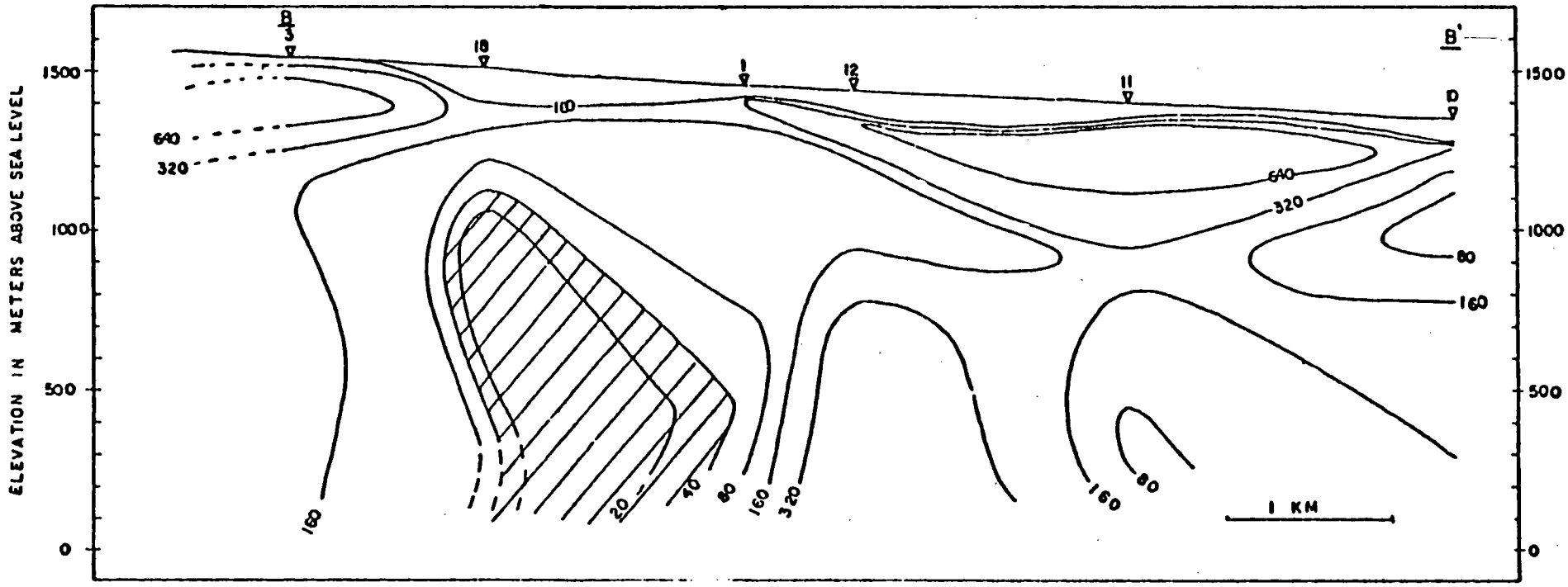

Figure 15.--Geoelectric cross-section B–B′ (fig. 13) compiled from interpreted resistivity sounding data. Contours increase from a value of 20 ohm-meters. Dashed contours indicate inferred values of resistivity. Patterned areas are those intervals considered to be composed primarily of argillaceous argillite of the Eleana Formation. Vertical exaggeration is 2X. From Anderson and others (1980).

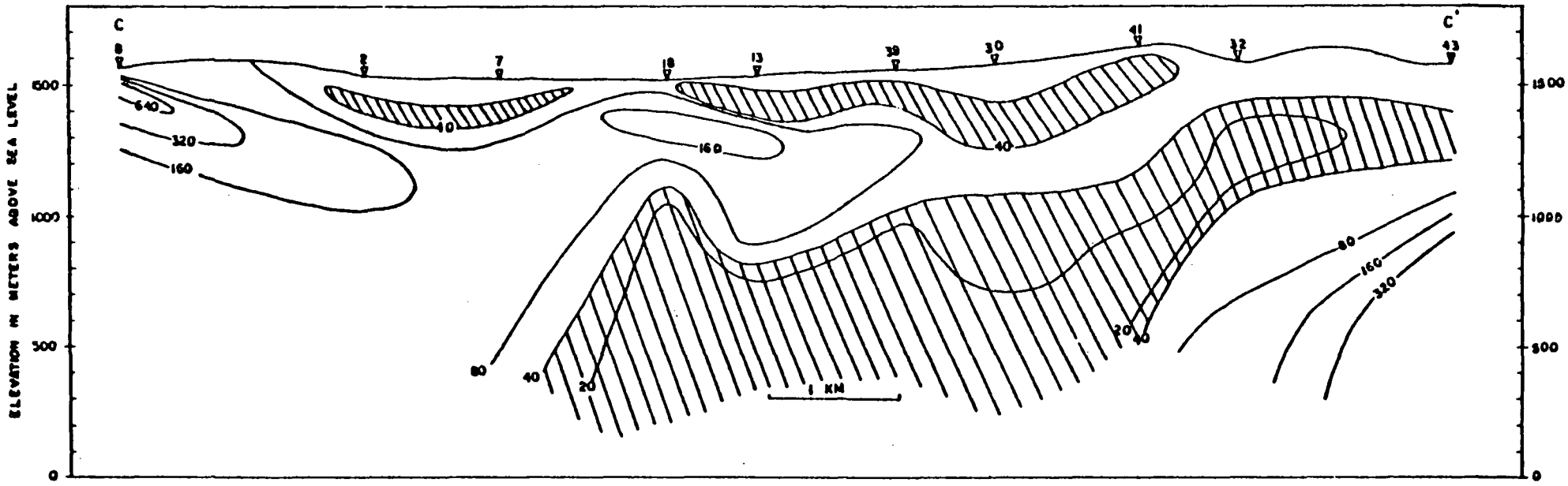

Figure 16.--Geoelectric cross-section C-C′ (fig. 13) compiled from interpreted resistivity sounding data. Contours increase in geometric progression from a value of 20 ohm-meters. Patterned areas are those intervals considered to be composed primarily of argillaceous argillite of the Eleana Formation. Vertical exaggeration is 2X. From Anderson and others (1980).

very nearly the same for the Tippipah and Eleana Formations yet the resistivities vary over such a wide range. The seismic refraction data however does indicate a wide range in velocity for the Eleana Formation.

Figure 14 shows geoelectric section A-A′ along the eastern edge of Syncline Ridge. A thick section of argillite is seen on VES 5 and 23 both within the central block. But a distinct discontinuity exists between VES 23 and VES 6 also within the central block. This electrical discontinuity and by inference lithologic discontinuity occurs rapidly as VES 23 and VES 6 are separated by only 750 m. On VES 6 and further north no resistivities were observed which are consistent with a thick section of the argillite subunit of unit J within the depth of exploration. Yet drill hole UE1-L 500 m east of VES 6 as well as VES 16 and 4 show a thick interval of argillite. VES 15 was made normal to VES 6 to help assess the effect of lateral inhomogeneities. Sounding 15 shows less evidence of lateral effects but yields the same results. These data constrain the location of what is inferred to be a major fault and indicate a northeast strike, at least in the central block. A fault interpreted near station 55 on the SSC seismic line 1 would be consistent with this trend and shows downdropping of the northwestern block. This would be consistent with the electrical data which suggests a thick section of limestone is beneath VES 6. Note the similarity with VES 3 made at the center of the Ridge in the southern block (fig. 16).

Figure 15 shows section B-B′ which runs across the structure following Gap Wash. This electrical section shows that the only thick unit of argillite lies in the valley to the west of Syncline Ridge. As would be expected it also shows the limestone is thickest at VES 11 on the syncline axis.

Section CC′ (fig. 16) is a north-south section along the front of the Eleana Range. This shows a major electrical discontinuity between VES 18 and

7. The lateral fault separating the central and southern blocks passes between these two stations. The electrical discontinuity is an expression of this fault and shows that distinct lithologic units occur on either side. From VES 18 to 41 a fairly uniform electrical section is observed also showing a thick interval of argillite in both the central and northern blocks. The lateral fault separating these two blocks is not clearly seen in this electrical data. VES 32 on Red Canyon marks the northern end of the zone containing a thick sequence of argillite. Faulting near this location is suggested by the electrical data.

Additional details may be found in Anderson and others (1980). The Schlumberger data, however, clearly shows that a great deal of heterogeneity exists in the central block and that the argillaceous unit considered for the repository has undergone significant vertical movement. This electrical data shows that the largest block of thick argillite is in the northwest part of the study area suggesting that it may be the least disturbed. A similar conclusion was drawn from the seismic reflection data.

Slingram surveys

Figure 17 shows the location of slingram traverses run on the eastern flank of Syncline Ridge to assess the usefulness of the technique for identifying faulting in the alluvium. Commercially available equipment was used operating at frequencies of 222, 444, 888, 1777, and 3555 Hz. Details of the survey are given by Flanigan (1979). Coil separation was 244 m selected as optimum based on modeling of a resistive alluvium overlying conductive argillite. Seven lines were run across the graben in the southern block and 24 east-west lines in the central block starting at the outcrop of the Tippipah Limestone going east. Two parallel northeast lines were also run along and adjacent to seismic line H Road.

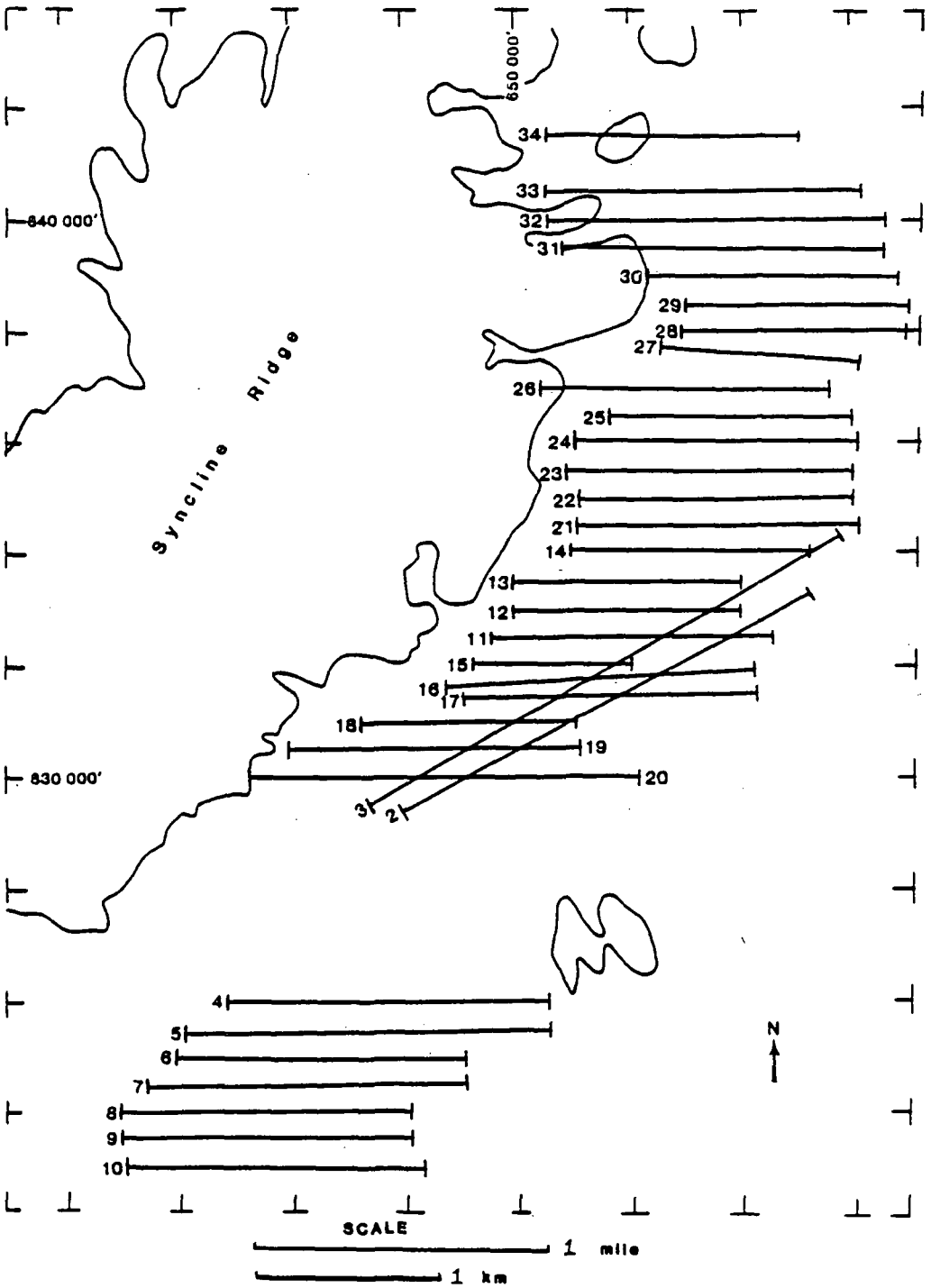

Figure 17.--Location map showing slingram traverses run over alluvium on the eastern side of Syncline Ridge. The outcrop line of Tippipah limestone is shown for reference. Adopted from Flanigan (1979).

A contour map of the slingram response from the southern block is shown in figure 18. Gradients on the eastern and western edges of the map separate regions on the edges where conductive rocks are at shallow depth as opposed to the center of the graben where thicker resistant alluvium is present. Although numerous faults have been mapped trending north to northeast across the graben (Hoover and Morrison, 1980), the thickness of the alluvial cover in the center probably masked the response of the deeper structure.

A contour map of data obtained in the central block taken from Flanigan (1979) is shown in figure 19. The most prominent feature is a northeast trending low in the real component which identifies an area of more conductive rock. This feature is just east of the outcrop of the Tippipah Limestone but is abruptly terminated at each end. On the southwest it terminates on the lateral fault separating the southern and central blocks. The northeastern end terminates south of VES 6 (fig. 13) apparently by an east-west trending feature.

Flanigan (1979) inverted selected portions of the data to derive a layered earth model for a few lines, and observed that models could not be made to satifactorally fit both the real and imaginary data sets. He attributes this principally to too complex a near surface geoelectric section which cannot be represented by his one-dimensional models.

The slingram results show various trends on the east side of Syncline Ridge which correlate in part with similar trends in other data sets. The data however is ambiguous because it is not clear how much of the response is due to bedrock topography. The method appears to have little utility in this area for identifying Quaternary faulting.

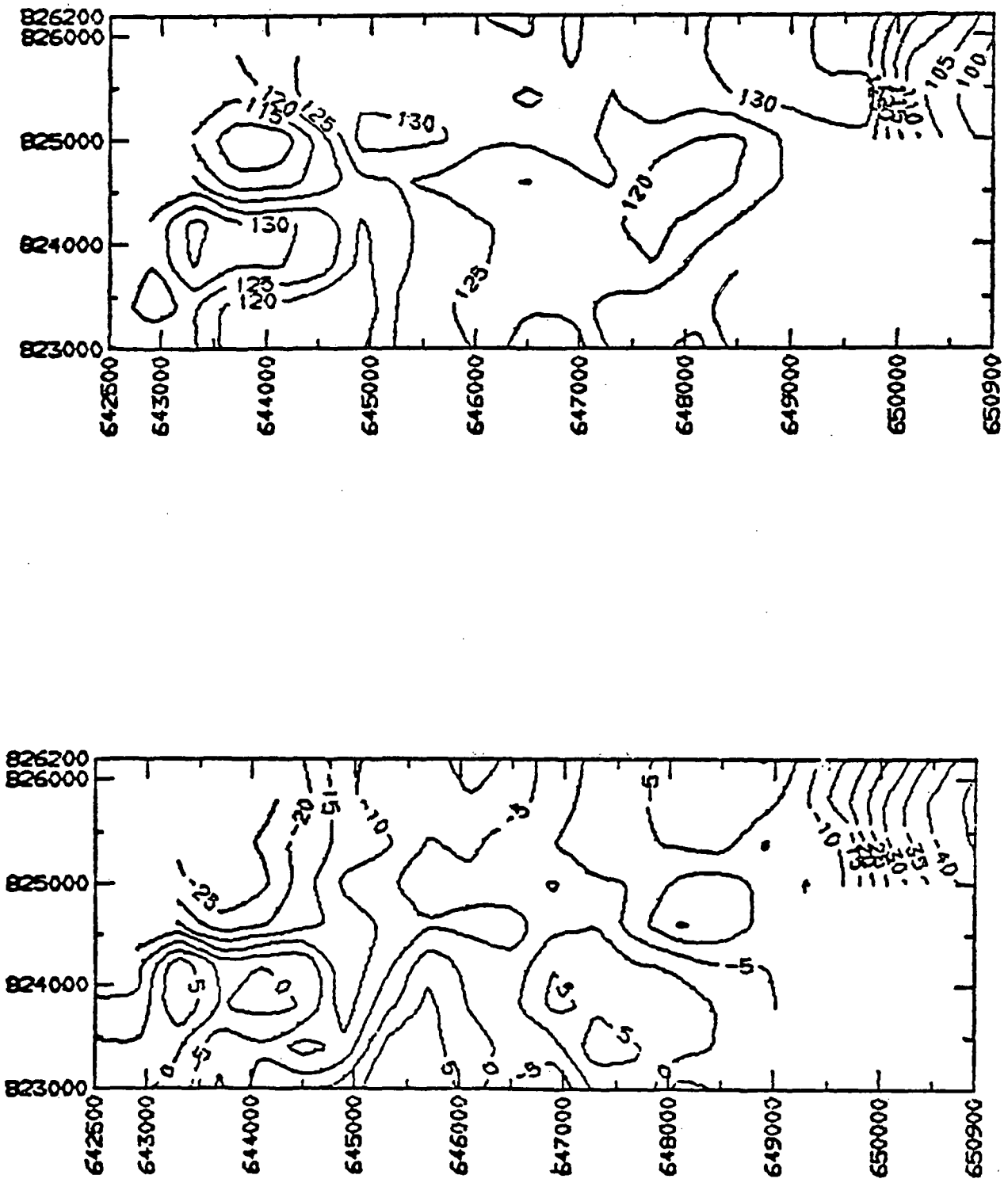

Figure 18.--Contour map in the southern block of Syncline Ridge showing slingram real and imaginary response at 444 Hz, from Flanigan (1979). Contour values are in percent of the primary field.

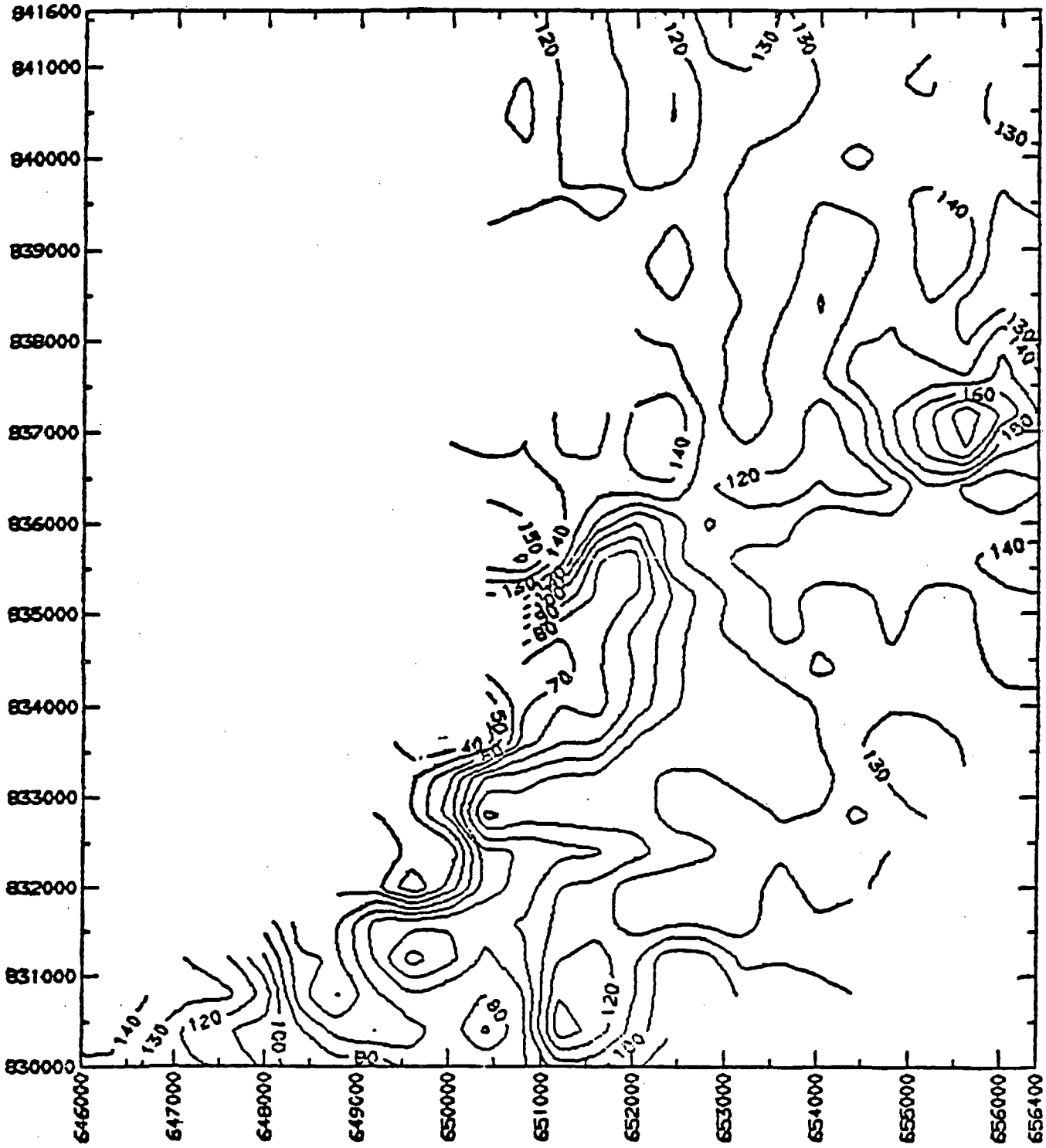

Figure 19.--Contour map in the central block of Syncline Ridge showing the slingram real response at 1777 Hz, from Flanigan (1979). Contour values are in percent of the primary field.

Magnetotelluric surveys

In February 1978 a contract was issued to Williston, McNeil and Associates, Golden, Colo., for a series of tensor magneto-telluric (MT) soundings covering the frequency range of 0.001 to 25 Hz. A digital data acquisition system was used based on a PDP-1103 computer system. A three component cryogenic magnetometer was used for sensing the magnetic field. Further details of the instrumentation are given in the final report by the contractor (Williston, McNeil and Associates, 1979). Data processing was by proprietary codes of the contractor but following the approach described by Vozoff (1972).

Locations of the MT sounding sites obtained in the study area are shown on figure 7. The sites were selected so as to give a detailed cross section normal to the structure in the central block and to tie to a previous survey. NTS 1 (fig. 7) was made at the same site as a station of the previous survey which revealed a highly conductive crust at 3 km depth. In general the data obtained were noisy with significant scatter observed on the sounding curves. This was attributed both to non-natural noise sources and to low natural signals. Data quality was so poor on station 1 that no attempt was made to invert the sounding. An estimate of the depth to the crustal conductor however was made by identifying the descending branch of the sounding curve and assuming infinite conductance for the basement layer giving a depth of 13.5 km.

Figure 20 gives the results of one-dimensional inversions and asymptotic interpretations for the line of MT stations 8, 2, 6, 4, 5 and 9. The section shows a conductor of 1 ohm-m present beneath the site at depths of 6 to 10 km. However station 8 in Yucca Flat shows a thick resistive section (1000 ohm-m) extending to 38 km. This same general picture was observed on two

previous detailed MT lines in Yucca Flat about 7 km north of Syncline Ridge and for which data quality was significantly better. These data show that a significant crustal discontinuity exists on the western side of Yucca Flat separating the flat from the proposed site. The discontinuity in electrical properties also appears to correlate with the boundary separating areas of poor seismic records from good record areas.

MT surveys are often limited by data scatter which puts rather wide limits on model resolution. The method, however, is the only practical means at present for obtaining deep crustal electrical information. For this reason the method has recently been extensively used in geothermal exploration in the western United States. One of the most interesting results to come from this work is the widespread observation of conductive zones in the crust at depths of 2 to 20 km such as observed at NTS. The resistivity of these conductive regions are typically less than 1 ohm-meter, and in geothermal areas often at depths less than 10 km. The mapping of such zones is an important aspect of geothermal exploration. The physical nature of these conductive zones is not fully understood at this time.

The MT results in the study area by themselves do not constitute strong evidence for a geothermal resource beneath the site. However, an anomalous crustal condition is present suggesting the potential for a geothermal system. This potential would have to be thoroughly evaluated at the site for it ever to be reconsidered for nuclear waste disposal.

Telluric traverses

Beginning in January 1978 four E-field ratio telluric traverses were run across the study area (fig. 21). The method and instrumentation have been described by Beyer (1977). Work was done by a U.S. Geological Survey

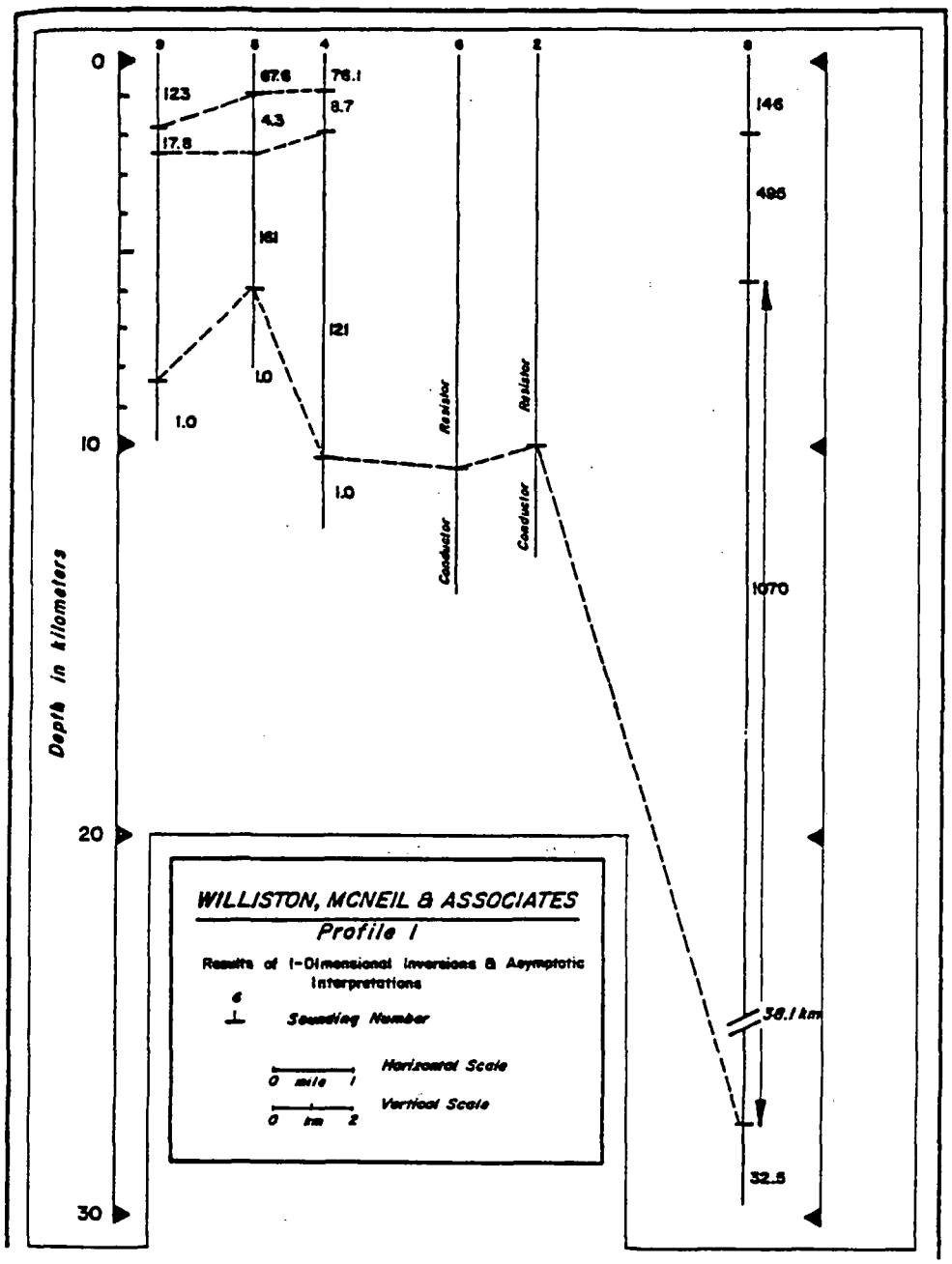

Figure 20.--Magnetotelluric geoelectric section at Syncline Ridge derived from one-dimensional inversion and asymptotic interpretation of sounding data, from Williston, McNeil and Associates (1979).

crew using equipment manufactured by the USGS. For the survey 500 m in-line dipoles were used and measurements of the Earth's natural field were made in the 20-40 sec period range. While the electrical fields at this period range sample a large part of the crust short spacial wavelength anomalies represent features of comparable extent.

Data reduction was accomplished as described by Beyer (1977). At least three sets of electric field ratio's were obtained at each recording site to insure data quality and input connections were reversed at each station to prevent cumulative error due to small differences in each recording channel. Typical station error is estimated at 3%.

Lines were referenced to each other by simultaneously recording signals at one dipole position on two lines and computing the ratio of the observed signals from the two parallel dipoles. This permitted contouring between the lines. We had hoped to be able to tie the telluric map to the MT data so as to obtain a resistivity map of the region at 20-40 sec periods. However because of the larger MT data, heterogeneity of the site, and non-correspondence of stations, only a telluric field ratio map was made (fig. 21). The resistivity map values would be proportional to the square of the electric field which was mapped. The MT data suggests that the unity contour in figure 21 would correspond to a resistivity in the range of 2 to 20 ohm-m.

The telluric map shows north to northeast trends generally following the surface structural trends. In the central and southern blocks, northeast trending lows are found on the eastern and western margins of Syncline Ridge and along or just east of the ridge crest. These lower values may be due to lower resistivity caused by fracturing along fault zones or to structural thickening of the Eleana Formation or both. On line 4 across the southern block the graben on the east side is defined by two lows correlated

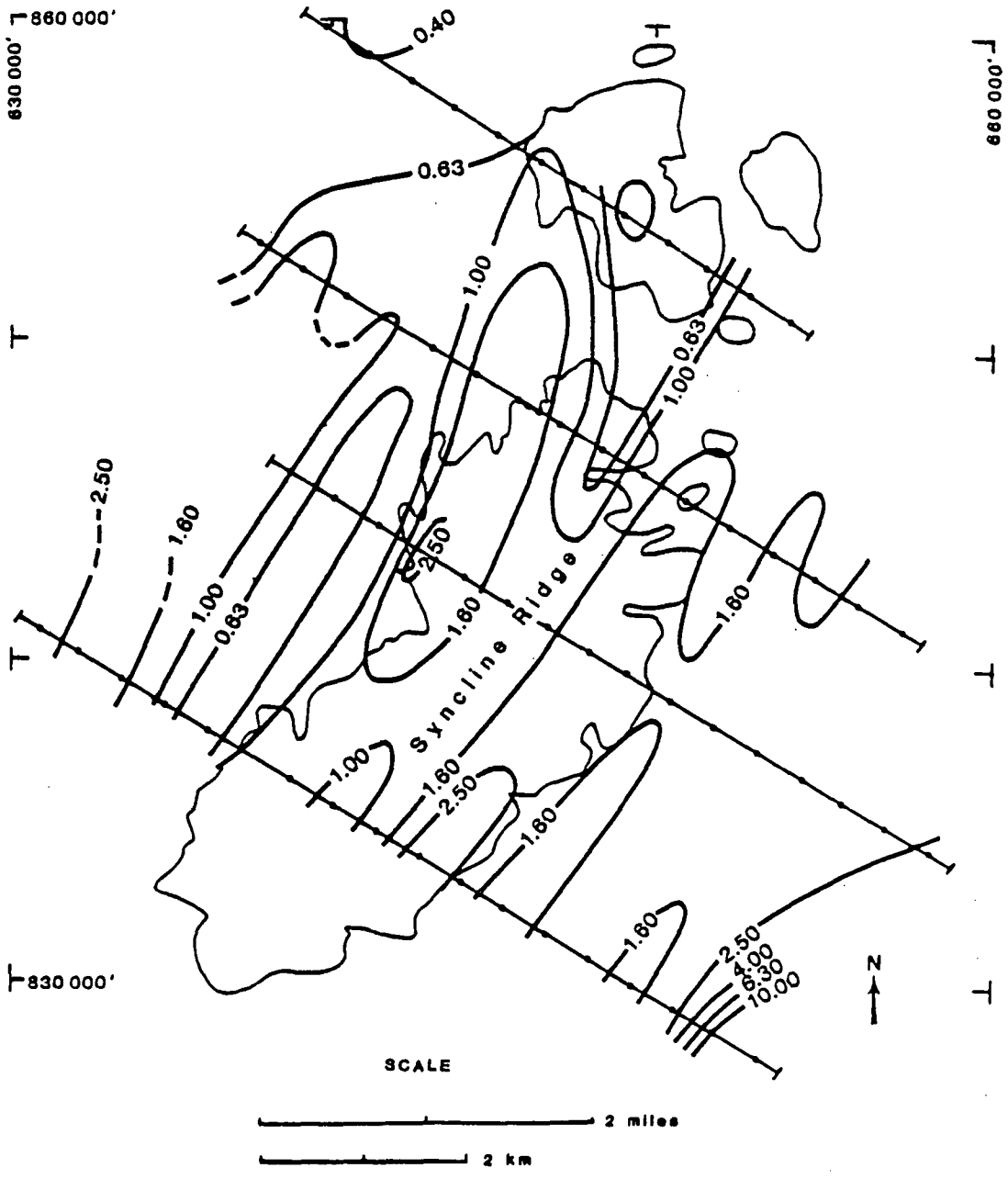

Figure 21.--Contour map of the relative electric field at 20-40 sec periods in the Syncline Ridge study area, derived from the four E-field ratio telluric traverses shown.

with the boundary faults. Very high resistivities are evident on the extreme southeastern end of this line on the flank of Mine Mountain.

Line 3 crosses the northern block where the resistivity is generally lower. Two regions on this line have values more typical of the other lines. One is over the western part of the outcrop of Tippipah Limestone and the other is on the eastern end of the line, presumably underlain by Eleana Formation. While contouring was carried between line 2 and 3 structural conditions on Gap Wash between the lines may cause the contouring to be misleading. The low values in the northwestern part of the survey show a broad region of low-resistivity rock supporting the VES data which showed a thick section of low-resistivity argillite in the same area.

Summary

The geophysical studies show that the Syncline Ridge study area is structurally complex. The general geological framework presented by earlier studies is supported. The geophysical work, however, reveals more extensive faulting and larger vertical offset than had been recognized earlier, and extensive variation in the proposed host rock within the site. Although the geophysical work was quite extensive many structural questions remain due to the complexity of the site.

The lateral fault separating the southern and central blocks is supported in the geophysical data. The lateral fault separating the central and northern blocks is not as clearly defined in part due to insufficient data. Lateral physical properties contrast across the inferred trace however are not distinct as further south. The graben on the east side of the southern block was identified by several methods. The general synclinal structure is verified by the seismic reflection data. The central axis appears displaced west of the axial fault. The central portion of the syncline has been down dropped between the axial fault along the ridge crest and a northeast-trending fault on the western edge of the ridge. The eastern half of the ridge proper appears to have suffered more extensive faulting with significant vertical movement along a fault on the eastern margin of the ridge. The axial fault which had not been considered to have undergone much displacement from earlier geological studies, appears as a major geophysical discontinuity, the geophysical data implying significant movement and fracturing. Faulting cutting alluvium was identified on the eastern side of the ridge, thus probably of Quaternary age, which implies recent movement.

The Eleana Formation, which is the proposed host medium here, appeared from electrical studies to lack continuity. This is inferred to be due to structural complexity. A small area in the northwest part of the study area was identified where the Eleana argillite subunit appears relatively undisturbed and of sufficient thickness for repository use.

Several deep crustal structural features were noted which could have significance for the repository siting. A north-trending crustal feature identified by seismic and electrical studies bounds the eastern margin of the site approximately along Nevada coordinate E 662,000. West of this line, very conductive rocks were identified at less than 10 km depth, possibly implying a potential geothermal system and resource. Gravity and MT data also show that the deeper crustal structural trends are realigned from the north to northeast direction seen at the surface to northwest at depth.

References

Anderson, L. A., Bisdorf, R. J. and Schoenthaler, D. R., 1980, Resistivity sounding investigation by the Schlumberger method in the Syncline Ridge area, Nevada Test Site, Nevada: U.S. Geological Survey Open-File report 80-466.

Bath, G. D., 1968, Aeromagnetic anomalies related to remanent magnetism in volcanic rock, Nevada Test Site, in Eckel, E. B., ed., Nevada Test Site: Geol. Soc. America Mem. 110.

Beyer, J. H., 1977, Telluric and D.C. resistivity techniques applied to the geophysical investigation of Basin and Range geothermal systems: Univ. of Calif. Lawrence Berkeley Lab. report LBL-6325.

Flanigan, Vincent J., 1979, A slingram survey on the Nevada Test Site: U.S. Geological Survey Open-file Report 79-277.

Gardner, P. G., 1978, Final report of vibroseis survey of the Syncline Ridge area of Nevada Test Site: unpublished report for the U.S. Geological Survey by Western Geophysical Co., on file in Denver office of United States Geological Survey.

Healey, D. L., 1968, Application of gravity data to geologic problems at Nevada Test Site; in Eckel, E. B., ed., Nevada Test Site: Geol. Soc. America Mem. 110.

Hodson, J. N. and Hoover, D. L., 1979, Geology of the UE17e drill hole, area 17, Nevada Test Site: U.S. Geological Survey report USGS-1543-2.

Hoover, D. L. and Morrison, J. N., 1980, Geology of the Syncline Ridge area related to nuclear waste disposal, Nevada Test Site, Nye County, Nevada: U.S. Geological Survey open file report 80-942.

Keller, G. V. and Frischknecht, F. C., 1966, Electrical methods in geophysical prospecting: New York, N. Y., Pergamon Press, 517 p.

Mossman, R. W. and Garrette, F. I., 1972, Report on a vibroseis seismic survey conducted in Nye County, Nevada: unpublished report for U.S. Atomic Energy Commission by Seismograph Service Corp., on file in Denver office of the United States Geological Survey.

Orkild, P. P., 1963, Geologic map of the Tippipah Spring Quadrangle, Nye County, Nevada: U.S. Geological Survey Quadrangle Map GQ-213.

Vozoff, K., 1972, The magnetotelluric method in the exploratin of sedimentary basins: Geophysics, v. 37, no. 1.

Williston, McNeil and Associates, 1979, Nevada Test Site magnetotelluric survey: unpublished report for U.S. Geological Survey,on file in Denver office of United States Geological Survey.

Wollard, G. P. and Rose, J. C., 1963, International gravity measurements: Menasha, Wisc., Geo. Banta Co. Inc.

Word, D. R., Halpin, D. and Owens, K., 1977, Magnetotelluric survey in the Yucca Flats area of southern Nevada: unpublished report for Lawrence Livermore Laboratories, Univ. of Calif., by Geotronics Corp., on file in Denver office of United States Geological Survey.

Zohdy, A. A. R., 1974, A computer program for the automatic interpretation of Schlumberger sounding curves over horizontally layered media: NTIS (National Technical Information Service) PB-232 703/AS, 25 p, Springfield, Va.

_____1975, Automatic interpretation of Schlumberger sounding curves using modified Dar Zarrouk functions: U.S. Geological Survey Bulletin 1313-E, 39 p.

Appendix 1.

The following seismic refraction velocity sections were derived from an interactive computer program of H. D. Ackermann (unpub. program, 1981).

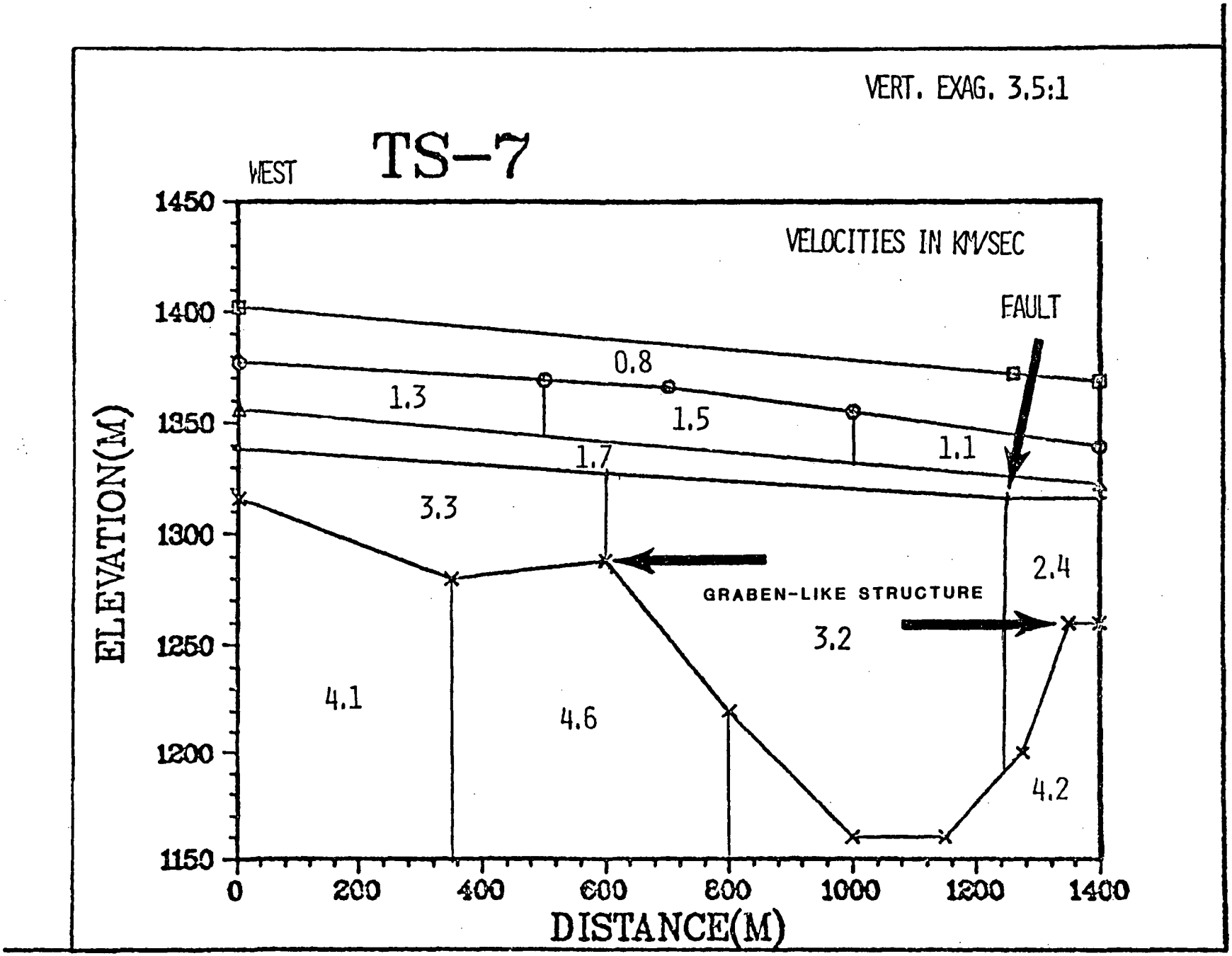
VERT. EXAG. 3.5:1
TS-7
WEST
VELOCITIES IN KM/SEC
FAULT
0.8
1.3
1.5
1.1
1.7
3.3
2.4
GRABEN-LIKE STRUCTURE
3.2
4.1
4.6
4.2
ELEVATION(M)
1450
1400
1350
1300
1250
1200
1150
0
200
400
600
800
1000
1200
1400
DISTANCE(M)

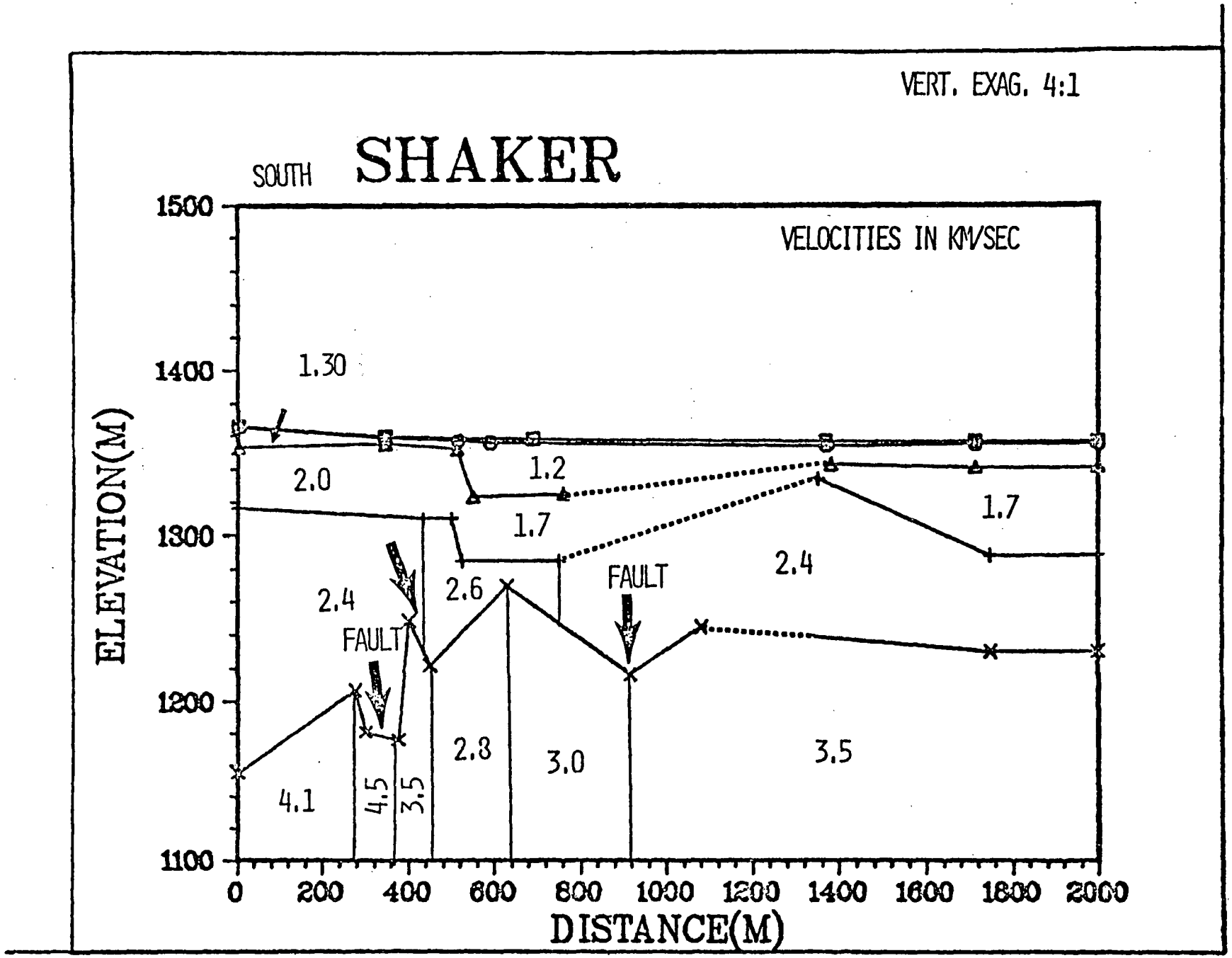
VERT. EXAG. 4:1
SHAKER
SOUTH
VELOCITIES IN KM/SEC
ELEVATION(M)
DISTANCE(M)
1500
1400
1300
1200
1100
0
200
400
600
800
1000
1200
1400
1600
1800
2000
1.30
2.0
1.2
1.7
1.7
2.4
2.6
2.4
FAULT
FAULT
4.1
4.5
3.5
2.8
3.0
3.5

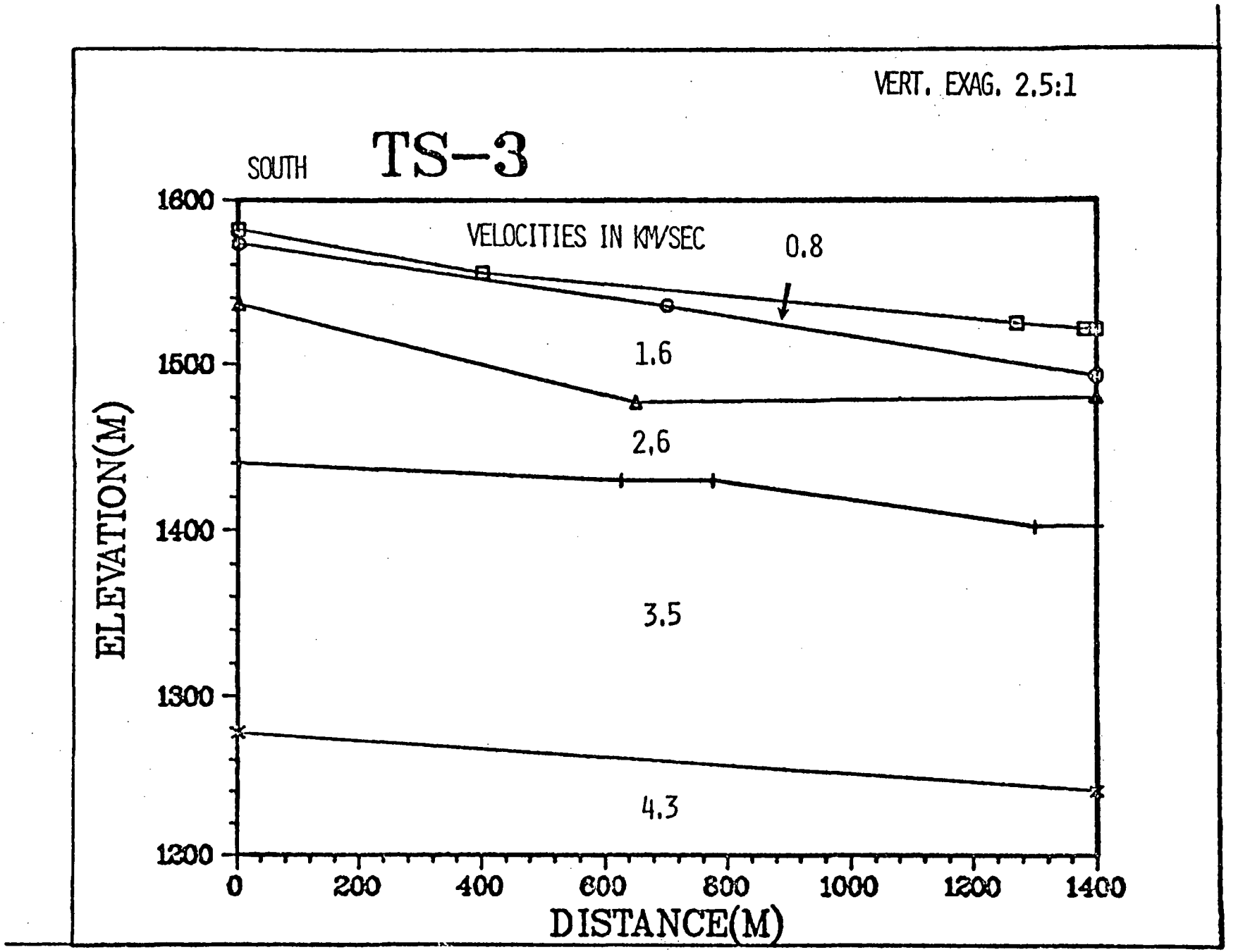
VERT. EXAG. 2.5:1
TS-3
SOUTH
VELOCITIES IN KM/SEC
0.8
1.6
2.6
3.5
4.3
1600
1500
1400
1300
1200
ELEVATION(M)
0
200
400
600
800
1000
1200
1400
DISTANCE(M)

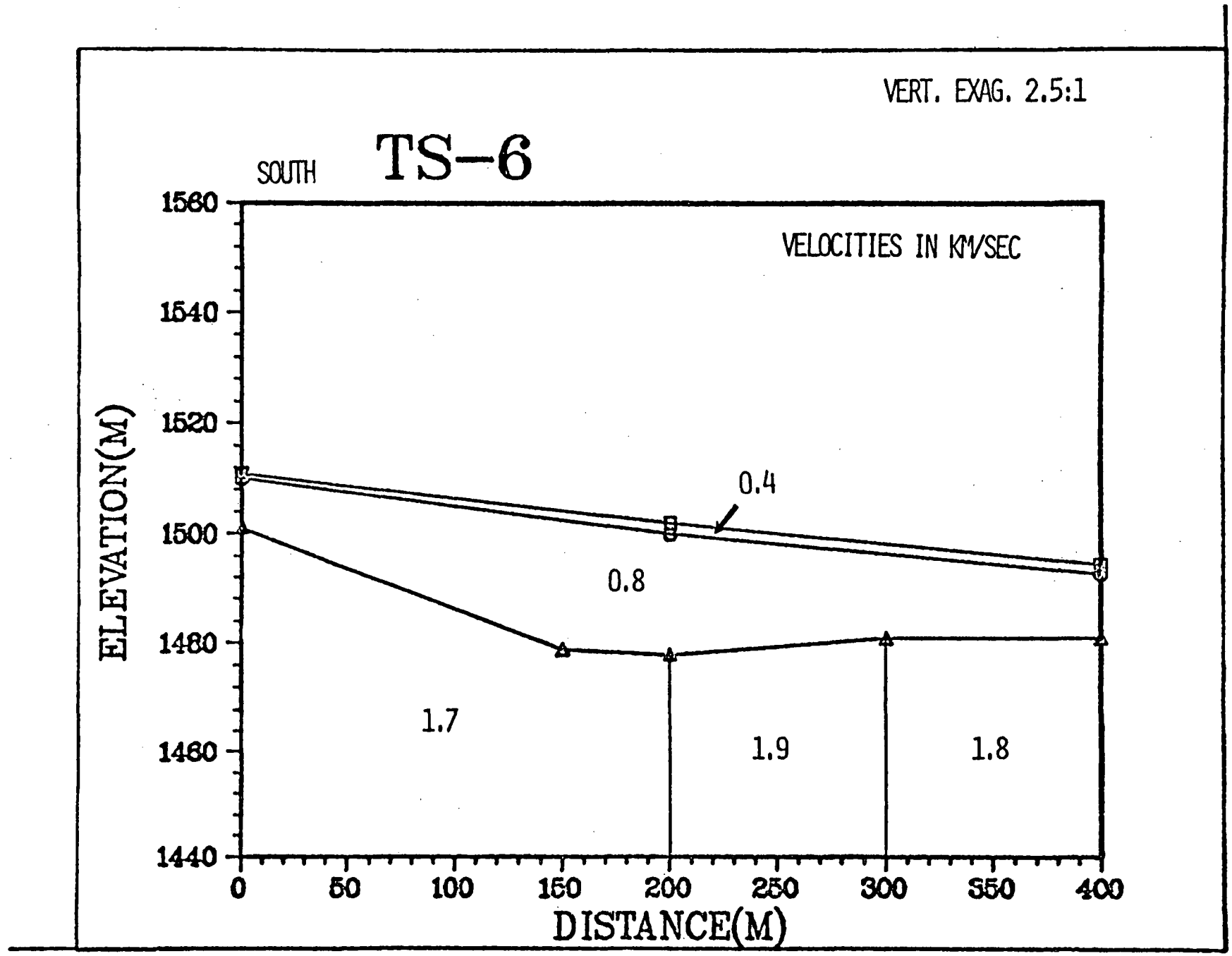
VERT. EXAG. 2.5:1
TS-6
SOUTH
VELOCITIES IN KM/SEC
0.4
0.8
1.7
1.9
1.8
1560
1540
1520
1500
1480
1460
1440
ELEVATION(M)
0
50
100
150
200
250
300
350
400
DISTANCE(M)

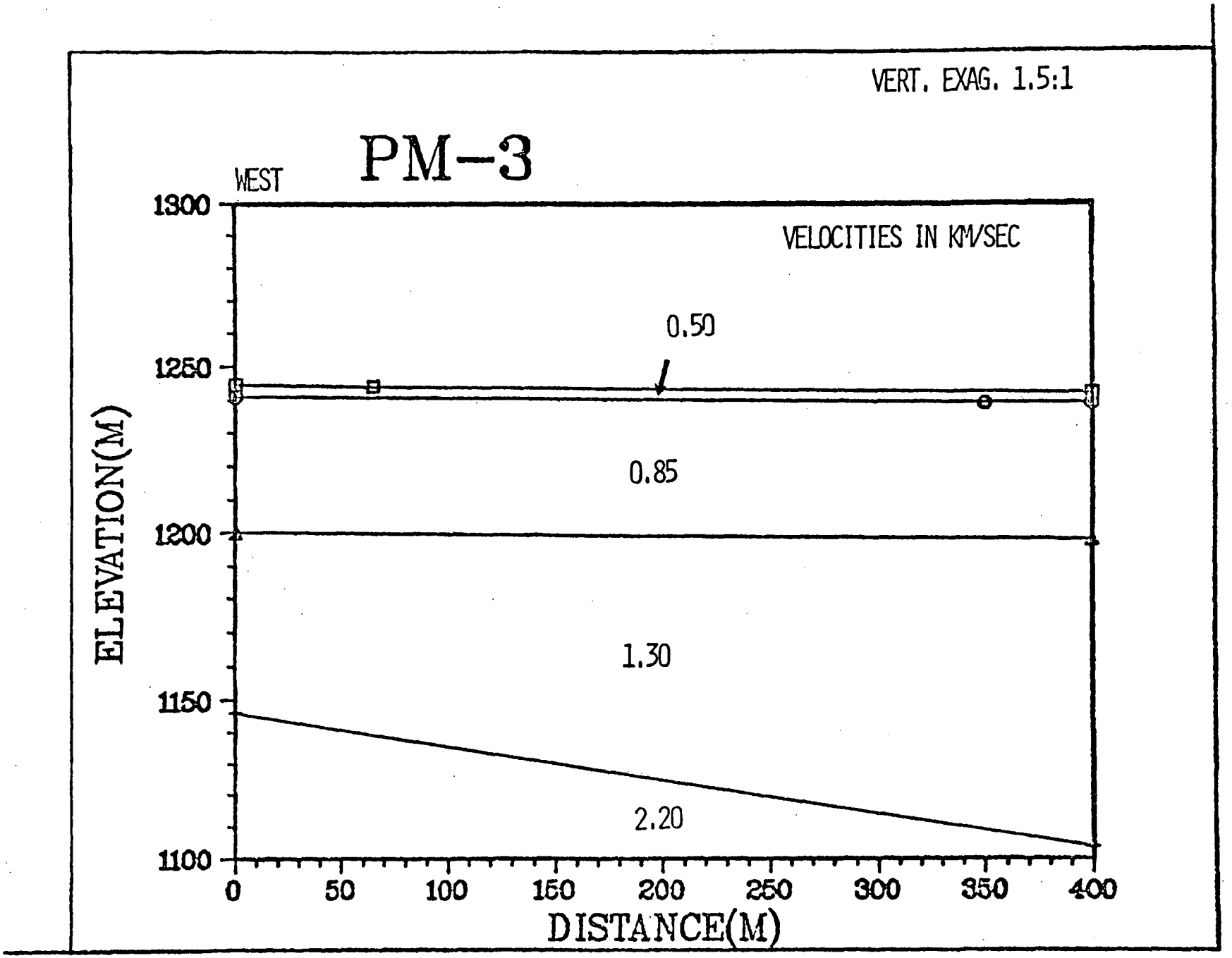
VERT. EXAG. 1.5:1
PM-3
WEST
VELOCITIES IN KM/SEC
0.50
0.85
1.30
2.20
1300
1250
1200
1150
1100
ELEVATION(M)
0
50
100
150
200
250
300
350
400
DISTANCE(M)

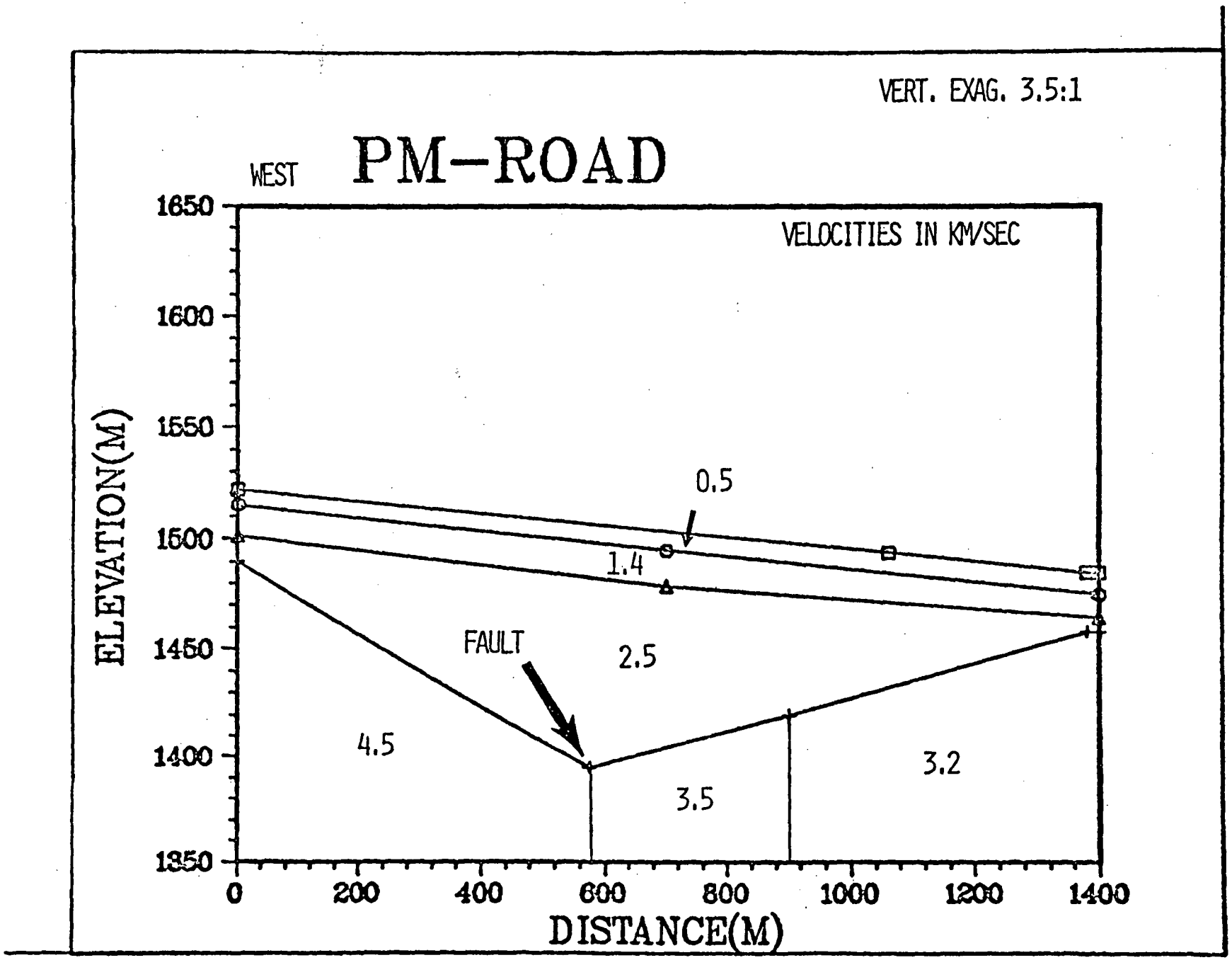
VERT. EXAG. 3.5:1
PM-ROAD
WEST
VELOCITIES IN KM/SEC
ELEVATION(M)
1650
1600
1550
1500
1450
1400
1350
0.5
1.4
FAULT
2.5
4.5
3.5
3.2
0
200
400
600
800
1000
1200
1400
DISTANCE(M)

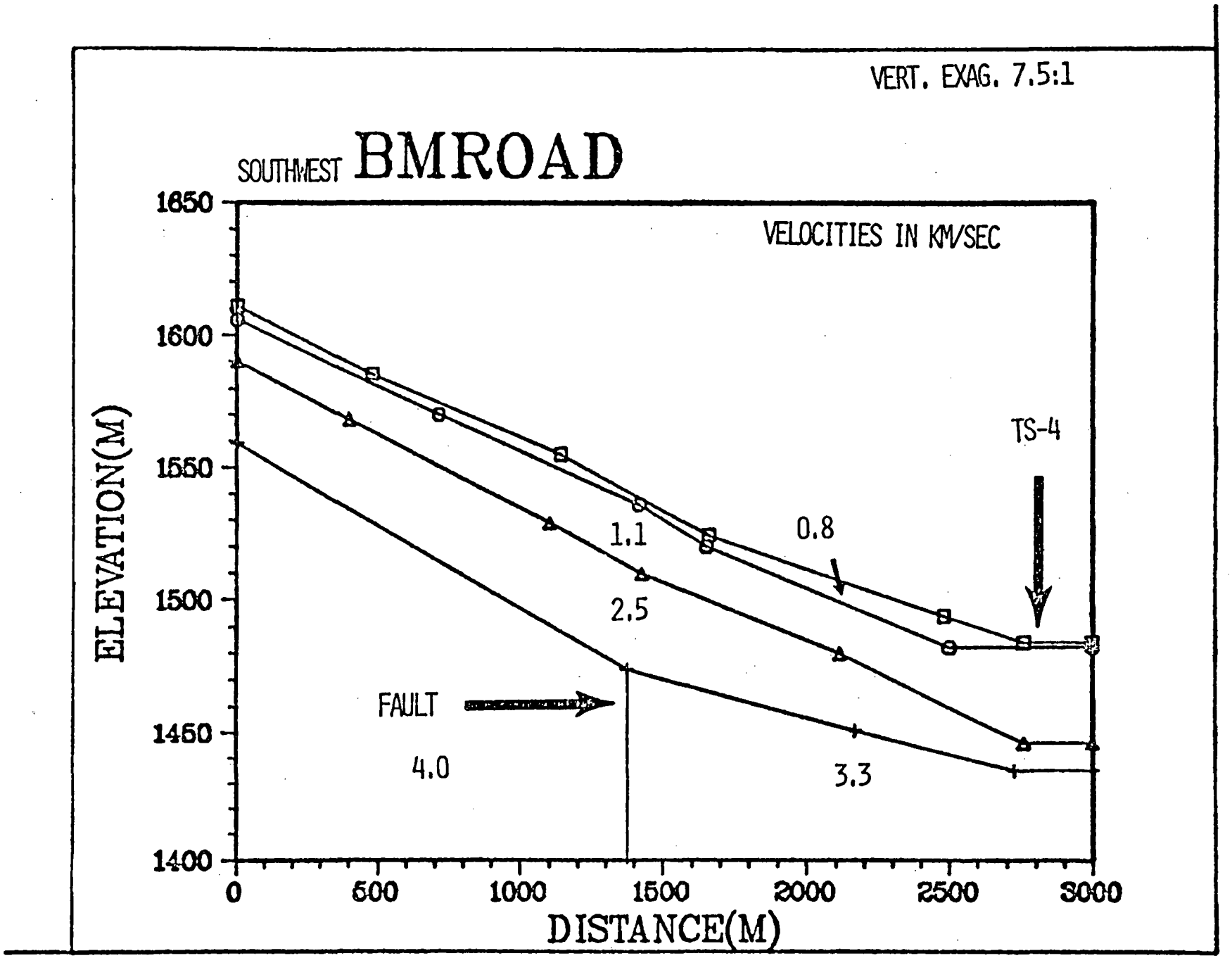
VERT. EXAG. 7.5:1
SOUTHWEST
BMROAD
VELOCITIES IN KM/SEC
TS-4
0.8
1.1
2.5
3.3
4.0
FAULT
ELEVATION(M)
1650
1600
1550
1500
1450
1400
0
500
1000
1500
2000
2500
3000
DISTANCE(M)

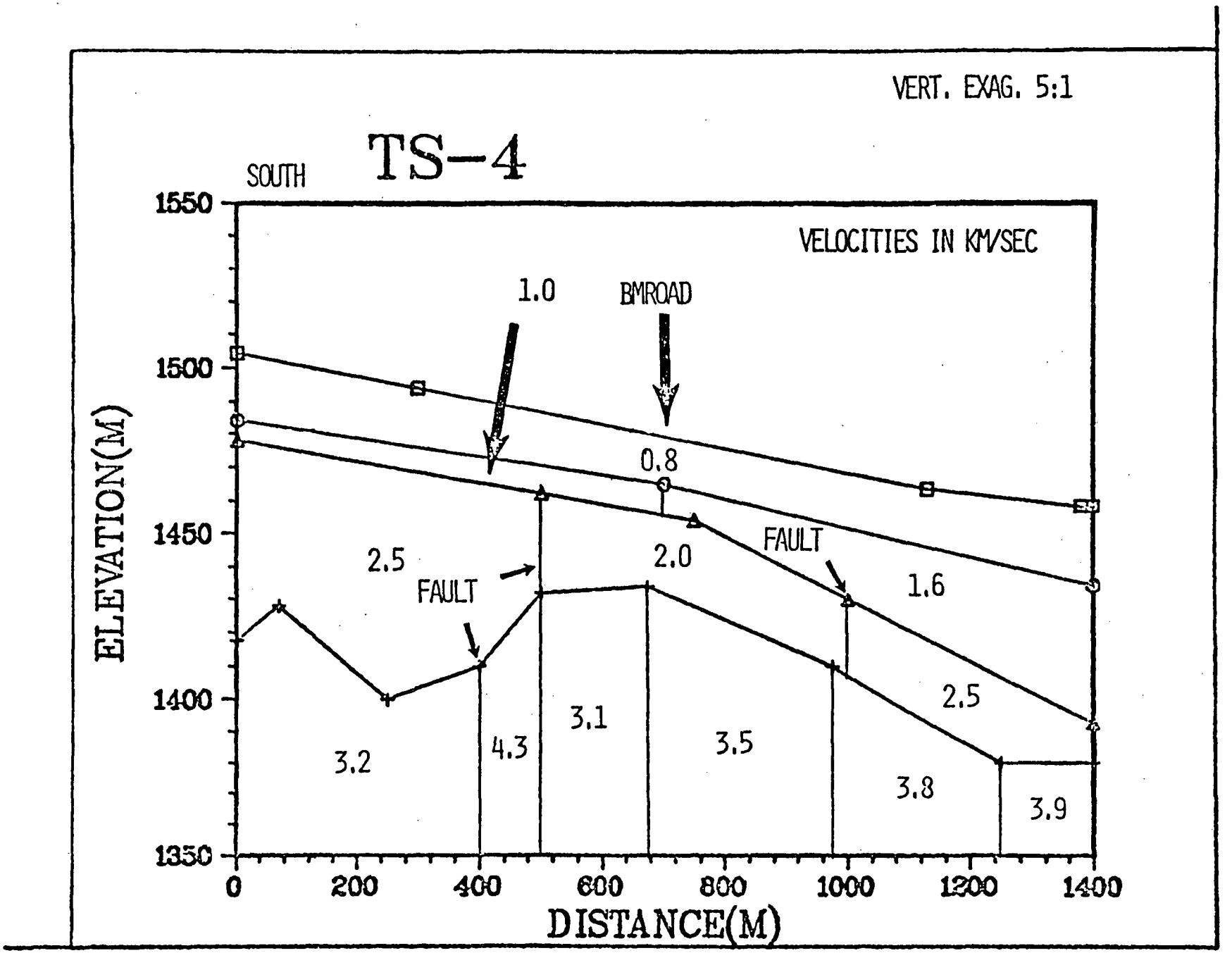
VERT. EXAG. 5:1
TS-4
SOUTH
VELOCITIES IN KM/SEC
1.0
BMROAD
0.8
FAULT
2.5
FAULT
2.0
1.6
2.5
3.1
4.3
3.2
3.5
3.8
3.9
1550
1500
1450
1400
1350
ELEVATION(M)
0
200
400
600
800
1000
1200
1400
DISTANCE(M)

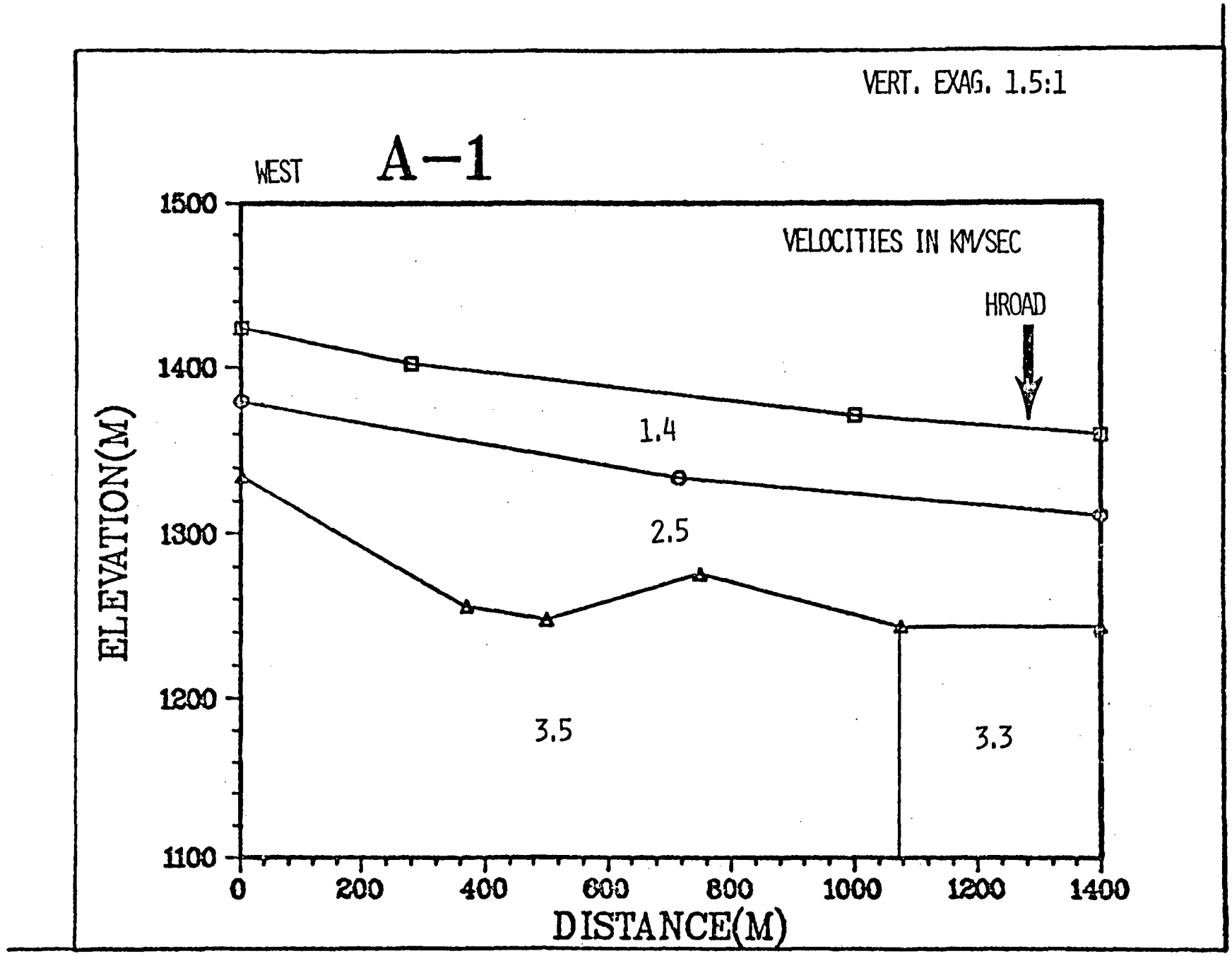
VERT. EXAG. 1.5:1
A-1
WEST
VELOCITIES IN KM/SEC
HROAD
1.4
2.5
3.5
3.3
1500
1400
1300
1200
1100
ELEVATION(M)
0
200
400
600
800
1000
1200
1400
DISTANCE(M)

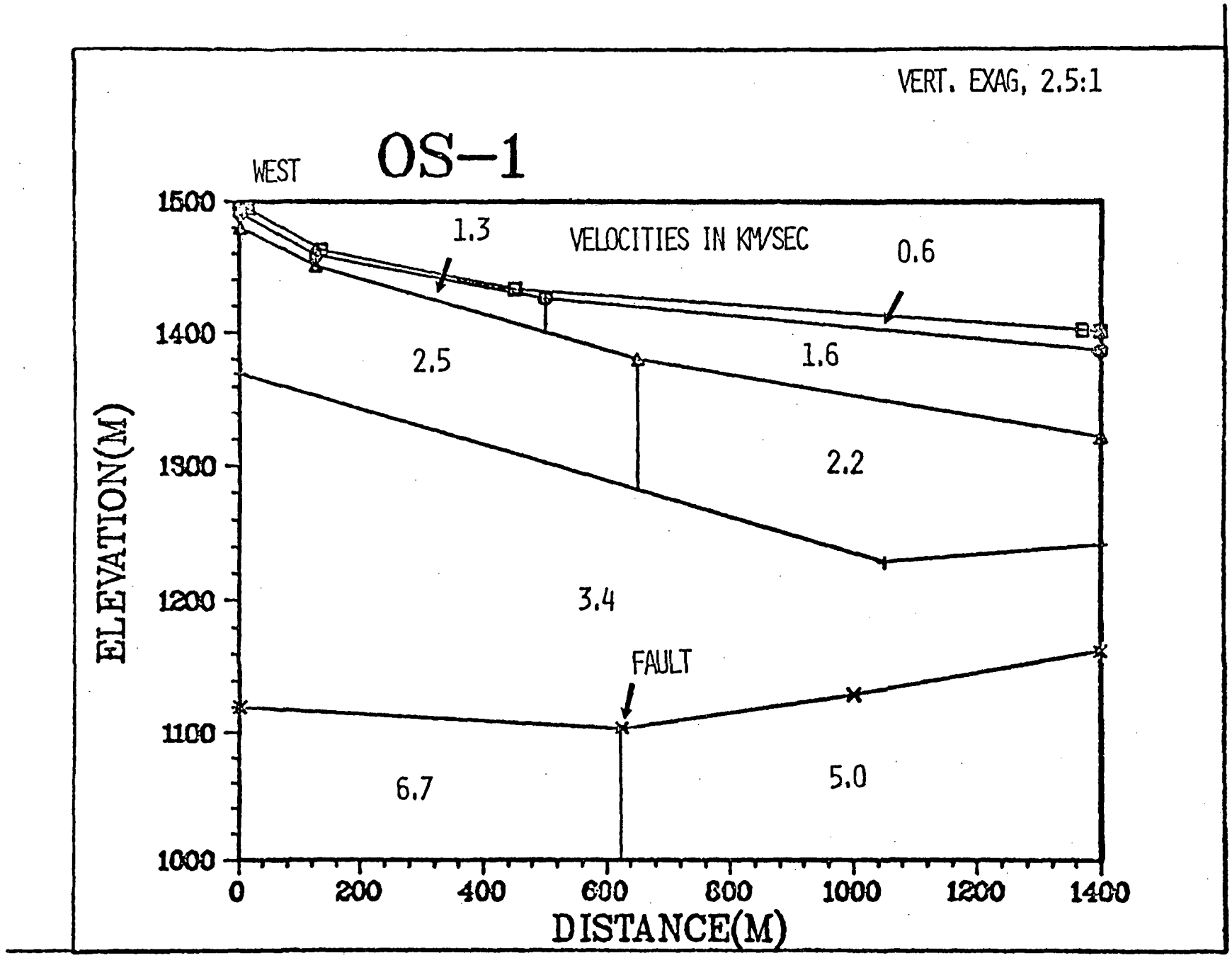
VERT. EXAG, 2.5:1
OS-1
WEST
VELOCITIES IN KM/SEC
1.3
0.6
2.5
1.6
2.2
3.4
FAULT
6.7
5.0
1500
1400
1300
1200
1100
1000
ELEVATION(M)
0
200
400
600
800
1000
1200
1400
DISTANCE(M)

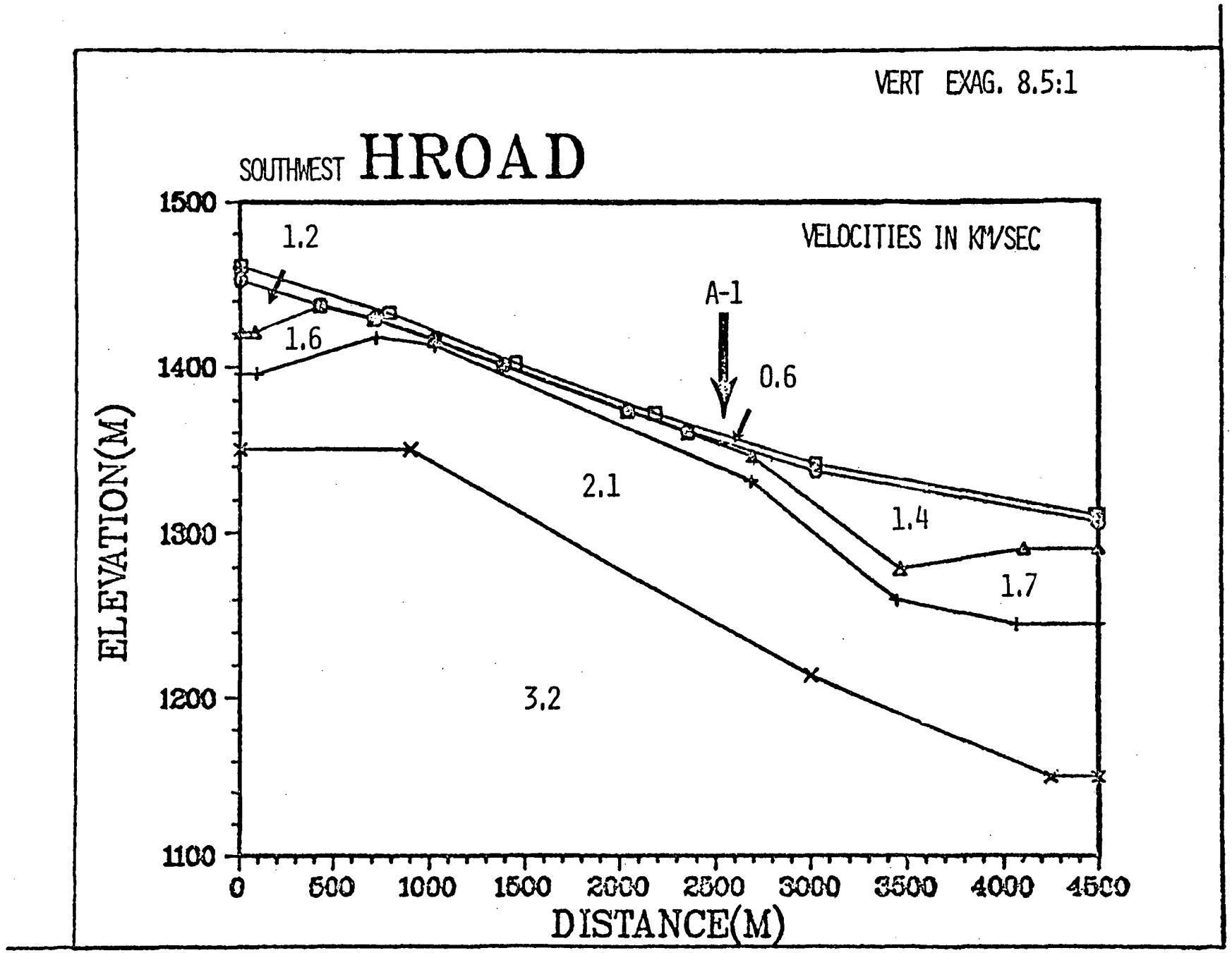

☆ U.S. GOVERNMENT PRINTING OFFICE: 1982—579-218/268 REGION No. 8

VES-ER, aeromag

USGS-OFR-82-897

USGS-OFR-82-897

UNITED STATES
DEPARTMENT OF THE INTERIOR
GEOLOGICAL SURVEY

A SCHLUMBERGER RESISTIVITY SURVEY OF THE AMARGOSA DESERT, SOUTHERN NEVADA

by

Michael R. Greenhaus

and

Charles J. Zablocki

Open-File Report 82-897

1982

Prepared by the U.S. Geological Survey

for the

Nevada Operations Office
U.S. Department of Energy
(Interagency Agreement DE-AI08-78ET44802)

A SCHLUMBERGER RESISTIVITY SURVEY OF THE AMARGOSA DESERT, SOUTHERN NEVADA

by

Michael R. Greenhaus

and

Charles J. Zablocki

INTRODUCTION

During 1978-1980, the U.S. Geological Survey carried out a geoelectric survey consisting of 136 Schlumberger resistivity soundings in the Amargosa Desert, Nevada, in support of hydrological studies being performed by the Water Resources Division in this area. These studies are part of the Radwaste Program effort to find a suitable site for nuclear waste storage within the Nevada Test Site, north of the Amargosa Desert. The aim of the geoelectric survey was to define basement structure and basin-fill characteristics, which may or may not be influencing the hydrological systems of the region.

SURVEY DESCRIPTION AND METHODS

Figure 1 shows the region of the geoelectric survey and the locations and azimuths of the 136 Schlumberger resistivity soundings. Maximum electrode separations ranged from AB/2=4000 feet (1219 meters) to AB/2=8000 feet (2438 meters). Crossed pairs of soundings were made at several locations as a check for anisotropy. Also, several sounding locations were reoccupied in order to sound deeper at locations where the original sounding did not detect the basement.

The resulting sounding curves were processed and interpreted using an automatic interpretation program developed by Adel Zohdy (unpub. program, U.S. Geological Survey, 1973, 1975). The results, plotted on 3 cycle x 4 cycle

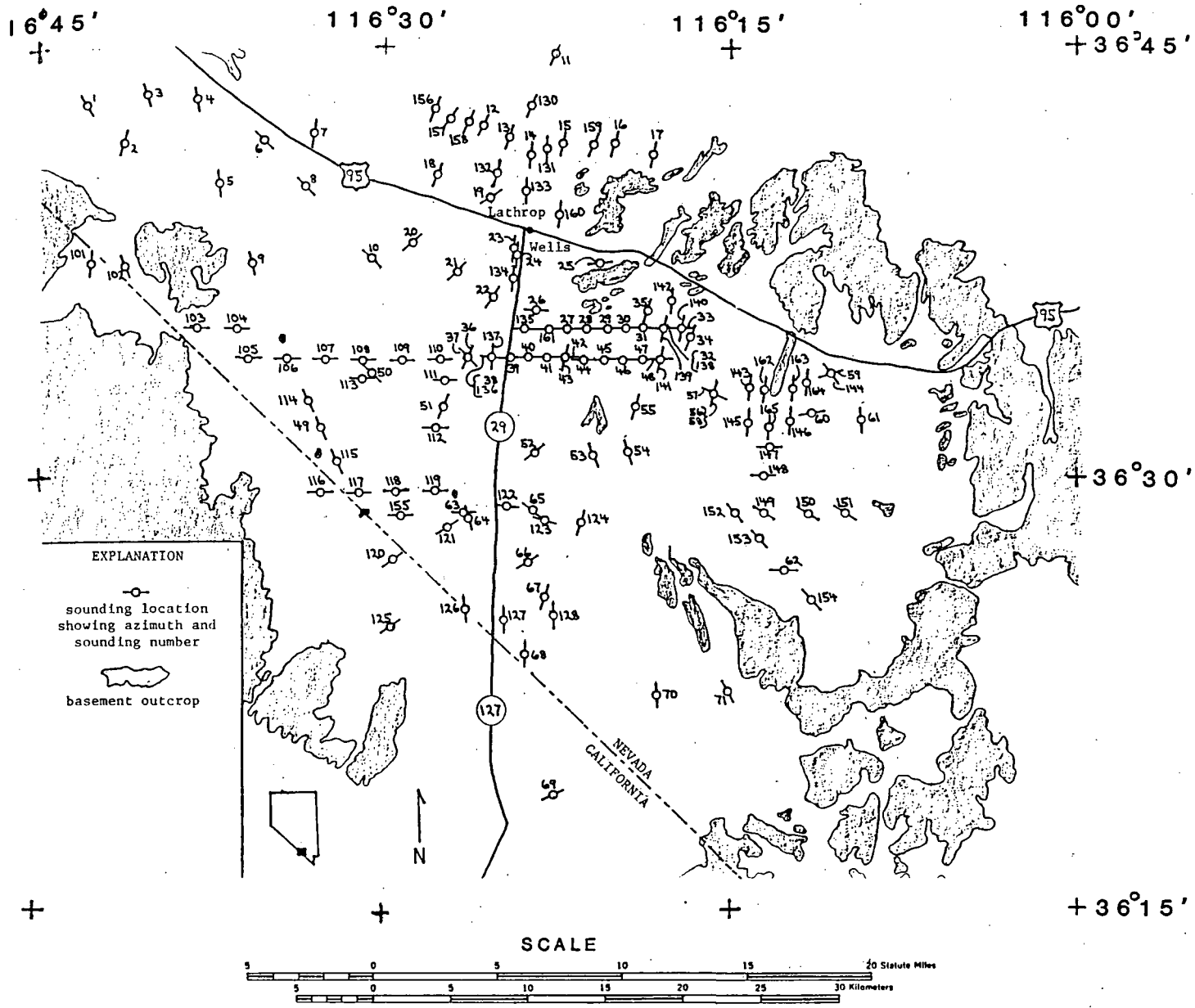

Figure 1. Schlumberger sounding locations, Amargosa Desert region.

log-log graphs, are included in the appendix. The soundings have been numbered AMAR 1 through AMAR 71, and AMAR 101 through AMAR 165. Each graph includes the following:

(1) The field data, shown by "x" symbols, which plot as a discontinuous curve of offset curve segments.

(2) A digitized-data curve shown by square symbols. This curve was obtained by shifting the offset segments of the field data with respect to the last segment to produce a continuous curve (Zohdy and others, 1973), and then digitizing this curve at a rate of six points per logarithmic cycle using a subroutine in a computer program for bicubic spline functions (Anderson, 1971).

(3) The layered model, represented by a solid-line step function, showing layers of various thicknesses and resistivities. This model is obtained by entering the digitized data points into the automatic interpretation program (Zohdy, 1973, 1975) which, through iteration, finds a horizontally layered model, the theoretical sounding curve of which best fits the digitized data curve.

(4) The best-fitting theoretical sounding curve, shown as a continuous, solid-line curve, computed from the layered model.

(5) The Dar Zarrouk curve for the layered model, plotted as "+" symbols. This curve has been shifted vertically by one logarithmic cycle in order to avoid confusion due to clutterring of the curves. The Dar Zarrouk curve can be used to simplify the model by reducing the number of layers (Zohdy, 1974).

RESULTS

The Amargosa Desert is a region which is well suited for resistivity soundings. It is basically a sediment-filled basin surrounded by ranges of outcropping basement rocks, the typical structure of the Basin and Range tectonic province.

Basement The basement rocks, composed of Paleozoic carbonates with some Precambrian and Cambrian clastics, will generally have resistivities greater than several hundred ohm-meters. The overlying basin-fill sediments, composed of clay, sand, gravel, and boulders, have much lower resistivities, particularly when clay content is high and when the sediments are saturated. This setting presents a large resistivity contrast between the basement rocks and the overlying sediments, allowing for fairly easy recognition of basement in the resistivity sounding curves. When the high resistivity basement has been reached after sounding through a medium of much lower resistivity, the curve swings up to a slope approaching $+45^{\circ}$, which is the theoretical limit of the slope (for horizontally stratified media) as the resistivity contrast approaches infinity. This can be seen on the deep end of many of the sounding curves in this report.

Figure 2 shows the sounding locations with the corresponding interpreted basement depths in meters. The shaded areas are basement outcrops. At stations where basement was not detected with the maximum electrode spacing, the letters "NB" ("no basement") appear. A question mark (?) indicates a sounding where the basement signature was not clear, or where the last data point (maximum electrode separation) just started to show what may have been basement signature, the uncertainty due to the absence of more data at greater electrode separation.

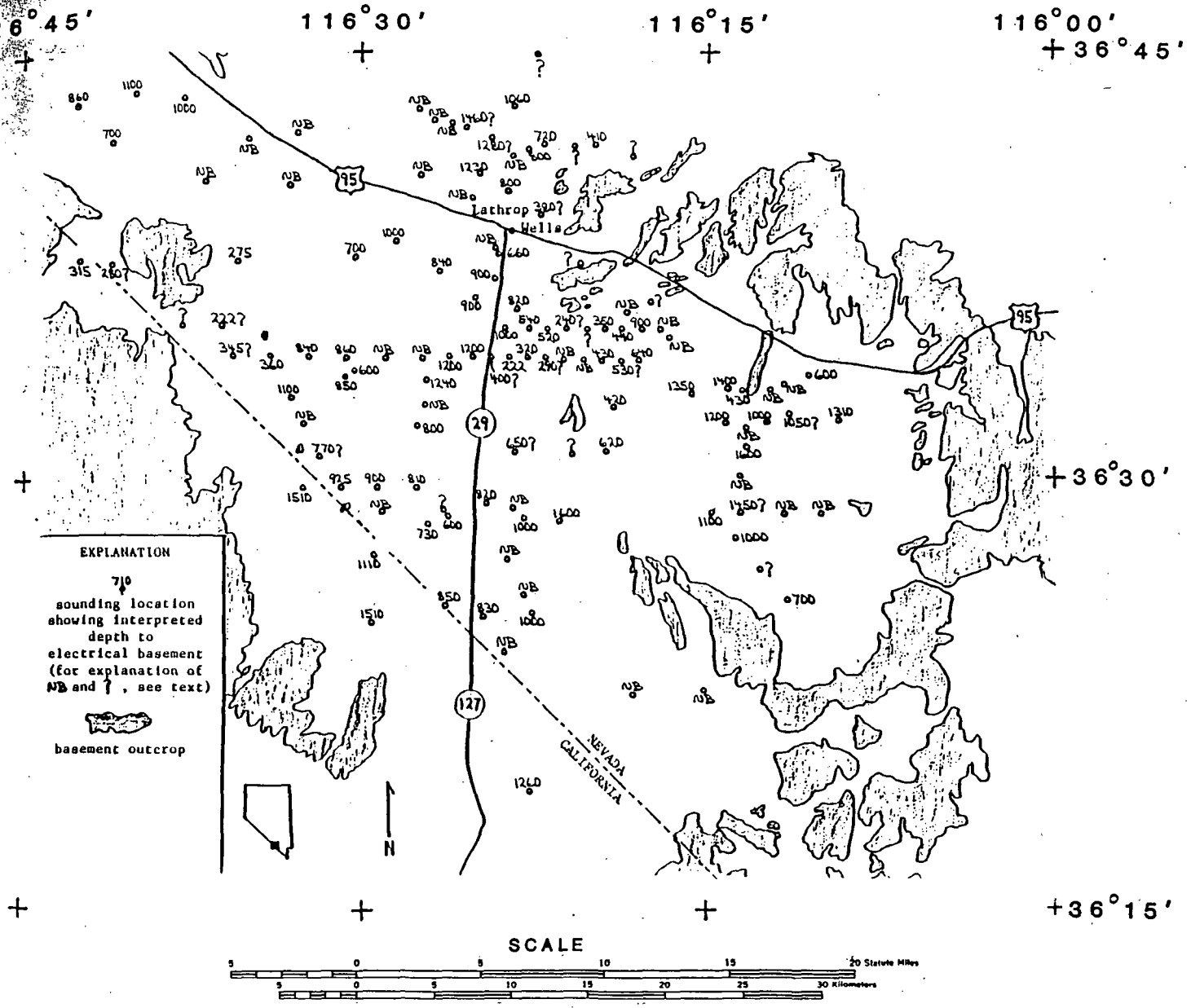

Figure 2. Interpreted depths to electrical basement from Schlumberger sounding results, Amargosa Desert region. Depths are in meters.

A cautionary word is necessary about what is being identified as basement from these sounding curves. As explained above, the basement surface is taken to be at the depth at which the top of the medium of much higher resistivity is encountered. This is commonly referred to as the "electrical basement." In the simplest case, this low resistivity-high resistivity interface would correspond to the actual geological interface between sedimentary fill and basement. However, if the uppermost section of the geologic basement has been fractured extensively, these fractures could be filled with clayey sediments and saturated with water, thus lowering the resistivity of this section. In this case, the top of the electrical basement inferred from the resistivity sounding would be at a greater depth than the top of the actual geologic basement. This is illustrated by an example from this survey. On correlation of one sounding, AMAR 162, with a lithological log for a nearby well (Johnston, 1971), a disagreement in depth to basement was seen. The well log indicated that basement rocks (in this case, dolomite and limestone) were encountered at 189 meters, where as the electrical sounding showed an apparent electrical basement depth of 430 meters. In this case, the depth to electrical basement is probably the depth to coherent basement, which is overlain by a section of highly fractured basement rock.

It should also be noted that when basement is identified by the upswing of only the last few data points in a sounding, and the last and highest resistivity value is still below the expected range of resistivities for the basement, it is possible that this is due to a thick, relatively high resistivity layer within the basin-fill sediments, and that the basement surface is at an even greater depth. However, the existence of such a high resistivity layer within the sedimentary section throughout the entire region of the survey is not likely.

The general picture of basement relief from the soundings shows the expected shallowing of basement toward the basement outcrops, with the greater depths occurring beneath the valleys between outcrops. The most pronounced feature of basement structure made apparent by this survey is the large vertical offset south of Lathrop Wells (figures 2 and 3). This north-south trending feature, downthrown on the west side, and probably the result of normal faulting, was first recognized in a regional gravity survey of the region by Healey and Miller (1971). It is most apparent between soundings 136 and 39, showing about 800 meters of vertical offset within a lateral distance of 2438 meters. The offset is not as abrupt to the north, and probably occurs as a series of sub-parallel, lesser normal faults west of the basement outcrops. To the south, all the soundings appear to be on the down-dropped side of the fault. This offset appears to be the southern continuation of the east side of the Forty-mile Wash graben to the north. Figure 3 shows the approximate location of this feature as derived from the regional gravity data (Healey and Miller, 1971), and its apparent location in one area as determined by three different methods; Schlumberger soundings (this report), tellurics (D. B. Hoover, unpublished data, 1979) and detailed gravity (H. W. Oliver, unpublished data, 1980), all along the same profile. The fairly close agreement in fault location among the three detailed profiles, and their difference from the fault location as modelled from the regional gravity, may be due to the expected lack of accuracy in locating structural features from the sparse distribution of the regional gravity data, or may be an indication that this offset is distributed among several parallel or sub-parallel normal faults.

Basin-fill Due to the complexity of the basin-fill sediments encountered over the large area covered in this survey, the basin-fill characteristics that are

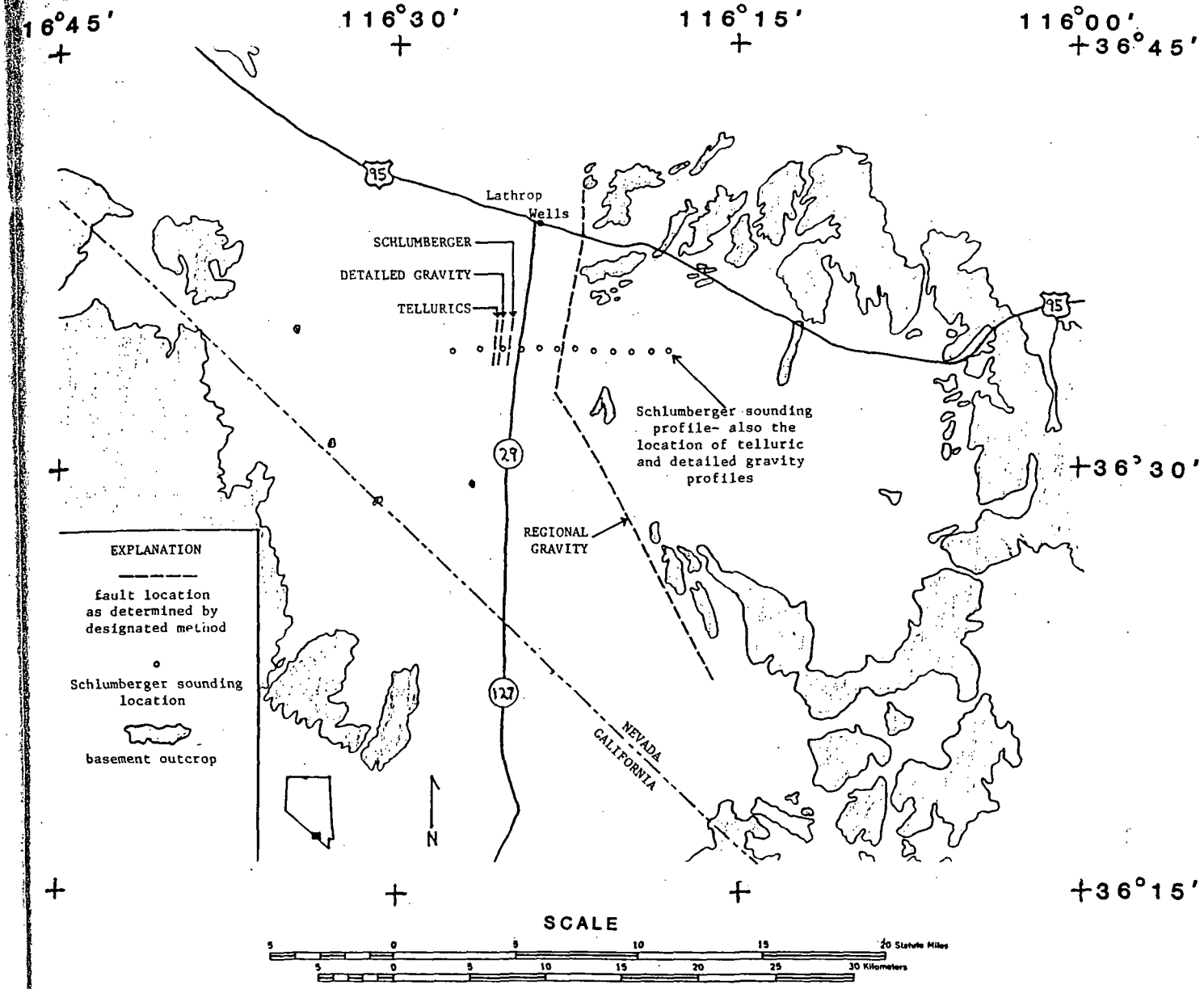

Figure 3. Comparison of four geophysical methods in determining the location of an inferred fault concealed beneath the Amargosa Desert (see text).

reflected in the resistivity soundings will be discussed in general terms. Lithologic logs for wells throughout the Amargosa Desert indicate a basin-fill composed of clay, sand, gravel, and boulders. In the area just south of Lathrop Wells, south of highway 95, a top sedimentary section, varying in thickness from about 7 to 25 meters, with resistivities from several tens to several hundred ohm-meters, can be seen in most of the sounding curves. Beneath this, and down to the top of the basement, is a section with resistivities mostly in the range of 10-100 ohm-meters. This grouping of layers of relatively higher resistivities overlying layers of generally lower resistivities probably represents a section of essentially dry sand and gravel layers at the surface overlying a section of saturated clayey sand, with varying amounts of clay throughout the section. The layers with resistivities less than 10 ohm-meters could be clay beds, or perhaps indicate the presence of saline groundwater. North of the highway, the soundings show a thicker top section of dry sediment, with the saturated and perhaps more clayey sediments starting at a depth of about 100 meters, and continuing down to the basement.

Toward the western margin of the survey area, the soundings show evidence of layers of clay, sand, and gravel. Resistivities range from less than 10 ohm-meters, probably for water-saturated sediment or possibly high clay content, to near 1000 ohm-meters, for dry layers of sand and gravel. Most of the resistivities are between 10 and 100 ohm-meters, most likely representing various layers of the sediment types mentioned above.

The soundings in the southern part of the survey area, near the state border, again show evidence of various layers of clay, sand, and gravel, with resistivities ranging from less than 10 ohm-meters to several hundred ohm-meters. In one sounding AMAR 118, layers of over 1000 ohm-meters (probably caliche) are possible. Again, the high resistivities in this area occur at shallower depths and can thus be attributed to dry layers.

The eastern part of the survey area, in addition to having the typical sounding results discussed thus far, contains three adjacent soundings (AMAR 149,153, and 62) which show a simple three-layer picture. The uppermost layer, from the surface to a depth of about 25 meters, has resistivities of 1-3 ohm-meters, among the lowest resistivities in this survey. As all three soundings are located within a playa, this thin, top layer most likely consists of playa deposits. The second layer, from 25 meters to about 1000 meters depth, with resistivities from 10 to 30 ohm-meters, probably represents a layer of sand and silt, with varying clay content. The third and deepest layer is the basement, with resistivities over 100 ohm-meters (AMAR 153).

In most of the soundings on the downthrown, western side of the major normal fault discussed earlier, some of the lowest resistivities (10 ohm-meters) occur just before reaching electrical basement. This could indicate several hundred feet of sediments with very high clay content, or the presence of saline groundwater, just above the basement throughout this area.

AEROMAGNETIC SURVEY

An interesting feature in the magnetics of part of the study area sheds some light on the nature of the basin-fill sediments, and thus will be briefly discussed here. In 1978, Aero Service of Houston, Texas, under contract with the U.S. Geological Survey, flew an aeromagnetic survey over the Amargosa Desert at an elevation of 122 meters (400 feet). Figure 4 shows the contoured results of the survey, obtained by running the flight data through projecting, gridding, and contouring programs (Godson and Webring, 1981; Webring, 1981). The contour interval is 50 gammas. With the exception of three isolated anomalies, the aeromagnetics over the Amargosa Desert show little magnetic variation over most of the region, including the surrounding basement outcrops, varying up to about 100 gammas in a few areas, but exhibiting little

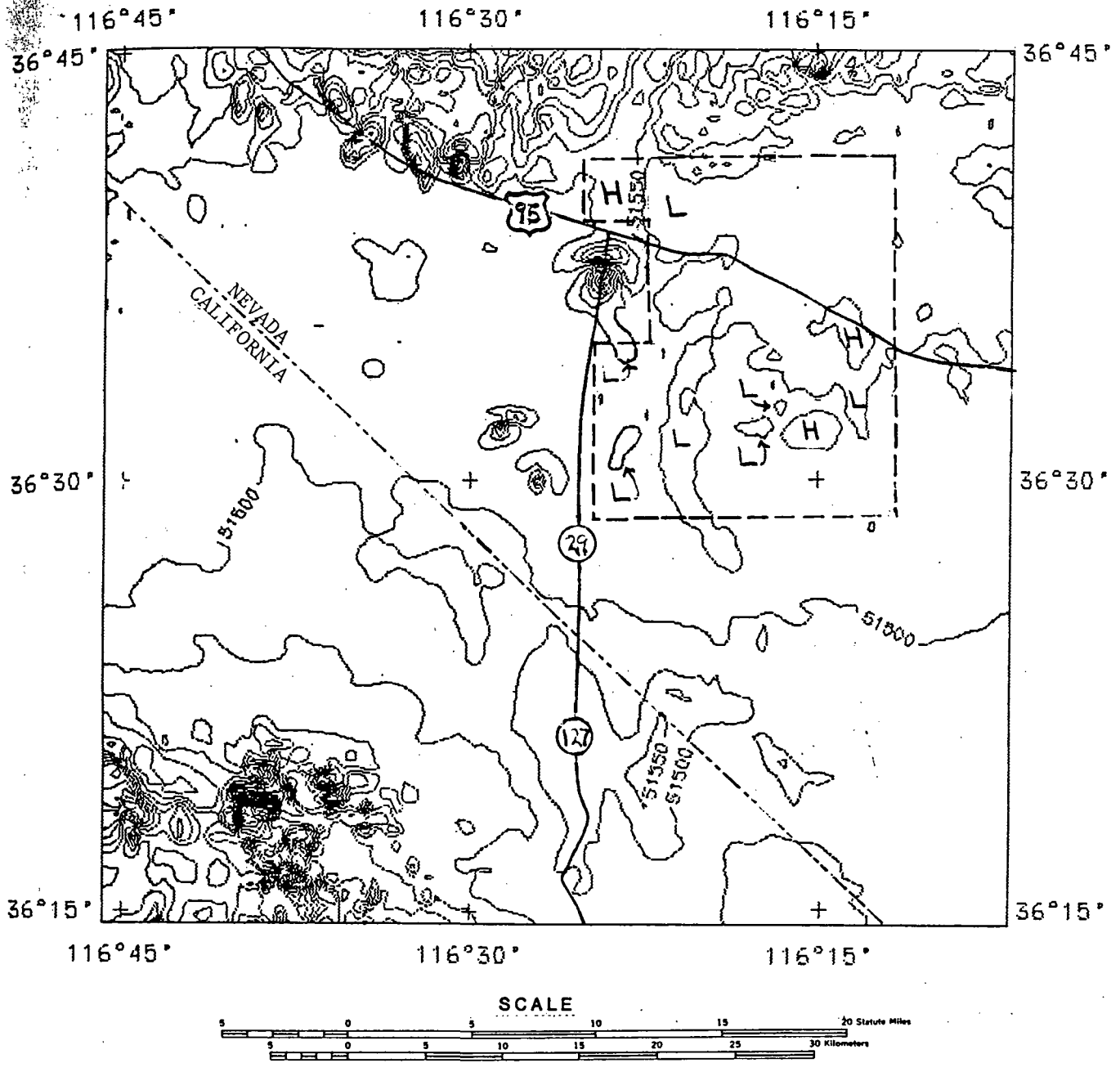

Figure 4. Contoured results of an aeromagnetic survey over the Amargosa Desert region. H = magnetic highs, L = magnetic lows. Dashed border encloses area where "reverse-relief" effect of magnetics is apparent (see text). Contour interval = 50 gammas.

more than about 20 gammas variation (low-frequency background) throughout most of the region, due to the weak magnetic nature of both the basement carbonates and the basin-fill sediments. The three isolated anomalies include one large, reversed anomaly just south of Lathrop Wells (580 gammas max. deflection), and two adjacent anomalies, one normal (220 gammas max. deflection), one reversed (260 gammas max. deflection), about 15 km south-southwest of Lathrop Wells. Also, strong (hundreds of gammas) high-frequency magnetic variation occurs along the northern edge of the Amargosa Desert, indicating the southern edge of the Tertiary volcanics found north of this region.

Although the magnetics over the Amargosa Desert are relatively quiet, the variation in the northeastern part of the desert (bordered area in Figure 4) seems to show a "reverse-relief" effect where basement relief is known. That is, there are magnetic highs where the basement surface is deepest (and thus where the basin-fill sediments are thickest), and magnetic lows where the basement surface is at shallower depths. This indicates that the magnetization producing these variations is within the basin-fill sediments, and that the three-dimensional distribution of magnetic particles within the sediments is uniform enough to produce this effect.

TDEM 81-988

36p -

U. S. Department of the Interior
Geological Survey

CALICO HILLS

INTERPRETATION OF TIME-DOMAIN ELECTROMAGNETIC SOUNDINGS IN THE CALICO HILLS AREA, NEVADA TEST SITE, NYE COUNTY, NEVADA

by

James Kauahikaua

Open-File Report 81-988

1981

INTERPRETATION OF TIME-DOMAIN ELECTROMAGNETIC SOUNDINGS IN THE CALICO HILLS AREA, NEVADA TEST SITE, NYE COUNTY, NEVADA

by James Kauahikaua

Abstract

A controlled source, time-domain electromagnetic (TDEM) sounding survey was conducted in the Calico Hills area of the Nevada Test Site (NTS). The goal of this survey was the determination of the geoelectric structure as an aid in the evaluation of the site for possible future storage of spent nuclear fuel or high-level nuclear waste. The data were initially interpreted with a simple scheme that produces an apparent resistivity versus depth curve from the vertical magnetic field data. These curves can be qualitatively interpreted much like standard Schlumberger resistivity sounding curves. Final interpretation made use of a layered-earth Marquardt inversion computer program (Kauahikaua, 1980). The results combined with those from a set of Schlumberger soundings in the area show that there is a moderately resistive basement at a depth no greater than 800 meters. The basement resistivity is greater than 100 ohm-meters.

Introduction

Between June 2 and 8, 1978, nine TDEM soundings were completed in the Calico Hills area of the Nevada Test Site using a grounded-wire current source and a cryogenic magnetometer sensor. The source wire was 2,250 m long oriented along a direction N78W, and continuously pulsed with a 4- to 6-amp current which changed polarity at 5 s intervals. The same source was used for all nine soundings. At each numbered location shown in Figure 1,

a three-component cryogenic SQUID magnetometer (X-axis parallel to the source wire) was set up to measure the magnetic field components generated by the switched current source. The magnetometer was partially buried and its top was covered with a plastic container to minimize wind noise. The vertical magnetic field (Hz) was digitized and recorded on a Gould data logger at 200 samples per second for a period of 4 min at each location. Horizontal fields perpendicular to the source wire (Hy) were similarly recorded at sounding locations 1, 5, 7, 8, and 9. Natural magnetic noise was low during the survey period, allowing much of the recording to be done without electronic filtering. Field operations were directed by Dick Sneddon (USGS, Denver, Colorado).

Figure 1 also shows the locations of eight Schlumberger soundings that are interpreted in this study. The vertical electric sounding (VES) data were provided by Don Hoover, USGS (written communication, 1979).

TDEM Data Reduction

The data-logger tape cartridges were transcribed to 9-track tape so that data reduction could be done on the Honeywell Multics computer maintained by the USGS in Denver, Colorado. Each 4-min record should contain 40 to 50 step responses and have a total of about 50,000 data points. The easiest way to stack this data is to search it for the start of the response (look for large first differences), store the next 5 s of data, search for the start of the next response, etc., until the whole 50,000 data points have been searched. The search-and-store step will convert the data string of 50,000 points into a 50-by-1000 matrix of points - each of the 50 rows is an individual step response, and each of the 1,000 columns correspond to the responses at a particular time relative to the source switching time.

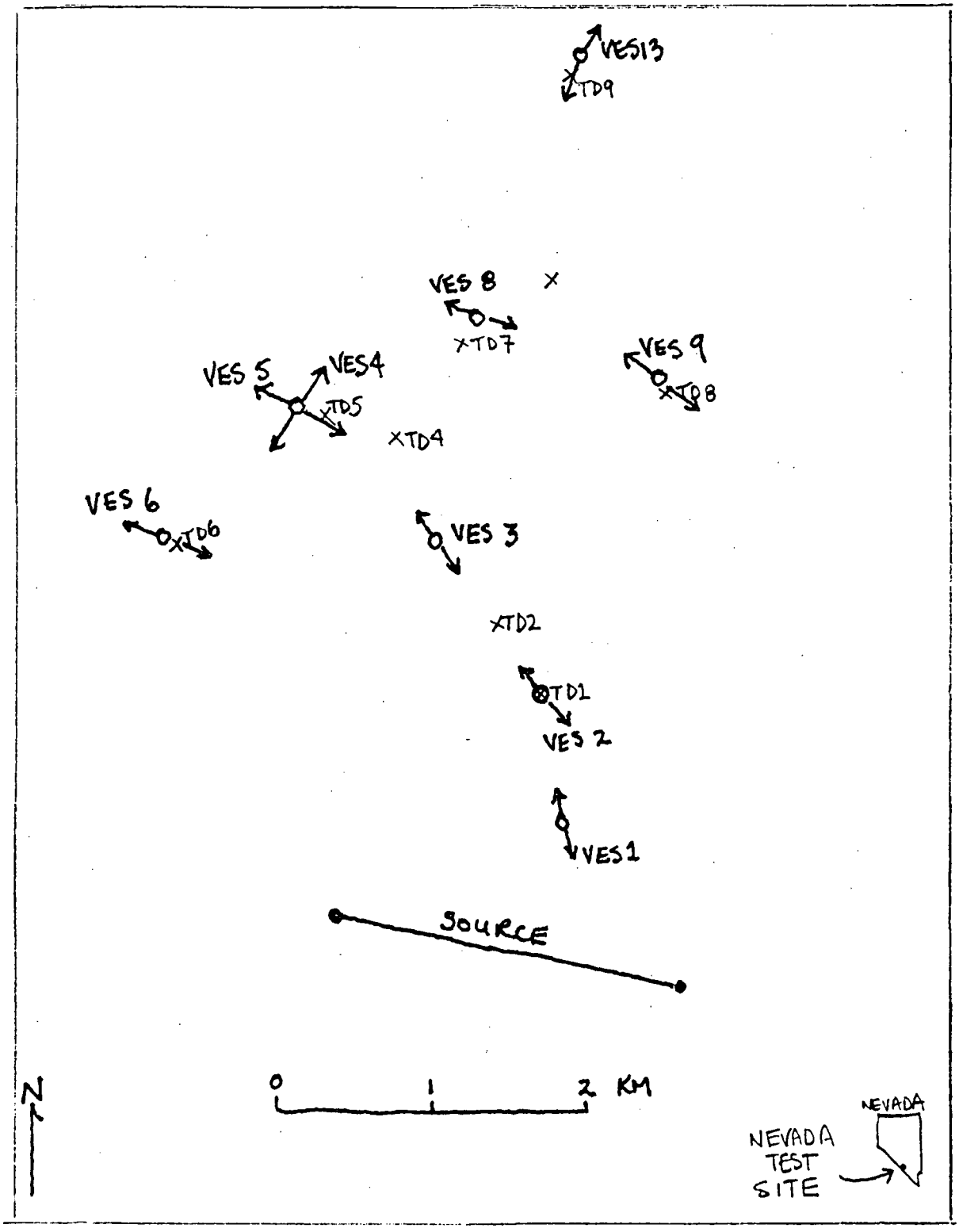

Figure 1. A topographic map of the Calico Hills area of the Nevada Test Site showing the locations of the grounded wire source and the nine cryogenic magnetometer receiver sites (prefixed by TD) used in this TDEM survey. Double-headed arrows are VES locations (prefixed by VES).

The stacking proceeds by computing an average and a standard deviation for each of the 1,000 columns. If data from any of the step responses fall more than two standard deviations from the average, those data are rejected and the average and standard deviations are recomputed. The stacking step, as described above, produces an average response and a corresponding standard deviation for each of the 1,000 columns. Finally, the stacked response is smoothed with a time-varying filter which emphasizes low frequencies at late times and higher frequencies at early times. The final reduced response data set consists of 49 averaged magnetic field values (and the corresponding standard deviations) spaced at logarithmically equal intervals of time.

The response data were not corrected for the response of the system. This is usually a standard step in TDEM data reduction; however, the numerical means available for deconvolution of the data can be unstable, particularly with data taken over resistive terrain, such as the Nevada Test Site. The approach preferred in this work is to use the system response as part of the model to which we are trying to match the data. This is numerically more stable and does not significantly increase the computations.

Data Interpretation Methods

The first stage in interpretation is to familiarize oneself with the TDEM responses to simple models. Figures 2 and 3b are two-layer step response models for a conductivity contrast (sig2/sig1) of 10 and 1/10 and d/r (ratio of first layer thickness to source-sensor separation) values of .05, .1, .25, .5, and 1. The modeled source is a horizontal electric dipole excited by a step function of current, and the received signal is not filtered. TDEM model responses were computed with a program written by Kauahikaua and Anderson (1977). Figure 2a shows the horizontal magnetic

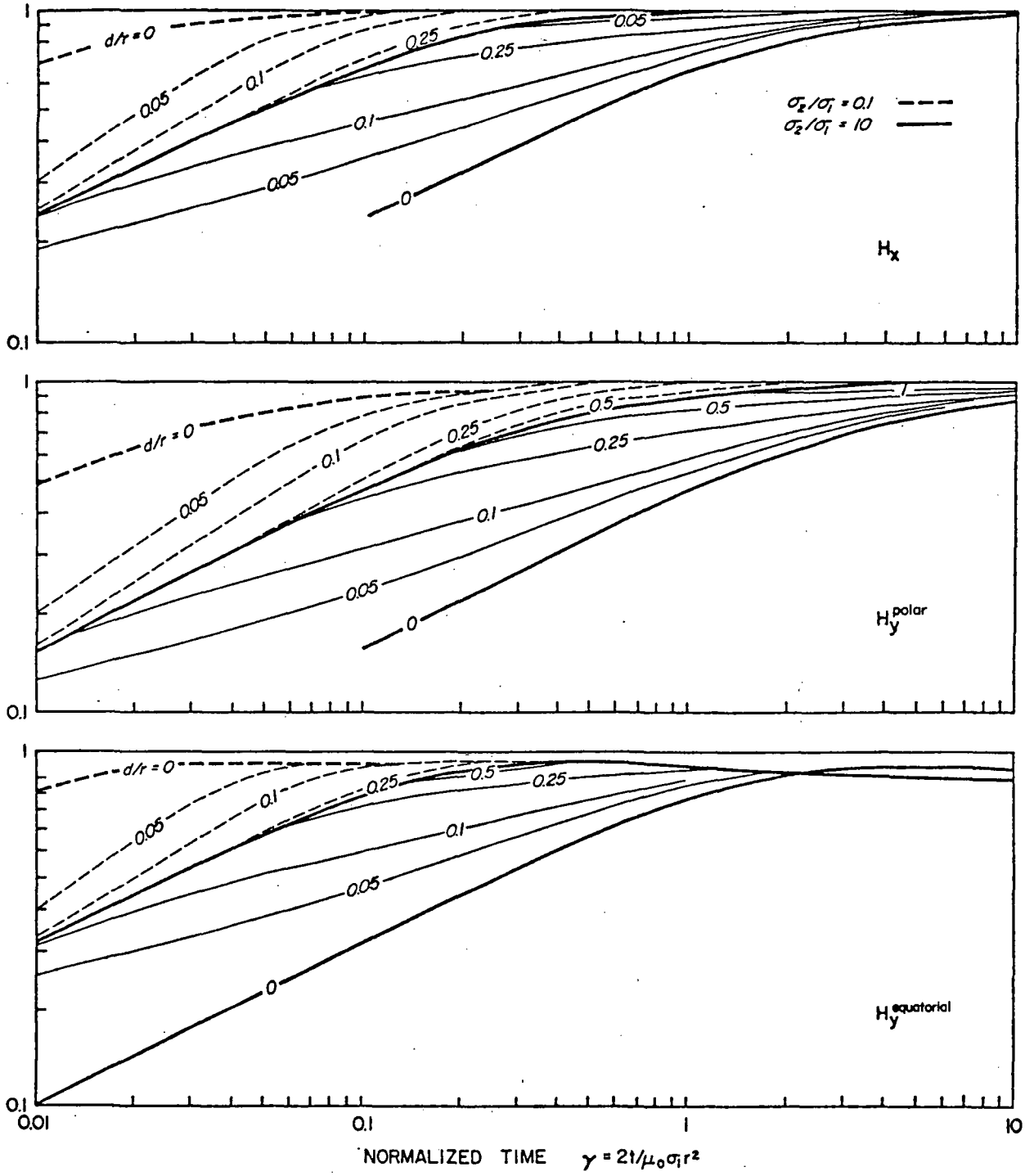

Figure 2. Plots of the theoretical transient horizontal magnetic field generated by a step current pulsed through a horizontal electric dipole. The fields are normalized by the appropriate free-space field values. Each figure shows model responses for two different conductivity contrasts of 10 and 1/10 and values of d/r (ratio of first layer thickness to source-sensor separation) of 0.0, 0.05, 0.1, 0.25, 0.5, 1.0, and infinity. a) magnetic field measured parallel to the dipole source, b) magnetic field measured perpendicular to the dipole source at a distance directly along the dipole direction, and c) magnetic field measured perpendicular to the dipole source at a distance measured perpendicular to the dipole direction.

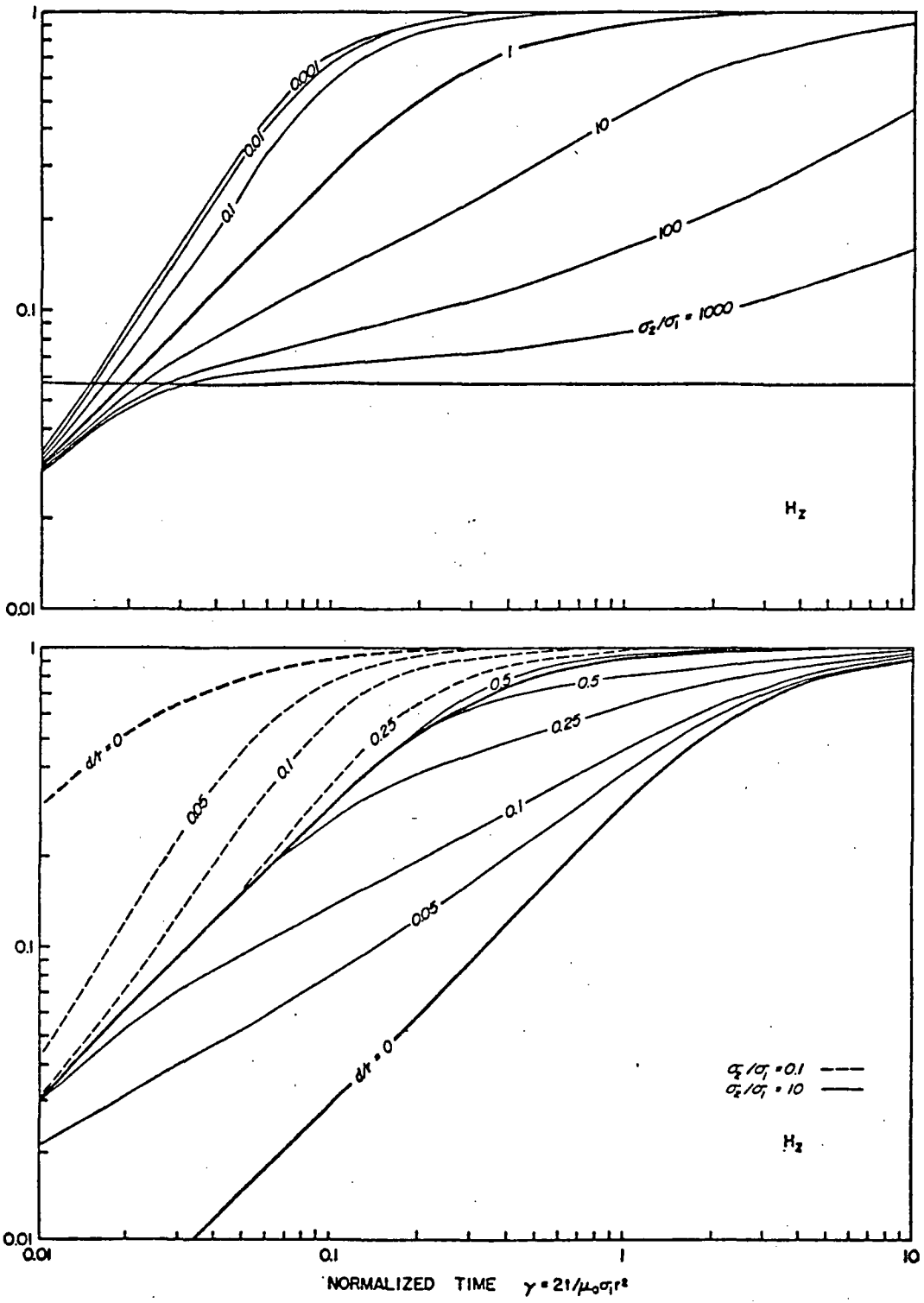

Figure 3. Plots of the theoretical transient vertical magnetic field generated by a step current pulsed through a horizontal electric dipole. The fields are normalized by the vertical free-space field value. a) first layer thickness is 1/10 of the source-sensor separation and the conductivity contrast varies from 10**-3 to 10**3. The dashed line is the asymptote for a conductivity contrast of infinity, and b) conductivity contrast of 10 and 1/10 and a d/r ratio of 0.0, 0.05, 0.1, 0.25, 0.5, 1.0, and infinity.

field in a direction parallel to the source dipole, and Figures 2b and 2c show the directionally-dependent horizontal magnetic field perpendicular to the source dipole. Figure 3b shows the vertical magnetic field. Note that the differences between the model responses are noticeably smaller for the horizontal fields than for the vertical field. This is because for early times, the horizontal fields build-up to the primary field value like 5**0.5 (1) whereas the vertical field builds up like t, where t is time. A half-space conductivity change of 10 times would change the vertical field by a factor of 10 in early time, but would only change the horizontal fields by 10**0.5 = 3. Therefore, to a first-order approximation, the vertical magnetic field of a horizontal electric dipole is about 3 times more sensitive to changes in earth conductivity structure than are the horizontal magnetic fields. It would seem most profitable to concentrate on the vertical magnetic field data.

At this point, the best fitting layered earth model could be determined directly by inversion using program MQLVTHXYZ (Kauahikaua, 1980); however, this should be avoided if possible because typical computer runs are expensive. Quite a good estimate of the electrical structure can be obtained by converting the TDEM data into apparent resistivities as a function of time (Morrison and others, 1969). That is, at successive times in the TDEM response, one can calculate "what the resistivity of a homogeneous half space would have to be to yield the observed field amplitude at that time". This can be done graphically as will be demonstrated first with the half-space response in Figure 3b, then with the actual data plots in Appendix I.

---

(1) exponentiation is denoted by '**'.

Computation of Apparent Resistivity from TDEM Data

First the data are normalized by the asymptotic late-time value. The date should then consist of values between zero and one. Next, the normalized time corresponding to each one of the normalized data points should be obtained using the half-space model curve in Figure 3B. Each of the normalized times can then be converted to an apparent resistivity using the corresponding real time and the source-sensor distance. As an example, let's use the data from a hypothetical sounding recorded at a distance of 1,000 m from a wire source. A normalized field value of 0.5 was measured at 70 ms after a break in the source current. Using Figure 3a, we see that a field value of 0.5 corresponds to a normalized time of 0.18. The equation defining normalized time in terms of real time is

normalized_time = 2*real_time*rho/(myu0*r*r)

where r is source-sensor distance in m, myu0 is 4*pi*10**(-7), pi is 3.1415927, and rho is the half-space resistivity. Using the actual source-sensor distance of 1,000 m, the resistivity of the half space that would have produced a normalized vertical magnetic field value of 0.5 at 70 ms is 1.62 ohm-m. This is the apparent resistivity at 70 ms for this point of the example sounding.

Taking this one step further and in the process approximately accounting for the system response, one can make a log-log graph paper with various half-space responses already plotted on it. The reduced data can be plotted on this customized graph paper and the apparent resistivity for each data point can be logarithmically interpolated using the two nearest half-space curves. For this study, the log-log graph paper has real time on its horizontal axis and normalized vertical magnetic field on the vertical axis. Half-space responses are

plotted on it for various values of the ratio rho/R**2 (R in kilometers). Because two different recording system configurations were used in the NTS study, two different types of customized graph paper were constructed. Some graphs were prepared using undistorted half-space responses and others were prepared using half-space responses distorted by a twin-T 60 Hertz notch filter. Apparent resistivities can even be estimated in the field in this way.

All nine vertical field TDEM sounding data sets are plotted in Appendix I on graph paper prepared in this manner. Each of the half-space responses have been labeled with the actual resistivity corresponding to the product of the rho/R**2 value of the half-space response and the square of that sounding's source-sensor distance, in kilometers. After logarithmically interpolating between half-space response curves for each data point, each apparent resistivitiy versus time function shows that the apparent resistivity increases with time. There is a slight decrease in resistivity at times greater than 50 msec for soundings 1 and 2, and at times greater than 100 msec for soundings 6 and 7. The exact depths to which these resistivities correspond can only be determined by modeling the TDEM responses themselves. The rule-of-thumb is that data at later times is information from greater depths. The NTS soundings are then depicting a structure with a conductive layer over a resistive one, with soundings 1, 2, 6 and 7 suggesting another conductive layer at still greater depths.

Computation of Apparent Depth of Penetration

This difficulty with quantitative depth estimates led to the concept of apparent depth of penetration as a function of normalized magnetic field amplitude. The idea behind this concept can be described most simply using

the two-layer model vertical magnetic field response curves in Figures 3a and 3b. Figure 3a shows responses to models with a fixed d/r ratio of 1/10 and varying conductivity ratios, and Figure 3b shows responses to models with fixed conductivity ratios of 10 and 1/10 and varying d/r ratios. These responses all show a conspicuous tendency to increase linearly with time from zero along the half-space response curve corresponding to the resistivity of the surface layer. The normalized field value at which these model curves depart from the half-space curve followed at early times can be seen to be characteristic of the particular d/r ratio of the model, and therefore could be used to estimate maximum penetration depth at a particular time.

A mathematical definition of this maximum penetration depth can be obtained from the model response of a perfect resistor overlying a perfect conductor. The significance of this particular model is that it is the most resolvable of all earth models for electromagnetic systems. The normalized vertical magnetic-field response for such a model can be shown to be

$$Hzn = 1 - (4*(d/r)**2 + 1)**(-3/2).$$

The field does not vary with time because of the choice of perfect conductors and resistors in the model. To show how this relates to the model responses with finite resistivities, the value of this function for d/r = 0.1 is plotted on Figure 3a as a horizontal dashed line. Obviously this is also the asymptotic (late-time) value of the induced vertical magnetic field for two-layer models with a finite-resistivity layer over a perfect conductor. For the case of d/r = 0.1, less-than-perfectly conducting lower half spaces significantly distort the response curve from that of a half space with the first-layer resistivity only at times greater than the time at which that half-space response intersects the dashed line. This is at a normalized

time of about 0.02. In general, the above equation can be solved for the d/r ratio, and each value in a set of TDEM response data could be converted to a d/r value as well as an apparent resistivity. The physical meaning of these d values is the maximum penetration depth at a given time for a given shallow resistivity structure. The d/r ratio will be called the normalized apparent depth of penetration. The normalized apparent resistivity versus normalized apparent depth curves corresponding to the set of two-layer model responses in Figure 3b are presented in Figure 4 as dashed lines. For comparison, Schlumberger model curves for the same two-layer models are plotted as solid lines in Figure 4. The Schlumberger electrode spacings (AB/2) have been normalized by r, the TDEM source-sensor distance, for ease of comparison. The great similarity between the two sets of curves suggests that the apparent depth conversion for TDEM data could be as diagnostic as the Schlumberger curves.

The shape of the TDEM apparent resistivity versus depth curves seems to depend only upon the parameters of the earth model and not on r, the source-sensor separation. An album of model curves for TDEM sounding could be constructed much like they have been for Schlumberger sounding. They would require a greatly reduced number of curves compared to the normal set of EM model curves which are commonly related to r. The same album of curves would also be applicable to frequency-domain sounding using the field amplitude data. This is because there is nothing implicitly time-or frequency-domain oriented about the approach except in the nature of apparent resistivity calculation (substitute reciprocal of 2*pi*frequency for time). The same approach could also be used in other systems (frequency- or time-domain) which employ electromagnetic fields. In this way, TDEM data can be compensated for the system response and reduced to a pseudo-Schlumberger form in the field.

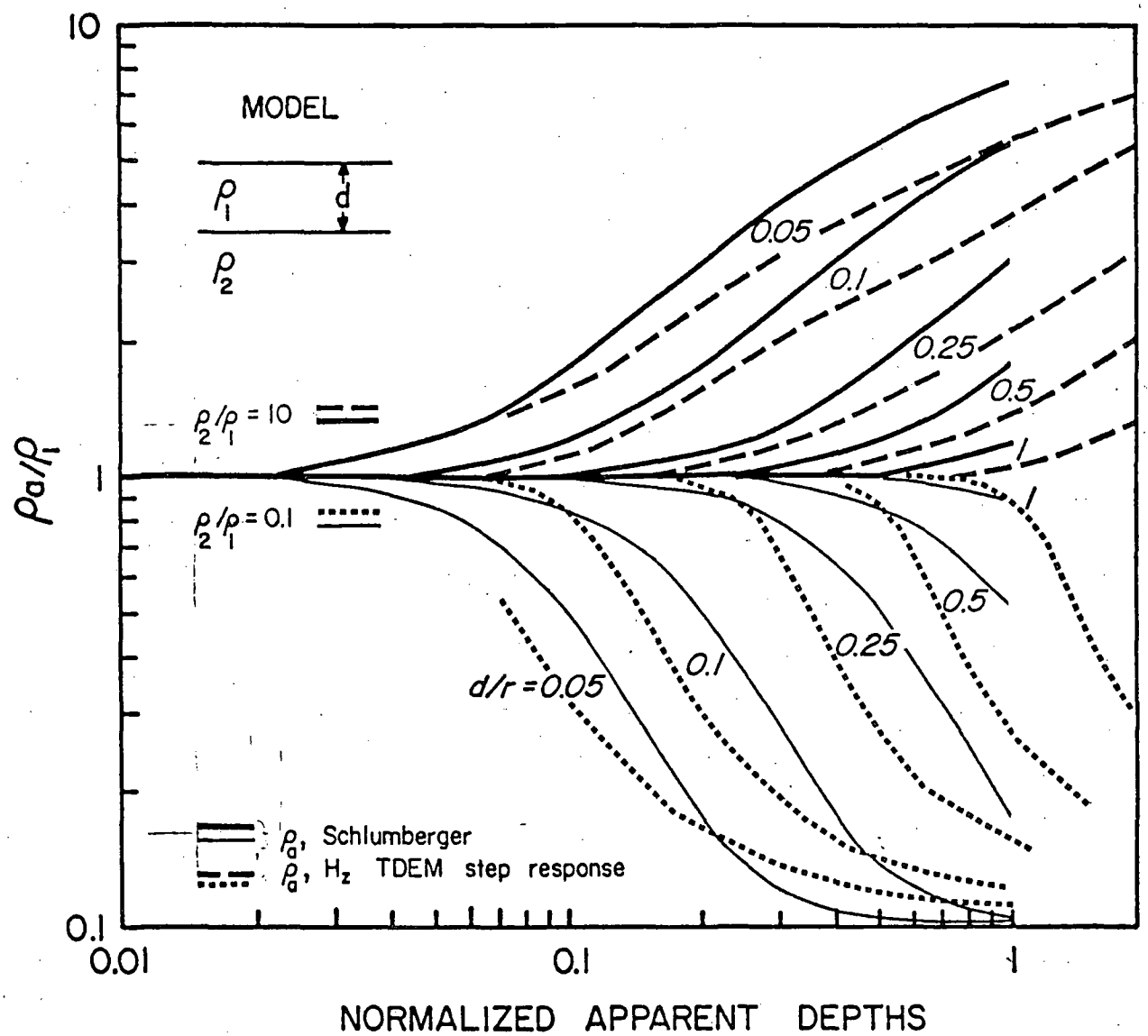

Figure 4. Solid lines are plots of normalized Schlumberger apparent resistivity versus normalized electrode spread length for conductivity contrasts of 10 and 1/10 and various first layer thicknesses. Dashed lines are plots of EM apparent resistivity versus normalized apparent depth. All lengths are normalized by r, the source-sensor distance.

Interpretation Results
Using the Converted TDEM and Schlumberger Data

The NTS TDEM sounding data have been reduced to the form described above and plotted on log-log paper in Appendix II along with the Schlumberger sounding data (locations in Figure 1) taken at the nearest location. With a few exceptions, the agreement between the TDEM and VES data, in terms of apparent resistivities and depths, is remarkable. The VES data cover electrode spacings (AB/2) of 3 m to 1,200 m whereas the TDEM apparent depths extend from about 450 m to over 3,000 m. Joint inversion of both sets of data would be possible but not very efficient because of the small amount of apparent depth overlap (400-1,200 m). Instead, the VES data alone were inverted using program MARQDCLAG (Anderson, 1979) with the intent of matching the TDEM data with the same model. Cost of this process was around $2/run as compared with $10 to $70/run for the joint inversion using MQLVTHXYZ (Kauahikaua, 1980). After just one or two runs, both sets of data were fit quite well with a single model for TD4, TD5, and VES4 (VES3 and VES5 were very similar to VES4), TD3 and VES8, TD8 and VES9, and TD6 and VES6. These models are summarized next to the VES number at the bottom of the appropriate figures in Appendix II. The parameter statistics reflect the resolution of the VES data alone.

At first, the TDEM data did not seem to be contributing any information about the earth structure that was not already indicated by the VES data. Soundings TD6 and TD7 indicate a moderate conductor at a depth greater than 3 km, but other than the deepest few points of these two soundings, TD3, TD4, TD5, TD6, TD7, and TD8 all had the same trends as the VES data did; however, after the first few VES inversions, it was clear that the TDEM data could be reasonably fit only by a model whose basement had a resistivity significantly

greater than that originally suggested by the VES data alone. In every case, the VES data accommodated the more resistive basement. As an example of the quantitative increase in resolution at greater depths brought about by combining the VES and TDEM sounding data, the data for TD4 and VES4 were inverted jointly. These results are presented for comparison in Appendix II. The parameter errors were decreased by significant amounts - 85% to 34% for d3 and 41% to 6% for rho3; the joint inversion cost $81.

TDEM Computer Inversion Using Multilayer Earth Models

Soundings TD1, TD2, TD6, TD7, and TD9 were inverted with program MQLVTHXYZ. The resulting models are presented at the bottom of the appropriate figures in Appendix II, while the TDEM model responses are plotted with the original data in Appendix I. The interpreted resistivities for TD1 and TD2 are significantly lower than those for VES2. Even rigorous correction for the nearness of these two soundings to a source wire longer than 2 km (apparent resistivity and depth calculations implicitly assume an infinitesimally small source) will raise the resistivity values by only 7%. Inversions of these two data sets resolve a moderately conductive basement at 1,200-1,300 m. The data from TD6 and TD7 also suggest a conductive basement, but at significantly larger depths; in fact, the suggested depths are precisely equal to the source-sensor distance for each sounding. Inversion failed to resolve the conductive basement in the TD6 and TD7 data, therefore we may conclude that apparent resistivities from TDEM data become of questionable accuracy when apparent depths exceed the source-sensor distance. Farther to the north, TD9 resistivities are significantly higher than those in the TDEM model response computed from the VES13 model earth; however, the data and model responses are very nearly parallel, suggesting that it will be fit by an earth model with the same geometry (layer thicknesses) but with

larger resistivities.

Comparison of Schlumberger VES and TDEM Soundings Data and Interpretations

In general, the two data sets compare very well. Two exceptions are the soundings nearest the source and the sounding farthest from the source (to the north). For those nearest the source, the TDEM apparent resistivities are much less than those determined from the Schlumberger data. One obvious cause for this discrepancy would be strong lateral changes in geoelectric structure. Examination of the Schlumberger data alone substantiates this hypothesis; VES1 and VES2 (the southernmost) are distinctly different from those farther north in that they do not having rising terminal branches. North of these two soundings, all VES data below 10 meters show an approximately uniform structure of 46 to 67 ohm-m overlying a basement of greater than 100 ohm-m. This lateral change is reflected in the TDEM data; TD1 and TD2 (the southernmost and nearest to the source) have descending terminal branches whereas all those farther north have rising terminal branches. Unfortunately, the actual interpretations of VES1 and VES2 do not compare favorably with those of TD1 and TD2. There is no way of determining which is the more accurate representation of the subsurface without other sets of electrical data. In spite of the disagreement, one could suggest that a fault exists between TD2 and VES3 on the basis of either set of data; it is uncertain whether the conductor below 1,300 m interpreted from the TDEM data is real or an effect of field distortion by the lateral resistivity changes.

The discrepancies noted between VES13 and TD9 at the northern edge of the study area are not as severe; both have ascending terminal branches. However, the TDEM apparent resistivities are significantly greater than

those for the VES. Again, the discrepancy is probably due to lateral changes. The basement is generally less than 200 m deep in the Calico Hills themselves, dropping to several hundred meters to the north and east. The TDEM data in each of these areas underestimates the conductance of the layers above basement thereby underestimating the basement depth. TD9 is the most severe example of this, but TD3, TD7 and TD8 all show similar discrepancies when compared to nearby VES data. This must be an averaging effect due to the utilization of a fixed source to the south of the hills for the TDEM soundings.

The TDEM and VES data obtained in and near the Calico Hills agree quite closely; however, there is a distinct difference in resolution. The VES data can resolve shallow structure to 800 or 900 m, which in this area is sufficient to resolve the conductive layers above basement (basement generally at 200 m). Deeper resolution could have been achieved with electrode spacings greater than the maximum of 1,200 m used here. The TDEM data is not sampled at small enough times to resolve anything shallower than 800 m and can only provide limits on the longitudinal conductance of the layers above basement, as well as a minimum basement resistivity. The combination of the two sets of data can yield uniformly good resolution from 10 m to 2-3 km.

References

Anderson, W. L., 1979, Program MARQDCLAG: Marquardt inversion of DC-Schlumberger soundings by lagged-convolution: U. S. Geological Survey Open-File Report 79-1432, 58 p.

Kauahikaua, J., 1980, Program MQLVTHXYZ: Computer inversion of three-component time-domain magnetic-field sounding data generated using an electric-wire source: U. S. Geological Survey Open-File Report 80-1159, 109 p.

Kauahikaua, J. and Anderson, W. L., 1977, Calculation of standard transient and frequency sounding curves for a horizontal wire source of arbitrary length: U. S. Geological Survey Open-File Report USGS-GD-77-007, 61 p., avail. from U. S. Dept. Comm. NTIS, Springfield, VA 22161 as Rept. PB-274-119.

Morrison, H. F., Phillips, K, J., and O'Brien, D. P., 1969, Quantitative interpretation of transient electromagnetic fields over a layered halfspace: Geophysical Prospecting, v. 17, p. 82-101.

APPENDIX I: Normalized TDEM Data Plots

Solid curves are TDEM half-space model responses which are either undistorted, or distorted by a twin-T 60 Hertz notch filter (depending on how each data set was measured in the field). The resistivities corresponding to each curve are in parentheses and were obtained by multiplying each curves' unique ratio of resistivity and the square of the source-sensor distance, in km, by the square of the actual source-sensor distance of each sounding. Data points are plotted as open circles with dots in the center, and error bars represent one standard deviation as derived by stacking. Dashed curves are the best-fit TDEM model responses; parameters and statistics for these fits are summarized in Appendix II.

HALFSPACE STEP RESPONSE, NO FILTERS

NTS SDG 1 ($R = 1.8$ km)

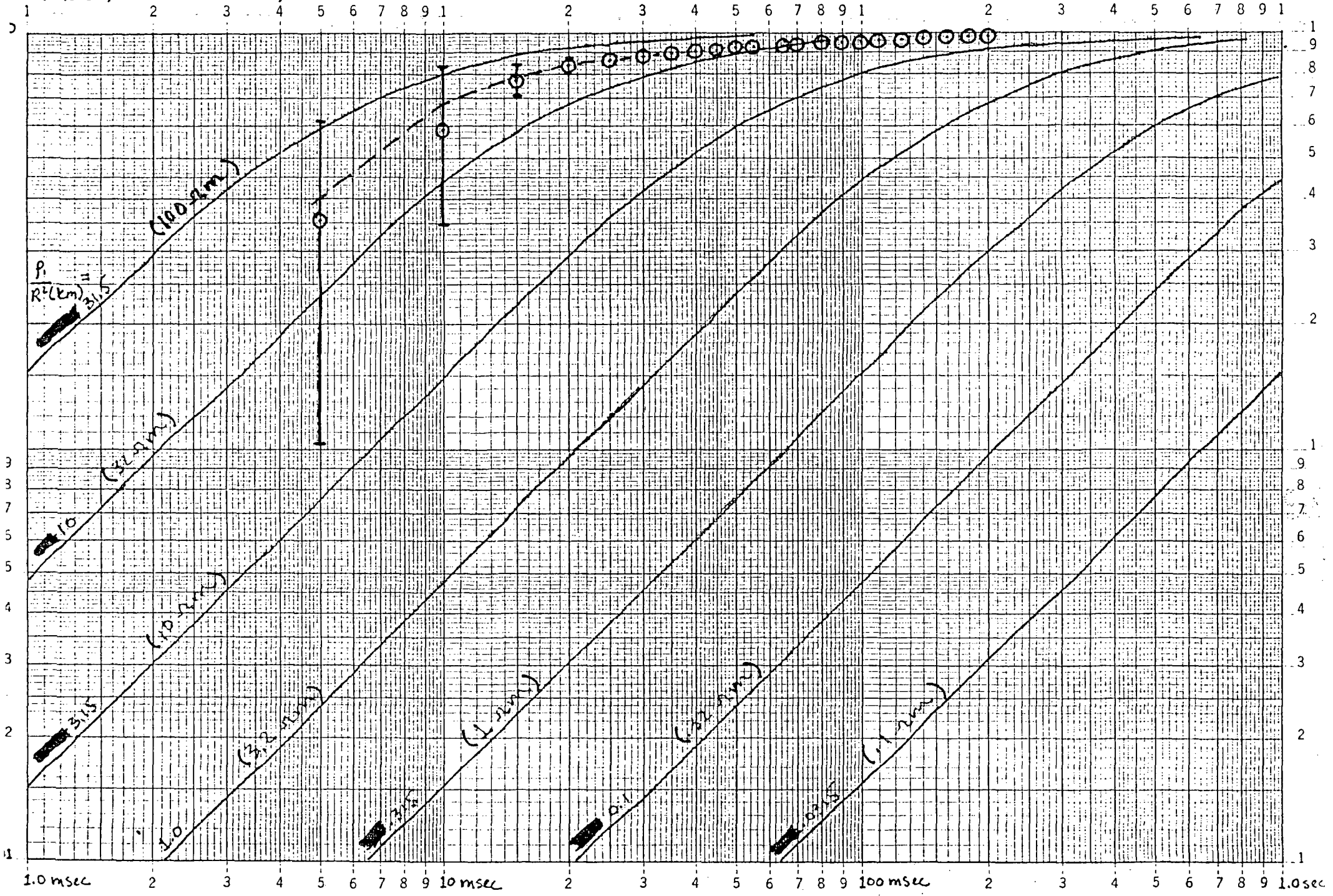

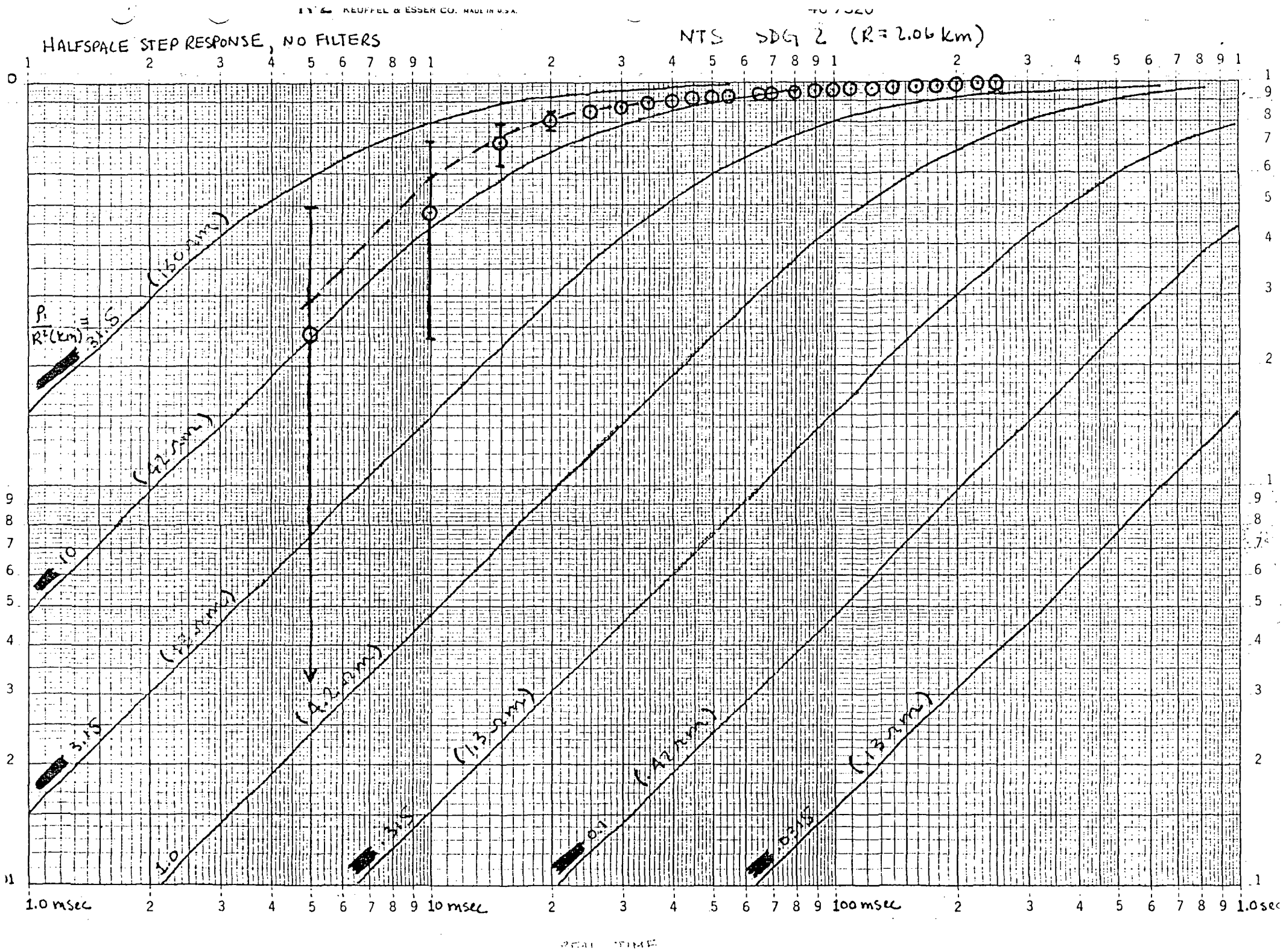
HALFSPACE STEP RESPONSE, NO FILTERS
NTS SDG 2 (R = 2.06 km)
$\frac{P_1}{R^2(km)} = 3.5$
(1.50 psi-ms)
(1.42 psi-ms)
(1.42 psi-ms)
(0.82 psi-ms)
(1.13 psi-ms)
(1.42 psi-ms)
(1.13 psi-ms)
10
3.15
1.0
.3
0.1
.03
1.0 msec
10 msec
100 msec
1.0 sec

HALFSPACE STEP RESPONSE, NO FILTERS

NTS SDG 3 (R = 4.3 km)

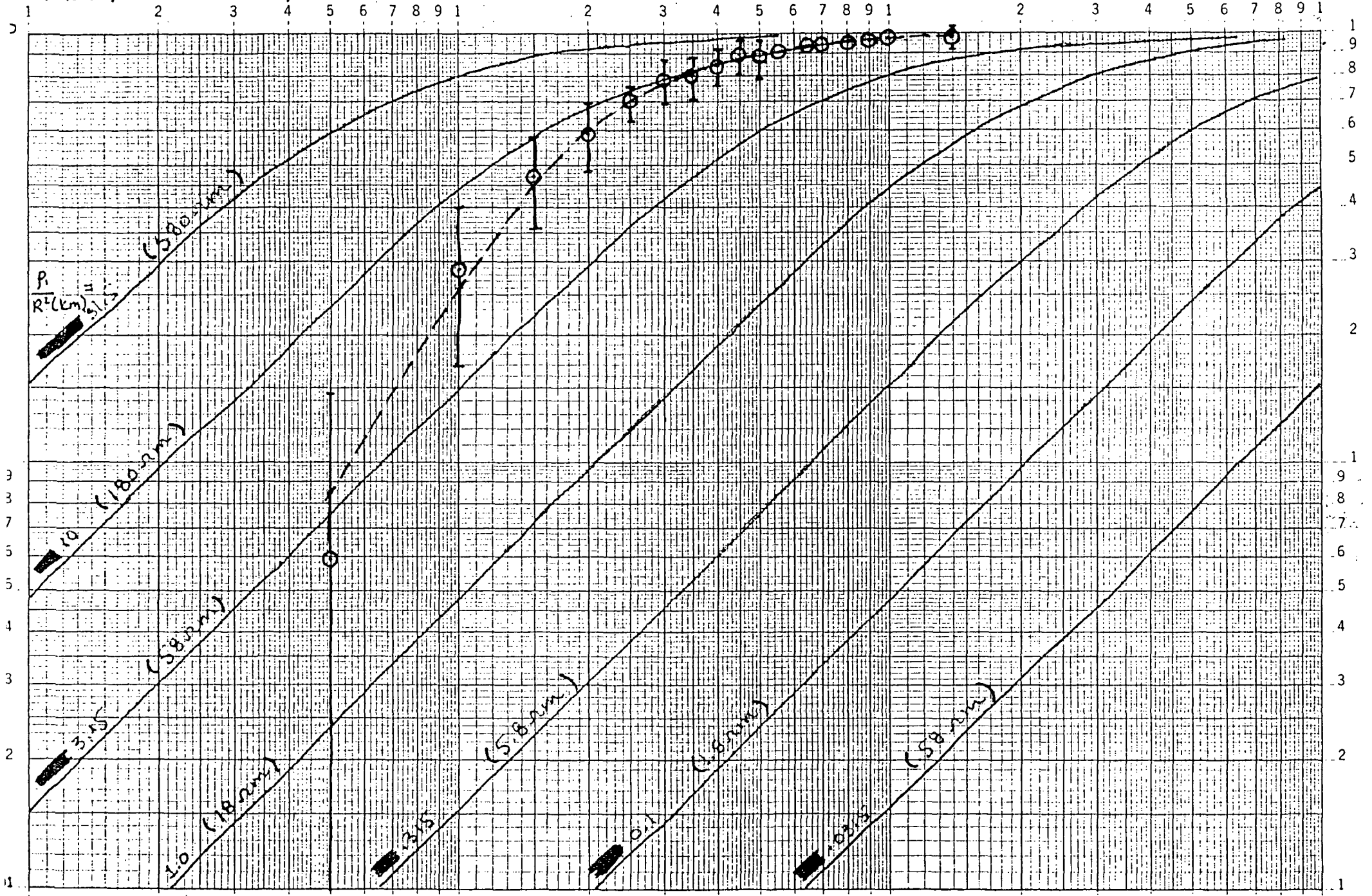

46 7320

HALFSPACE STEP RESPONSE, NO FILTERS

NTS SDG 4 (R = 3.3 km)

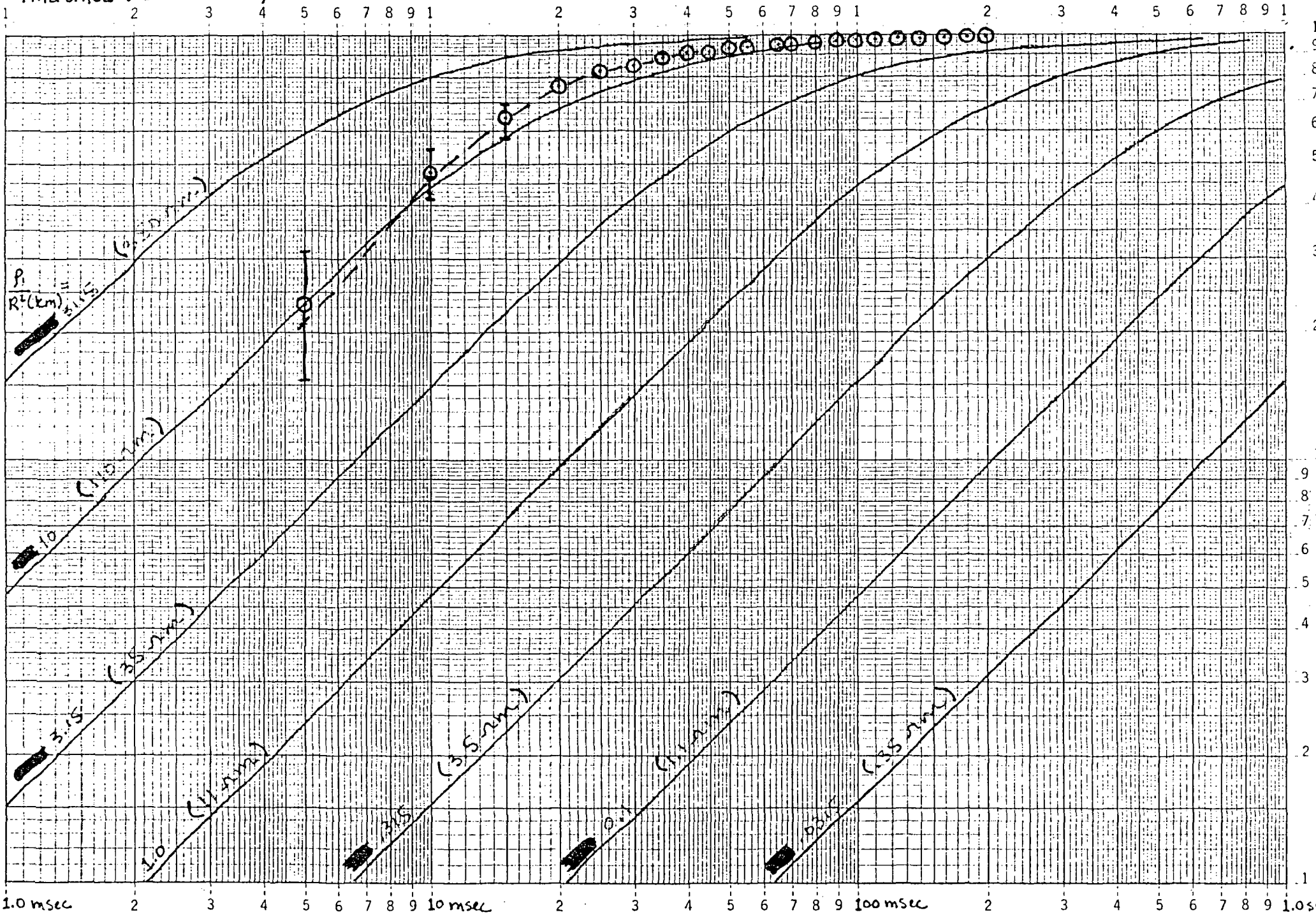

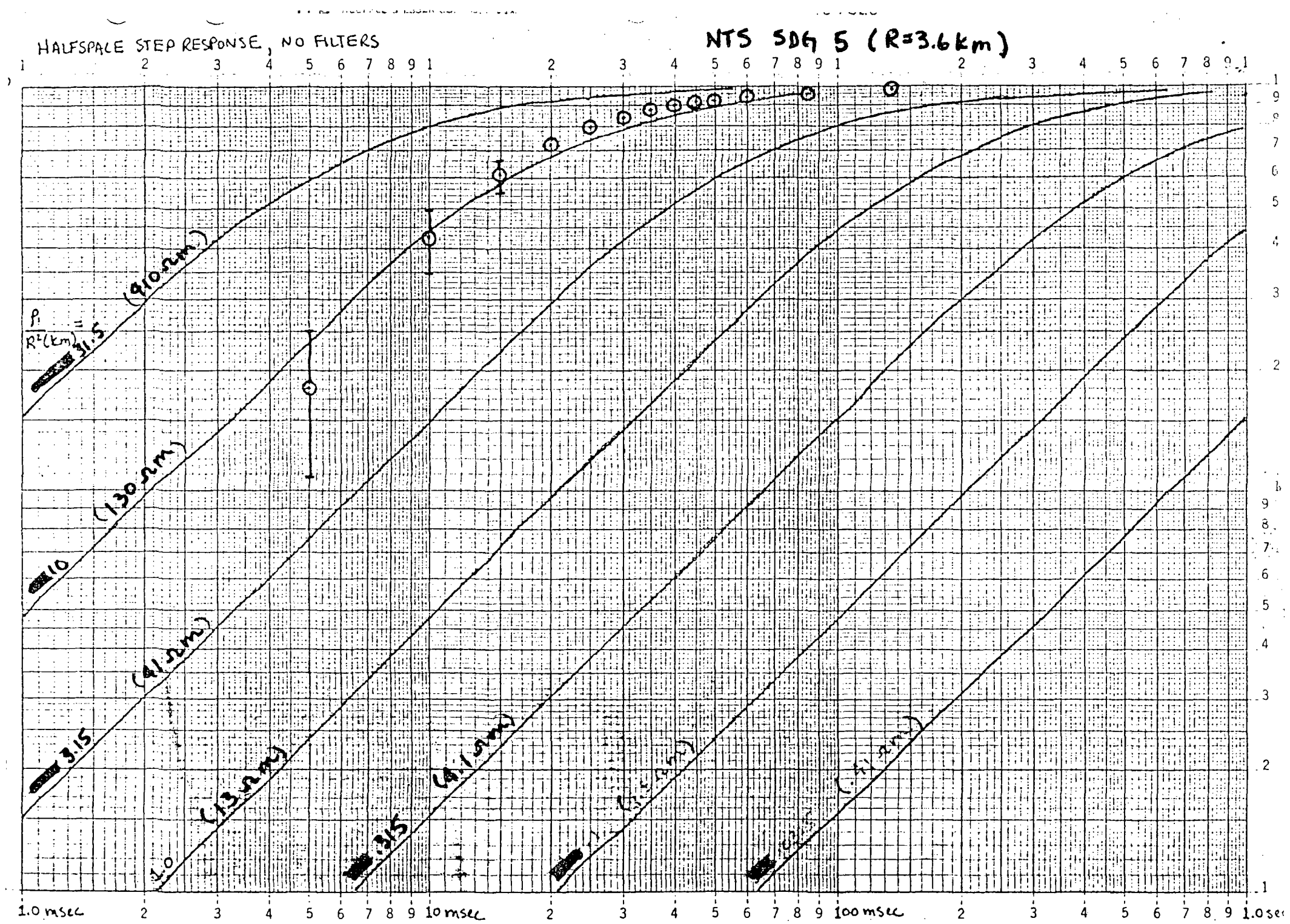
HALFSPACE STEP RESPONSE, NO FILTERS
NTS SDG 5 (R=3.6km)
$\frac{P_1}{R^2(km)}$ =
31.5
10
3.15
1.0
(910 nm)
(130 nm)
(41 nm)
(13 nm)
(4.1 nm)
(1.3 nm)
1.0 msec
10 msec
100 msec
1.0 sec

KEUFFEL & ESSER CO. MADE IN U.S.A.

40 7520

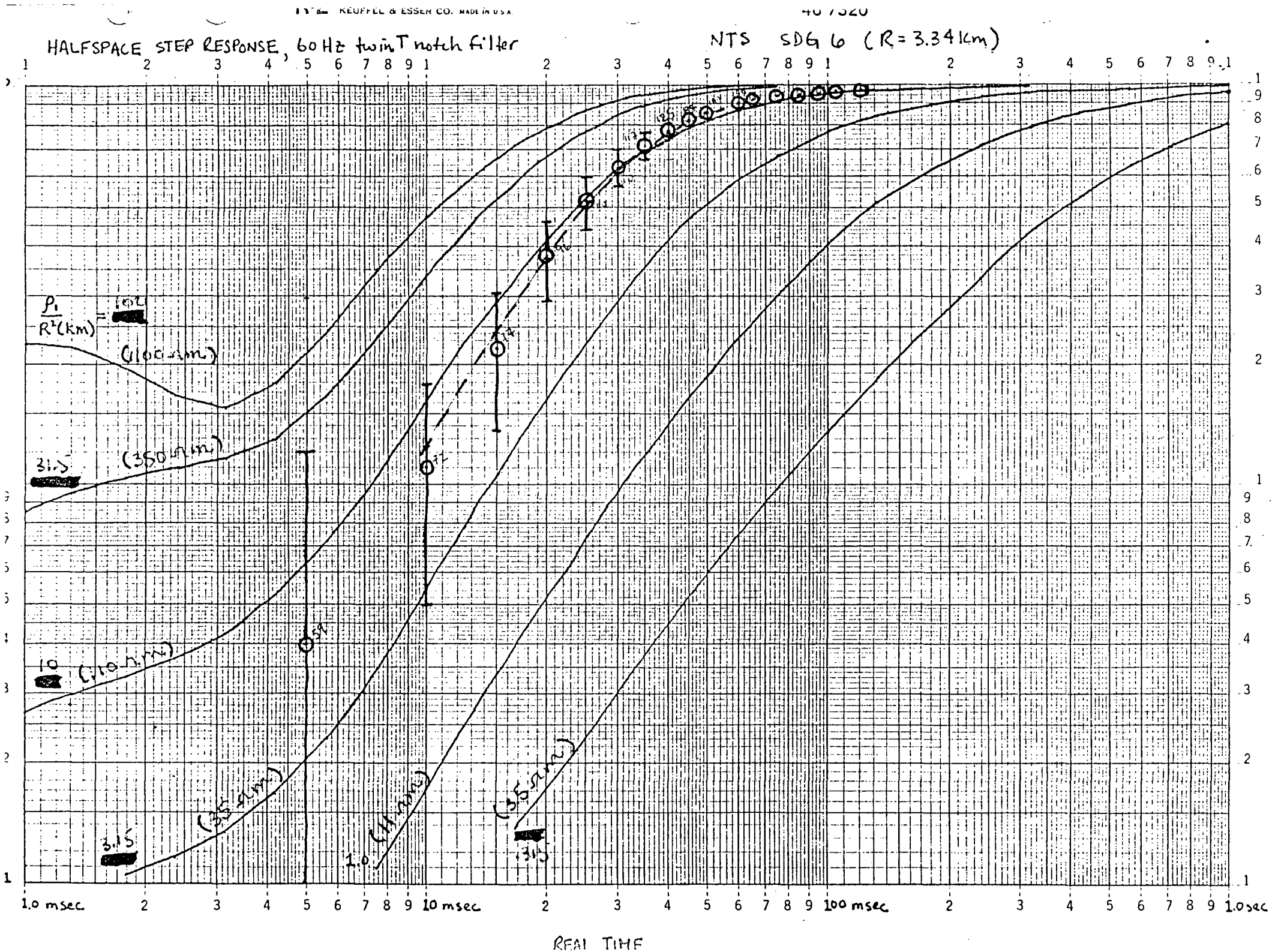

HALFSPACE STEP RESPONSE, 60 Hz twin T notch filter

MTS SD67 (R = 3.85 km)

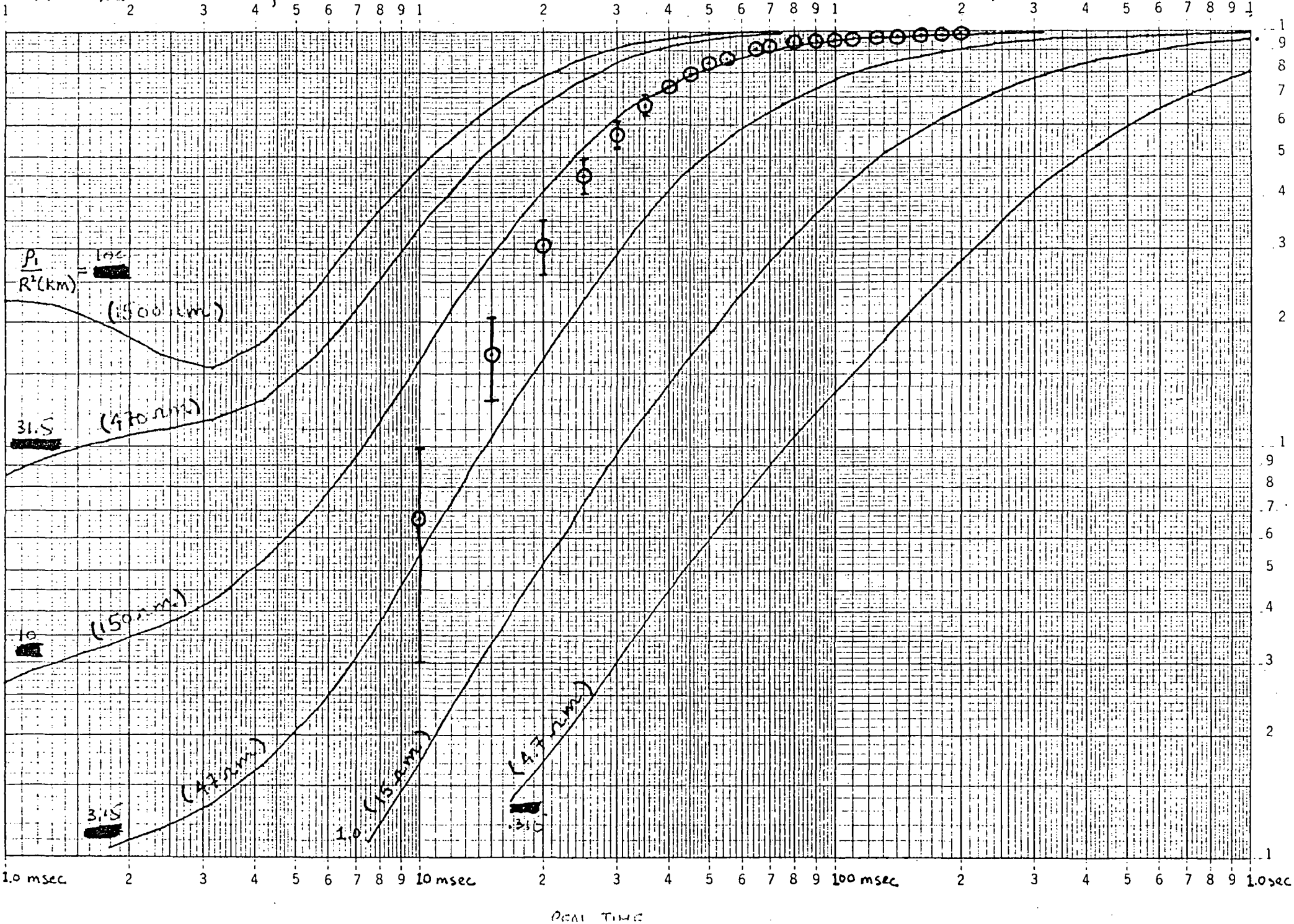

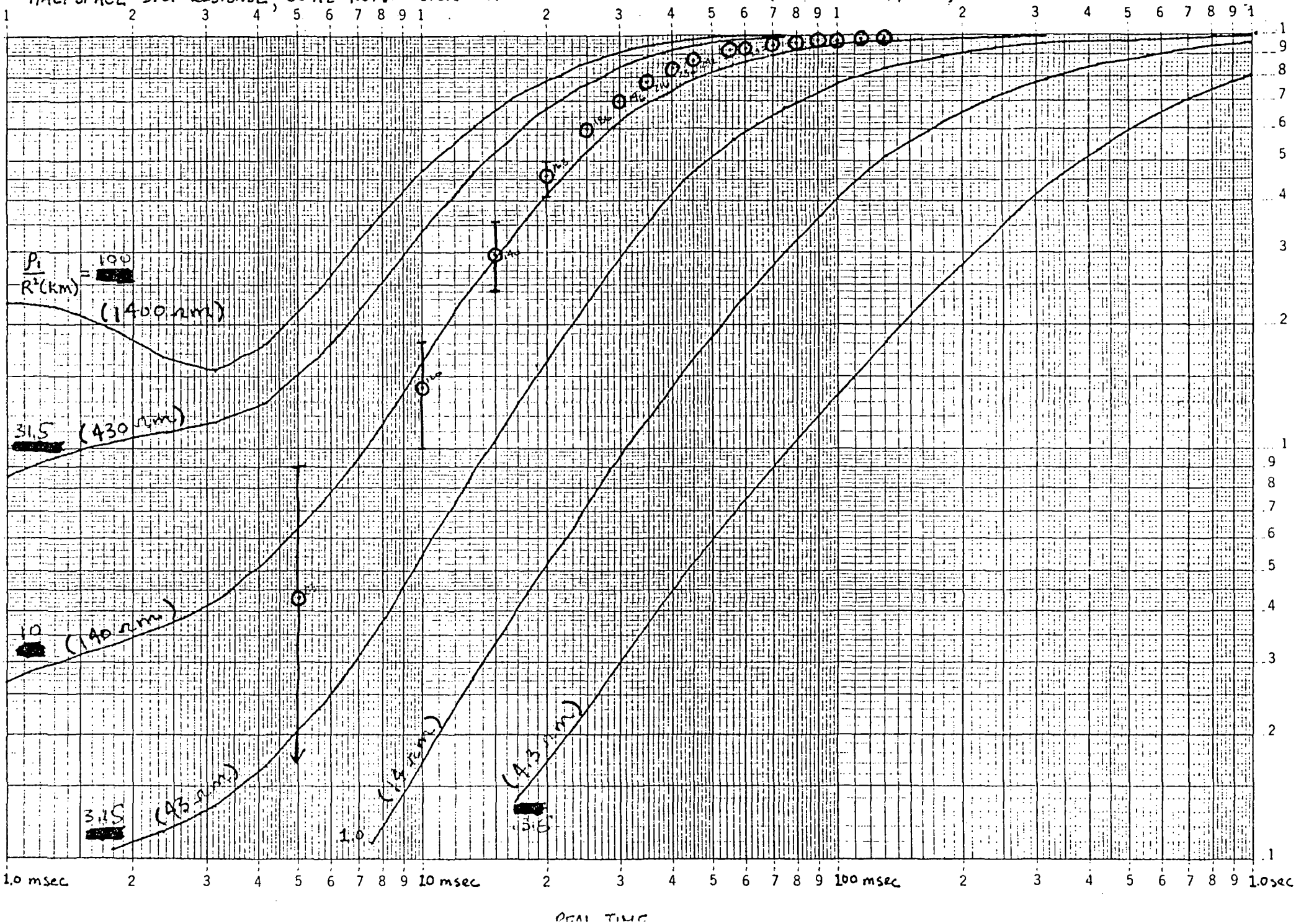

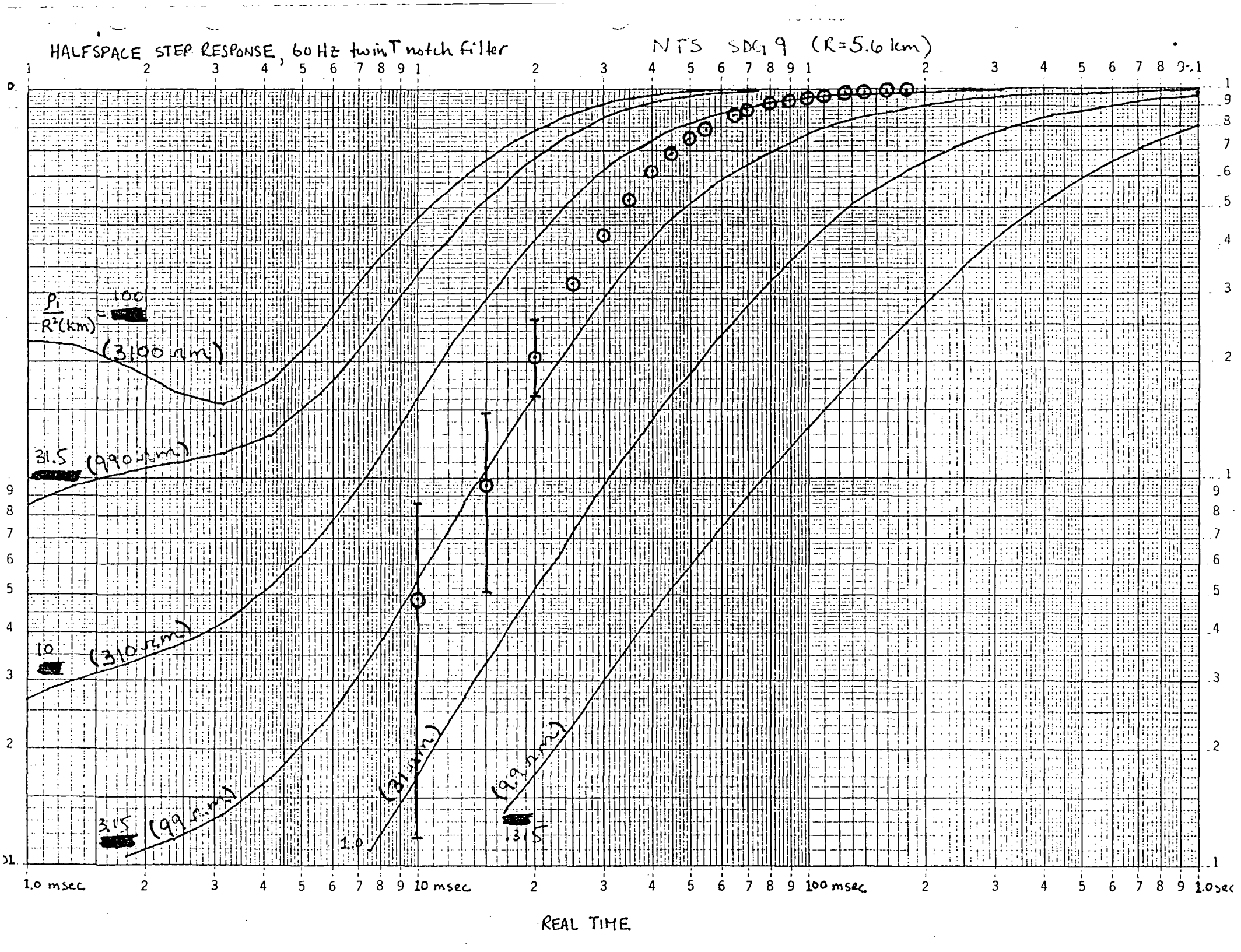
HALFSPACE STEP RESPONSE, 60 Hz twin T notch filter
NTS SDG 9 (R=5.6 km)
$\frac{P_1}{R^2(km)}$ = 100 (3100 nm)
31.5 (990 nm)
10 (310 nm)
3.15 (99 nm)
1.0 (31 nm)
.315 (9.9 nm)
1.0 msec
10 msec
100 msec
1.0 sec
REAL TIME

APPENDIX II: Combined Plots of Apparent Resistivity Versus Apparent Depth

Schlumberger data are plotted as the circled symbols, and TDEM data are the uncircled symbols. Solid curves represent the best-fit Schlumberger model whose parameters are summarized in bar form at the bottom of the plot. Dashed curves represent the TDEM model response computed using the Schlumberger best-fit model parameters. The parameters listed in bar form with the TDEM station numbers are the best-fit TDEM models produced by computer inversion. The numbers accompanying the parameters are the standard parameter errors produced by the inversion program. Those that have no errors explicitly listed had errors greater than 150%. An equal sign with three bars instead of two signifies a parameter that was constrained during inversion.

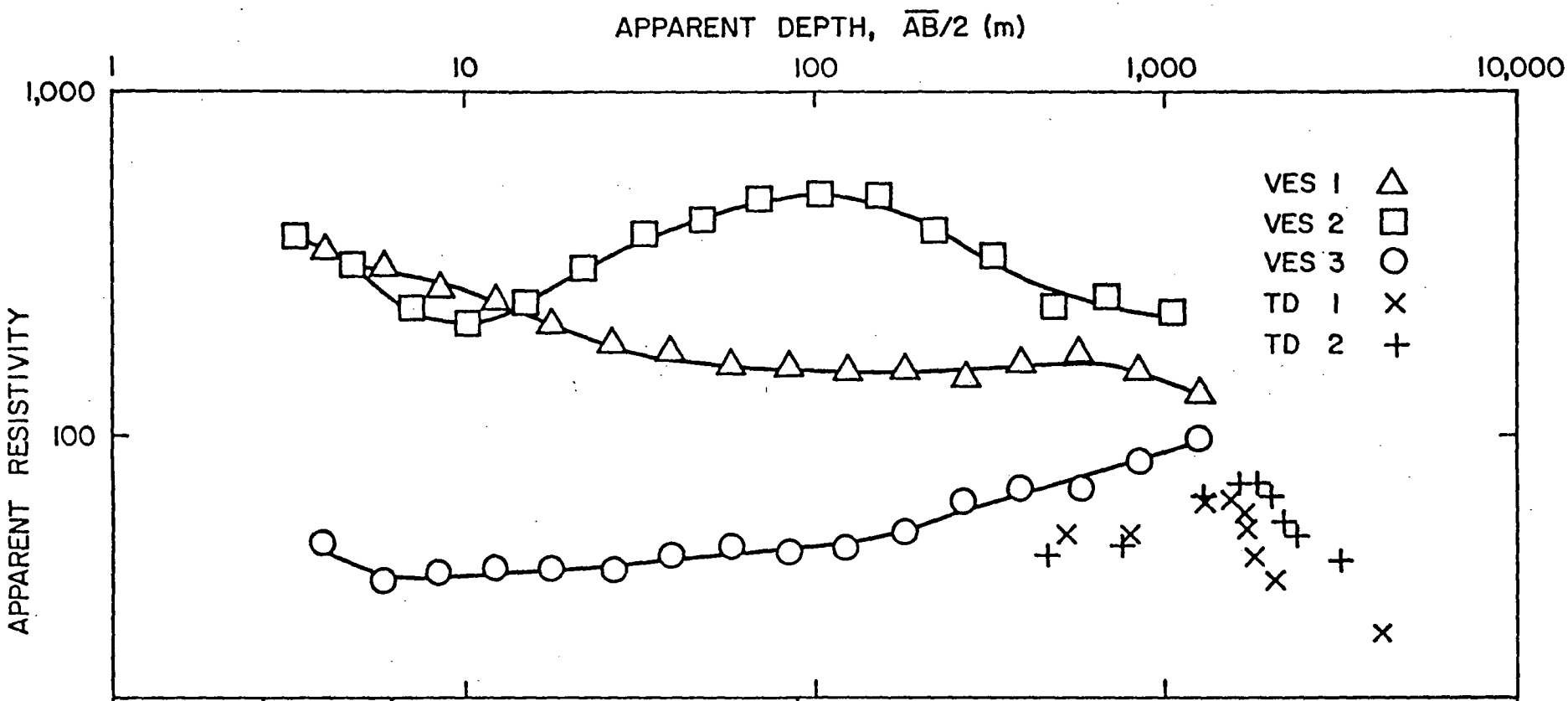

ρ=465 Ωm ± 7% d =2.6 ± 8 %	ρ=90 d=3.5 ± 8%	ρ=627 Ωm ± 6 % d = 83 ± 12 %	ρ=214 Ωm ± 5 %	VES 2
ρ=326 Ωm ± 3 % d = 6 ± 9 %	ρ=153 Ωm ± 3 % d = 358 ± 84 %	ρ=big d=201	ρ=41 Ωm	VES 1
ρ=38 Ωm ± 18 % d =9.4 ± 150 %	ρ=46 Ωm ± 8 % d =123 ± 20 %	ρ=99 Ωm ± 6 %		VES 3
ρ=50 Ωm d =445 ± 8 %	TD 1	ρ=200 Ωm d =734 ± 2%	ρ=11 Ωm ± 12 %	
ρ=40 Ωm d =326 ± 7 %	TD 2	ρ=200 Ωm d=1007 ± 5%	ρ=21 Ωm ± 11%	

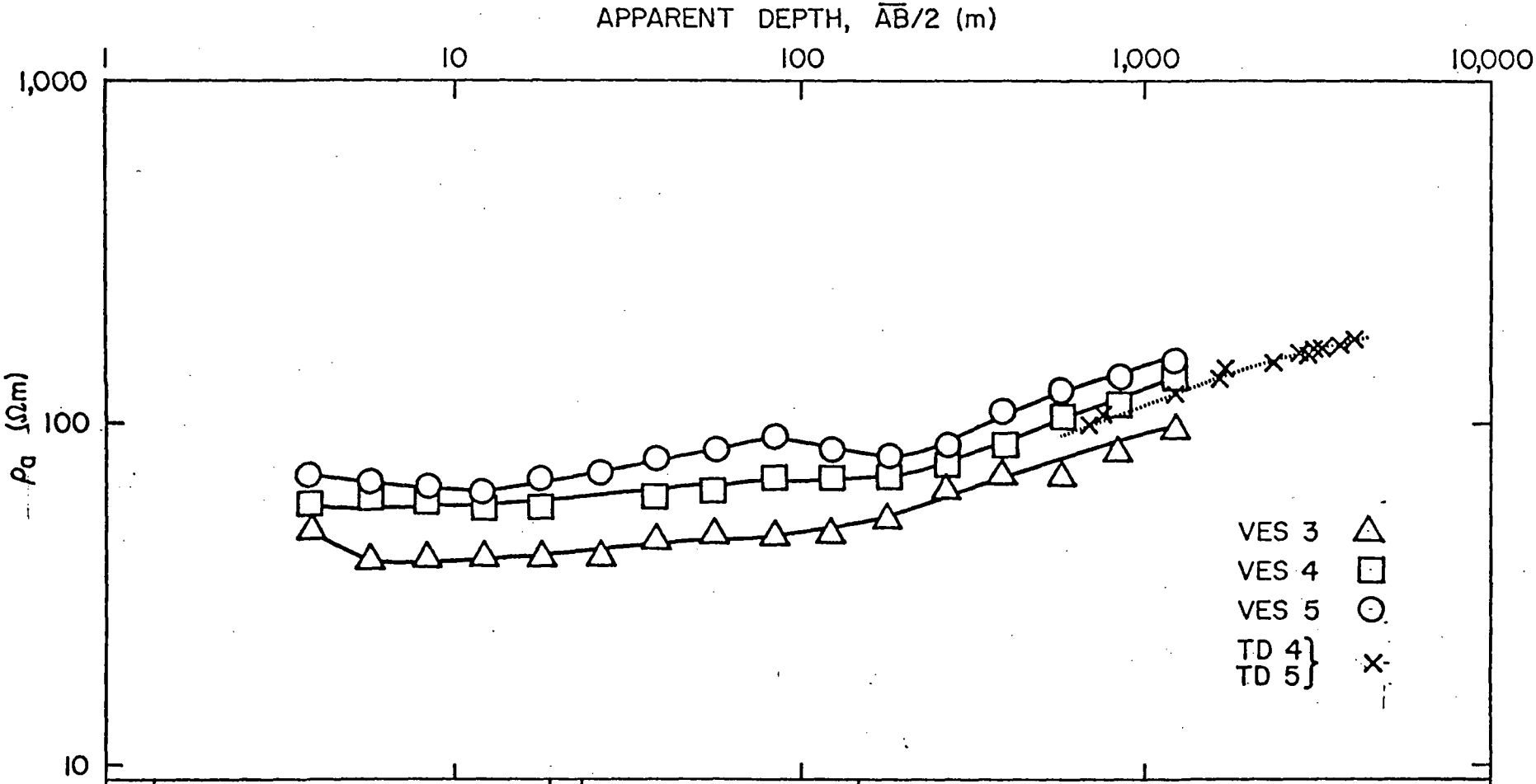

ρ=82 Ωm d=1.4 ± 34 %	ρ=62 Ωm ± 5 % d=20 ± 105 %	ρ=212 Ωm d=21	ρ=17 Ωm d=25	ρ=170 Ωm ± 5 % — VES 5
ρ=58 Ωm ± 4 % d=9.8 ± 77 %	ρ=67 Ωm ± 5 % d=163 ± 43 %	ρ=130 Ωm ± 41 % d=425 ± 85 %	ρ=210 Ωm (This model used to compute dashed line to model response)	
ρ=58 Ωm d=10	ρ=67 Ωm d=160	ρ=123 ± 6 % d=453 ± 34 %	ρ=250 Ωm ± 16 %	Joint VES 4 and TD 4
ρ=38 Ωm ± 18 % d=9.4 ± 150 %	ρ=46 Ωm ± 8 % d=123 ± 20 %	ρ=99 Ωm ± 6 %		VES 3

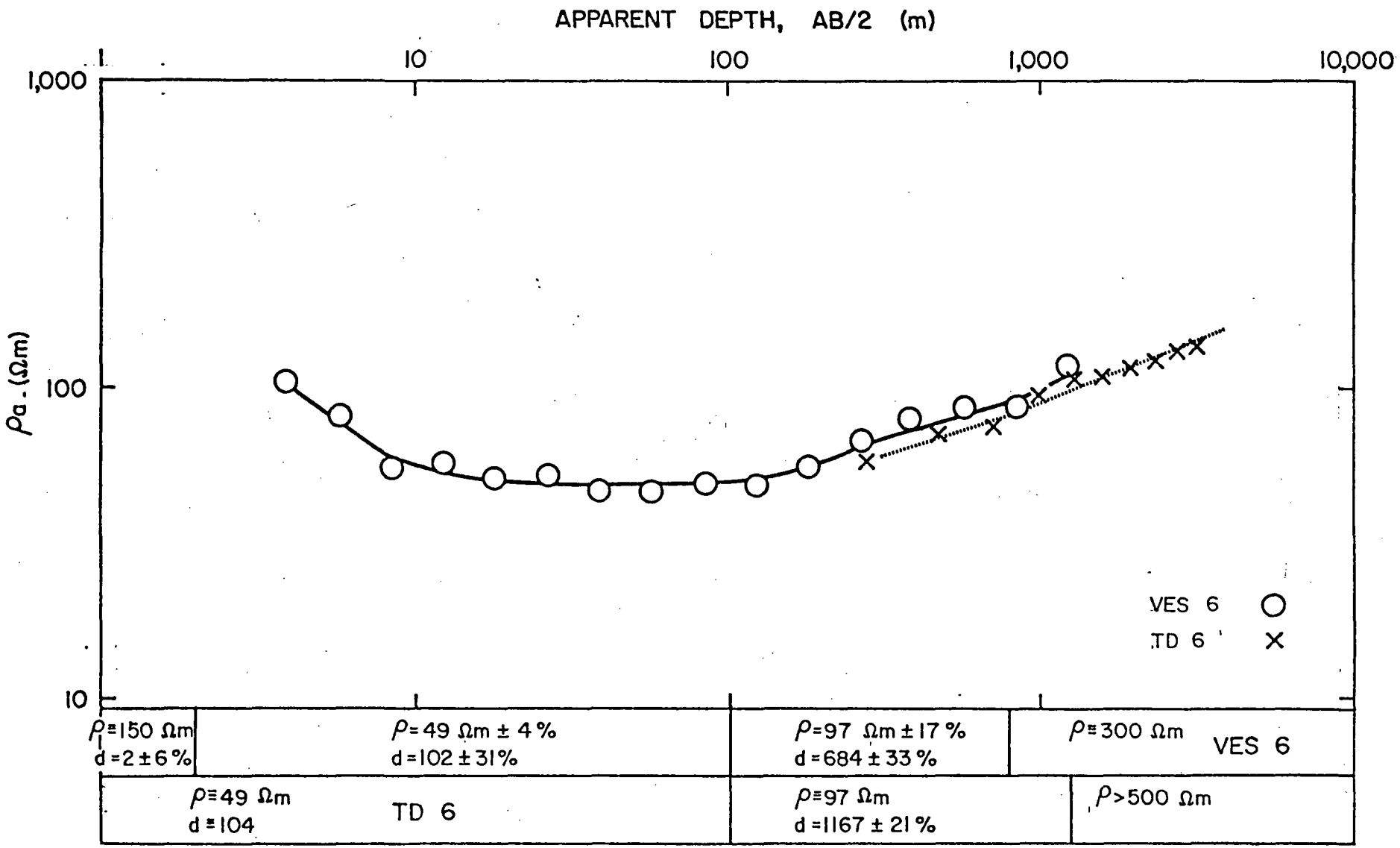
APPARENT DEPTH, AB/2 (m)
1
10
100
1,000
10,000
1,000
100
10
ρ_a . (Ωm)
VES 6
TD 6
ρ≡150 Ωm
d = 2 ± 6 %
ρ= 49 Ωm ± 4 %
d = 102 ± 31 %
ρ=97 Ωm ± 17 %
d = 684 ± 33 %
ρ≡300 Ωm
VES 6
ρ≡49 Ωm
d ≡ 104
TD 6
ρ≡97 Ωm
d = 1167 ± 21 %
ρ>500 Ωm

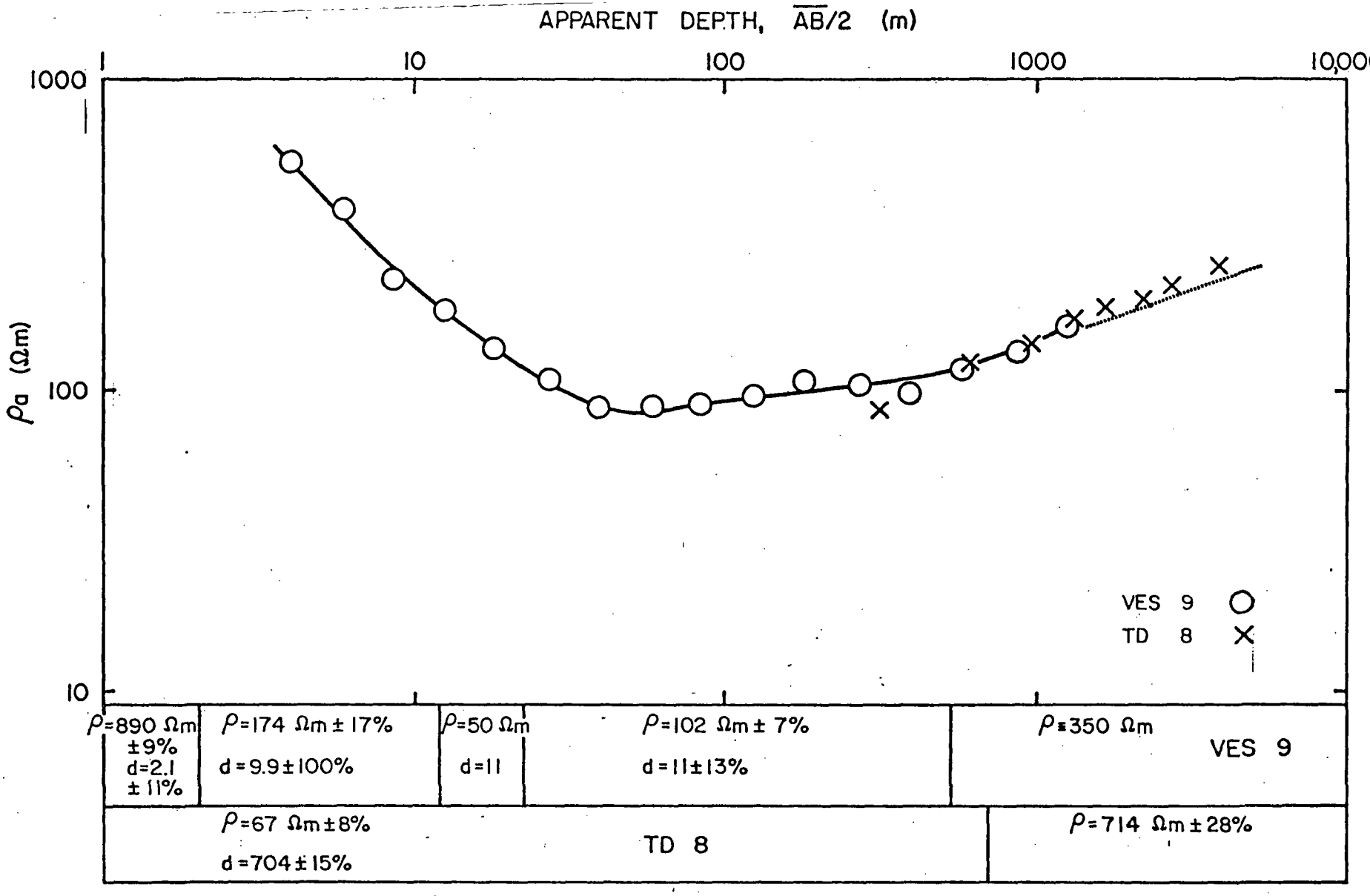
APPARENT DEPTH, AB/2 (m)
1
10
100
1000
10,000
1000
100
10
ρa (Ωm)
VES 9
TD 8
ρ=890 Ωm ±9% d=2.1 ±11%
ρ=174 Ωm ± 17% d=9.9±100%
ρ=50 Ωm d=11
ρ=102 Ωm ± 7% d=11±13%
ρ=350 Ωm
VES 9
ρ=67 Ωm±8% d=704±15%
TD 8
ρ=714 Ωm ± 28%

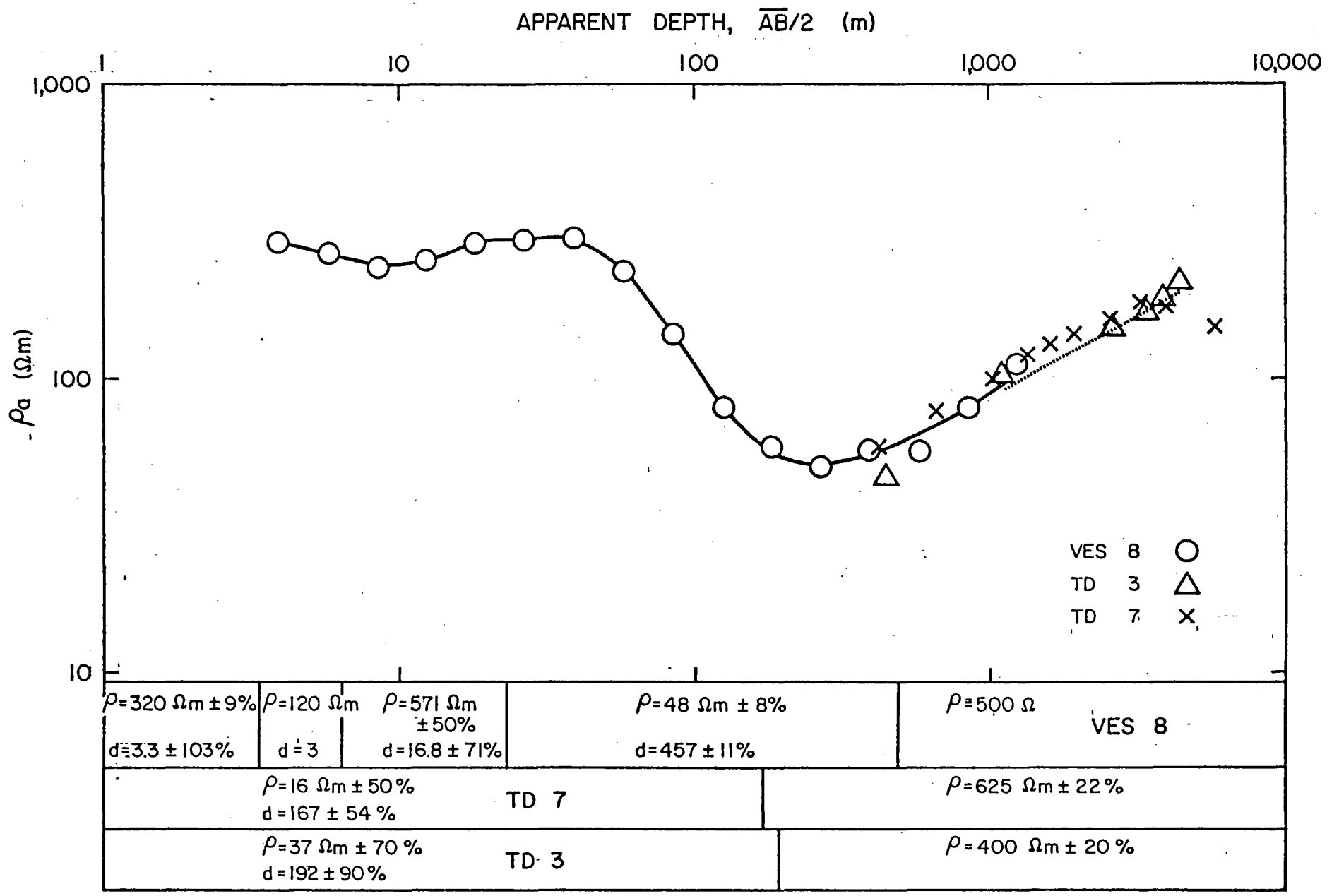
APPARENT DEPTH, $\overline{AB}/2$ (m)
1
10
100
1,000
10,000
1,000
100
10
ρ_a (Ωm)
VES 8
TD 3
TD 7
ρ=320 Ωm ± 9%
d=3.3 ± 103%
ρ=120 Ωm
d=3
ρ=571 Ωm ± 50%
d=16.8 ± 71%
ρ=48 Ωm ± 8%
d=457 ± 11%
ρ=500 Ω
VES 8
ρ=16 Ωm ± 50%
d=167 ± 54%
TD 7
ρ=625 Ωm ± 22%
ρ=37 Ωm ± 70%
d=192 ± 90%
TD 3
ρ=400 Ωm ± 20%

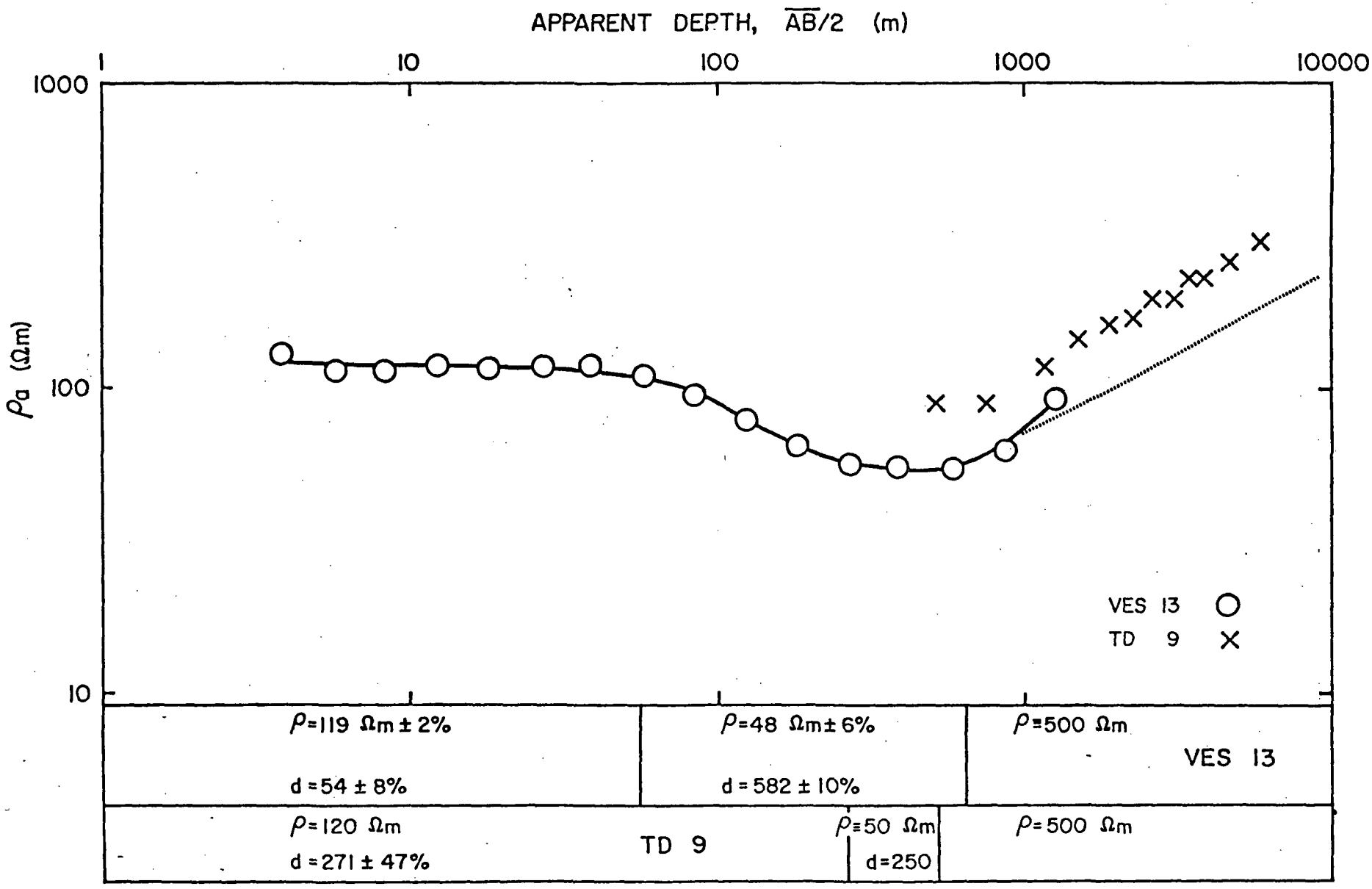
APPARENT DEPTH, AB/2 (m)
1
10
100
1000
10000
1000
100
10
ρa (Ωm)
VES 13
TD 9
ρ=119 Ωm ± 2%
d = 54 ± 8%
ρ=48 Ωm ± 6%
d = 582 ± 10%
ρ=500 Ωm
VES 13
ρ=120 Ωm
d = 271 ± 47%
TD 9
ρ=50 Ωm
d=250
ρ=500 Ωm